NORTH ATLANTIC TREATY ORGANISATION

RESEARCH AND TECHNOLOGY ORGANISATION

AC/323(SCI-033)TP/48

www.rta.nato.int

**RTO AGARDograph 160** **SCI-033**
**Flight Test Instrumentation Series – Volume 20**

# Optical Air Flow Measurements in Flight

(Mesures optiques de l'écoulement aérodynamique en vol)

This AGARDograph has been sponsored by SCI-122, the
Flight Test Technology Task Group of the
Systems Concepts and Integration Panel (SCI) of RTO.

Published December 2003

**This page has been deliberately left blank**

---

**Page intentionnellement blanche**

NORTH ATLANTIC TREATY ORGANISATION

RESEARCH AND TECHNOLOGY ORGANISATION

AC/323(SCI-033)TP/48

www.rta.nato.int

**RTO AGARDograph 160** **SCI-033**
**Flight Test Instrumentation Series – Volume 20**

# Optical Air Flow Measurements in Flight

(Mesures optiques de l'écoulement aérodynamique en vol)

This AGARDograph has been sponsored by SCI-122, the
Flight Test Technology Task Group of the
Systems Concepts and Integration Panel (SCI) of RTO.

Authored by

Mr. Rodney K. Bogue
NASA Dryden Flight Research Center
P. O. Box 273
Edwards, CA 93523-0273
UNITED STATES
email: rod.bogue@dfrc.nasa.gov

and

Dr. Henk W. Jentink
National Aerospace Laboratory (NLR)
Anthony Fokkerweg 2
1059 CM Amsterdam
THE NETHERLANDS
email: jentink@nlr.nl

# The Research and Technology Organisation (RTO) of NATO

RTO is the single focus in NATO for Defence Research and Technology activities. Its mission is to conduct and promote co-operative research and information exchange. The objective is to support the development and effective use of national defence research and technology and to meet the military needs of the Alliance, to maintain a technological lead, and to provide advice to NATO and national decision makers. The RTO performs its mission with the support of an extensive network of national experts. It also ensures effective co-ordination with other NATO bodies involved in R&T activities.

RTO reports both to the Military Committee of NATO and to the Conference of National Armament Directors. It comprises a Research and Technology Board (RTB) as the highest level of national representation and the Research and Technology Agency (RTA), a dedicated staff with its headquarters in Neuilly, near Paris, France. In order to facilitate contacts with the military users and other NATO activities, a small part of the RTA staff is located in NATO Headquarters in Brussels. The Brussels staff also co-ordinates RTO's co-operation with nations in Middle and Eastern Europe, to which RTO attaches particular importance especially as working together in the field of research is one of the more promising areas of co-operation.

The total spectrum of R&T activities is covered by the following 7 bodies:

- AVT Applied Vehicle Technology Panel
- HFM Human Factors and Medicine Panel
- IST Information Systems Technology Panel
- NMSG NATO Modelling and Simulation Group
- SAS Studies, Analysis and Simulation Panel
- SCI Systems Concepts and Integration Panel
- SET Sensors and Electronics Technology Panel

These bodies are made up of national representatives as well as generally recognised 'world class' scientists. They also provide a communication link to military users and other NATO bodies. RTO's scientific and technological work is carried out by Technical Teams, created for specific activities and with a specific duration. Such Technical Teams can organise workshops, symposia, field trials, lecture series and training courses. An important function of these Technical Teams is to ensure the continuity of the expert networks.

RTO builds upon earlier co-operation in defence research and technology as set-up under the Advisory Group for Aerospace Research and Development (AGARD) and the Defence Research Group (DRG). AGARD and the DRG share common roots in that they were both established at the initiative of Dr Theodore von Kármán, a leading aerospace scientist, who early on recognised the importance of scientific support for the Allied Armed Forces. RTO is capitalising on these common roots in order to provide the Alliance and the NATO nations with a strong scientific and technological basis that will guarantee a solid base for the future.



Published December 2003



ISBN 92-837-1112-2

# AGARDograph Series 160 and 300

The Systems Concepts and Integration (SCI) Panel has a mission to distribute knowledge concerning advanced systems, concepts, integration, engineering techniques, and technologies across the spectrum of platforms and operating environments to assure cost-effective mission area capabilities. Integrated defence systems, including air, land, sea, and space systems (manned and unmanned) and associated weapon and countermeasure integration are covered. Panel activities focus on NATO and national mid- to long-term system level operational needs. The scope of the Panel covers a multidisciplinary range of theoretical concepts, design, development, and evaluation methods applied to integrated defence systems.

One of the technical teams formed under the SCI Panel is dedicated to Flight Test Technology. Its mission is to disseminate information through publication of monographs on flight test technology derived from best practices which support the development of concepts and systems critical to maintaining NATO's technological and operational superiority. It also serves as the focal point for flight test subjects and issues within the SCI Panel and ensures continued vitality of the network of flight test experts within NATO.

These tasks were recognized and addressed by the former AGARD organization of NATO in the form of two AGARDograph series. The team continues this important activity by adding to the series described below.

In 1968, as a result of developments in the field of flight test instrumentation, it was decided that monographs should be published to document best practices in the NATO community. The monographs in this series are being published as individually numbered volumes of the AGARDograph 160 Flight Test Instrumentation Series.

In 1981, it was further decided that specialist monographs should be published covering aspects of Volume 1 and 2 of the original Flight Test Manual, including the flight testing of aircraft systems. The monographs in this series (with the exception of AG 237, which was separately numbered) are being published as individually numbered volumes of the AGARDograph 300 Flight Test Techniques Series.

At the end of each AGARDograph 160 Flight Test Instrumentation Series and AGARDograph 300 Flight Test Techniques Series volume is an annex listing all of the monographs published in both series.

# Optical Air Flow Measurements in Flight

## (RTO AG-160 Vol. 20 / SCI-033)

# Executive Summary

Optical measurements are increasingly becoming a part of measurement techniques in airborne systems. It has become important to avoid protuberances on military aircraft designed for stealthy radar characteristics. Optical measurement systems offer the possibility of accurate airspeed measurements that do not increase the radar cross-section. Although the experience base is small, cost studies show that substantial savings are possible for military applications. Applications of optical air flow measurements on highly maneuverable aircraft are expected to provide much more reliable information in regions of the flight regime where unacceptable measurement uncertainties plague conventional probe-based techniques.

Furthermore, with optical methods, the velocity of air masses at some distance from the aircraft can be measured. This feature can be utilized for several purposes. Air data measurement on helicopters beyond the rotor downwash and on first flights of prototype aircraft are improved. Warnings for turbulence and wind shear in front of the aircraft can be generated for prevention of engine unstarts and for improvement of flight safety. The researcher can study the atmosphere without flying through the air mass under study. The researcher measuring the air at very small distances from the aircraft learns about aerodynamics, and can be confident that the measurement process does not disturb the condition being measured. Parachute drop accuracy can also be improved.

The purpose of this AGARDograph is to bring attention to optical technology as it is currently being utilized in flight systems and to mention future technology prospects. The reader will become familiar with the vocabulary, components, and techniques in using optical components in airborne systems. Applications for airborne optical systems and case studies are also discussed.

# Mesures optiques de l'écoulement aérodynamique en vol

## (RTO AG-160 Vol. 20 / SCI-033)

# Synthèse

Les mesures optiques font de plus en plus partie des techniques de mesure utilisées dans les systèmes aéroportés. Il est désormais important de s'assurer que les avions militaires conçus pour la furtivité ne comportent pas de protubérances. Les systèmes de mesure optique offrent la possibilité d'exécuter des mesures précises de la vitesse aérodynamique sans augmentation de la surface équivalente radar. Bien que l'expérience acquise dans ce domaine soit limitée, des études de coûts ont montré que des économies de coûts considérables seraient réalisables dans le cas d'applications militaires. La mesure optique de l'écoulement aérodynamique appliquée à des aéronefs très manœuvrants devrait fournir des informations beaucoup plus fiables sur des parties du domaine de vol pour lesquelles les techniques à base de sondes actuelles sont entachées d'incertitudes de mesure.

En outre, les méthodes optiques permettent de mesurer la vitesse de masses d'air à différentes distances de l'aéronef. Cette caractéristique peut être mise à profit de différentes façons. L'enregistrement des données aérodynamiques est amélioré, tant pour les hélicoptères, en ce qui concerne le domaine de vol au-delà de la zone de déflexion vers le bas du rotor, que pour les premiers vols d'avions prototypes. Des signaux d'avertissement peuvent être générés en cas de détection de turbulence et de cisaillement du vent à l'avant de l'aéronef, afin d'éviter les décrochages et d'améliorer la sécurité en vol. Le chercheur peut étudier l'atmosphère sans traverser la masse d'air à l'étude. Lorsqu'il mesure l'écoulement d'air à des distances très rapprochées de l'aéronef et s'informe sur l'aérodynamique, il peut avoir la certitude que le processus de mesure ne perturbera pas le milieu étudié. La précision lors de parachutages peut également être améliorée.

Cet AGARDographe a pour objectif d'attirer l'attention sur les technologies optiques telles qu'actuellement employées dans les systèmes de navigation et d'évoquer les perspectives technologiques futures. Le lecteur pourra se familiariser avec le vocabulaire, les composants et les techniques d'intégration des composants optiques dans les systèmes aéroportés. Certaines applications pour systèmes optiques aéroportés et des études de cas sont également présentées.

# Acknowledgements

The development of this volume would not have been possible without the assistance and support of the Research and Technology Organization (RTO) of NATO who supported the authors' fact-finding visits in both Europe and the US and provided administrative assistance in the development and publication of this document. In particular, Mr. Glenn Bever of the NASA Dryden Flight Research Center in the US and Mr. Rob Krijn of the National Aerospace Laboratory in the Netherlands were instrumental in gaining RTO approval for publication and in continuing RTO support during the volume production when the project fell behind schedule.

The authors are indebted to the many researchers in the field of optical measurements who hosted fact-finding visits, willingly sharing their experience, and provided comments on the narrative text to improve the technical accuracy and the readability of the final product. Although there are many reference publications on optical theory, applying this theory in the flight environment requires knowledge from many other disciplines, most notably aeronautics, meteorology, atmospheric science, aerodynamics, signal processing, and mechanical design. A store of experience (in many cases experience in what did NOT work) is very valuable to the researcher in avoiding unproductive activities that do not yield useful results. The authors have incorporated comments reflecting the experience of many contributing researchers to provide guidance for the design of new systems that can acquire reliable optically based measurement in flight. Mr. James Meyers from NASA Langley Research Center, Hampton, Virginia was particularly helpful in providing information and feedback on the text. Others providing information and comments were:

Mr. Guy Destarac, Mr. Franck Innarelli – Airbus Industry, Toulouse, France

Mr. Rick McGann, Dr. David Soreide – The Boeing Company, Seattle, WA, US

Dr. Stephan Damp and Dr. Hans Pfeifer – French-German Research Institute ISL, Saint-Louis, France

Dr. Steven Hannon – Coherent Technologies Inc., Lafayette, CO, US

Mr. Friedrich Köpp – DLR, Oberpfaffenhofen, Germany

Mr. Wolfgang Förster, Dr. Chris Willert, Mr. Manfred Beversdorff – DLR, Cologne, Germany

Mr. Richard Richmond – US Air Force, Wright-Patterson Air Force Base, Ohio, US

Mr. Hubert Combe – Thales, Valence, France

Mr. Peter Tchoryk – Michigan Aerospace Corporation, Ann Arbor, MI, US

Mrs. Muriel Khachooni and Mr. Dennis Calaba provided editorial services and graphic assistance respectively. The text and graphics have been substantially improved through their efforts.

# Table of Contents

# List of Figures

# List of Tables

# Nomenclature

## Acronyms

| | |
|---|---|
| A/D | analog to digital |
| ACLAIM | airborne coherent lidar for advanced in-flight measurements |
| AGARDograph | Advanced Guidance for Alliance Research and Development volume |
| ALEV | Anémomètre Laser en Vol (Airborne Laser Velocimeter) |
| ANSI | American National Standards Institute, District of Columbia, US |
| AoA | Angle of Attack |
| AoS | Angle of Sideslip |
| ATADS | Advanced Technology Air Data System |
| CLIO | circle-to-line image optic |
| CLR | coherent laser radar |
| CTI | Coherent Technologies, Inc., Lafayette, CO, US |
| CW | continuous-wave |
| DGV | Doppler global velocimetry |
| DLR | German Aerospace Center DLR, Germany |
| DSP | digital signal processor |
| EADS | European Aeronautic Defence and Space Company |
| EML | enhanced mode lidar |
| FFT | fast Fourier transform |
| FL | flight level |
| IR | infrared |
| ISL | Institut Saint-Louis (French-German Research Institute), France |
| JOADS | joint optical air data system |
| L2F | laser two-focus anemometer |
| ladar | laser detection and ranging |
| laser | light amplification through stimulated emission of radiation |
| LDA | laser Doppler anemometry (a type of dual-beam Doppler) |
| LDV | laser Doppler velocimetry (a type of dual-beam Doppler) |
| LED | light emitting diode |
| lidar | light detection and ranging |
| LIF | laser induced fluorescence |
| LTA | laser transit anemometry |

| | |
|---|---|
| MEMS | microelectromechanical systems |
| MFLAME | multifunction future laser atmospheric measurement equipment |
| MOADS | molecular optical air data sensor |
| MPE | maximum permissible exposure |
| NASA | National Aeronautics and Space Administration, US |
| NCAR | National Center for Atmospheric Research, Boulder, Colorado, US |
| NLR | National Aerospace Laboratory, NLR, The Netherlands |
| PDV | planar Doppler velocimetry |
| PIV | particle image velocimetry |
| PMT | photomultiplier tube |
| RASP | real-time advanced signal processor |
| RTO | Research and Technology Organisation |
| SCI | Systems Concepts and Integration, one of seven RTO bodies |
| SL | sea level |
| SNR | signal-to-noise ratio |
| TAS | true airspeed |
| UN | United Nations |
| US | United States of America |
| USAF | United States Air Force |
| UV | ultraviolet |
| VFO | variable frequency oscillator |
| W | watt |

## Symbols

| | |
|---|---|
| B | system bandwidth, hertz |
| c | speed of light, electromagnetic constant, 299,792,458 m/sec |
| d | distance between light sheets, meters |
| D | effective optical diameter of lens or telescope |
| $\Delta L$ | measurement volume length |
| $\Delta t$ | time interval |
| e | energy |
| f | frequency |
| $f$ | focal distance of collecting optic |
| $f_D$ | frequency of intensity fluctuations on a detector that result from the Doppler effect |
| $h$ | Planck's constant, $6.55 \times 10^{-27}$ erg/sec |

| | |
|---|---|
| $I$ | scattered light intensity |
| $I_O$ | light beam intensity |
| $\bar{i}$ | illumination direction, vector |
| $\bar{k}$ | wave number, vector |
| $\bar{k}_s$ | scattered wave number, vector component in direction s |
| $L$ | range |
| nm | nanometer, one billionth of a meter |
| $\bar{o}$ | observation direction, vector |
| $P_T$ | transmitted light power |
| $Q$ | technique for switching pulsed lasers |
| $r$ | distance |
| $R$ | effective optical radius of lens or telescope |
| $s$ | distance between fringes |
| $\bar{v}$ | velocity vector |
| $v_{los}$ | velocity component in the line-of-sight direction (parallel to the light beam) |
| $v_\perp$ | velocity component in the direction perpendicular to the line-of-sight |
| $w_0$ | beam waist diameter |
| $\alpha$ | angle between beams in dual beam laser Doppler configuration |
| $\bar{\alpha}$ | polarizability |
| $\beta_\pi$ | atmospheric backscatter coefficient |
| $\delta f$ | frequency change of light, Hz |
| $\delta\bar{k}$ | wave vector change of light, caused by scattering |
| $\eta$ | detector quantum efficiency |
| $\nu$ | frequency, Hz |
| $\lambda$ | wavelength of light |
| $\theta$ | angle between laser beam axis and axis of light collection optics in DGV systems |

**This page has been deliberately left blank**

---

**Page intentionnellement blanche**

# Chapter 1 – INTRODUCTION

## 1.1 Background

The goal of this AGARDograph is to provide an introductory practical overview of in-flight optical flow measurement techniques. This document is written to aid an instrumentation engineer or research scientist in making non-intrusive flow measurements on an aircraft. It is hoped that this document will be particularly useful for the technologist with a limited background in optical theory and limited experience in applying optical technology. The experience of the authors and numerous other contributors has been infused here to provide guidance in avoiding expensive non-productive diversions that can occur when applying optical technology for the first time in the flight environment. This AGARDograph provides basic knowledge and techniques necessary for assessing the applicability of optical measurements and addressing effective optical measurement techniques in flight. Key aspects of optical measurements are discussed and the tradeoffs are identified, as they are currently understood. Basic components of optical measurement systems are discussed and key requirements are identified. Specific systems designed for a variety of applications are discussed to provide insight for the reader.

### 1.1.1 History

For many years, optical methods have been extensively used to perform detailed flow velocity measurements in wind tunnels. Non-intrusive optically based measurements have given researchers insight into the details of fluid dynamics that could not be obtained with any other technique. With optical methods, the researcher can be confident that the measurement process has not disturbed the condition being measured, and can therefore concentrate on results assessment instead of on developing calibrations or corrections for measurement-induced flow disturbances. The wind tunnel environment, being ground-based, affords ample space and power for equipment operation. Laser beams can be safely controlled in a ground situation. The air in a wind tunnel, unlike the free atmosphere in-flight, is confined so special operations (like seeding the flow with optical tracer particles) can be utilized. The enclosures of wind tunnels restrict the entry of light radiation from extraneous natural or artificial sources, thereby preserving the signal-to-noise ratio in the ground situation. For many of these reasons, the use of optical methods has become routine and one or more laser-based velocimetry systems have become standard fixtures for most production wind tunnels, on a worldwide basis. As conditions are often less favorable for aircraft in-flight testing, optical techniques have been less practical for flight applications.

Notwithstanding the difficulties in applying optical velocity measurements in flight testing, several systems were developed and operated, beginning in the early 1970s. About this time, carbon dioxide gas lasers (operating in the far infrared, at a wavelength near 10 μm) were developed that had the necessary coherence length to be able to generate a reliable Doppler frequency shift from aerosol backscatter through a coherent detector. These reference-beam systems measure flow velocity along the axis of the laser beam. Efficient systems at this wavelength require cryogenically cooled detectors, a limiting factor for flight use. These systems have been and continue to be used in special situations and for reference purposes, but have always been one-of-a-kind designs usually for specific research applications. Because of the large size and power needs of these early systems, large aircraft were usually required. With the passage of time, improvements in technology reduced the size and power requirements and systems were built and flown on helicopters and high-performance fighter aircraft. Table 1-1 summarizes several noteworthy early systems.

Table 1-1: Early optical-based flight flow measurement systems.

| Year | Organization/ Aircraft | Wavelength/ Mode/Power | Concept | Application/ Significance |
|---|---|---|---|---|
| 1971 | Honeywell, Inc./CV 990 | 10.6µm/CW/ 10 W and 50 W | Focused reference-beam velocimeter | Airspeed measurement at 20 meters. First known flight test of laser velocimeter |
| 1975 | Raytheon, Inc./UH-1 | 10.6µm/CW/ 3.5 W/ scanned | Focused reference-beam velocimeter | Correction of helicopter-fired rocket ballistics. Range of 1 to 32 m. First scanned system, first real-time rotor downwash correction |
| 1984 | Lockheed/ L1011, F-104 | .8µm/CW/9W | Sheet pairs time-of-flight velocimeter | Airspeed measurement at 2.5 m. First flight test of a sheet-pairs system. (ref. Smart-1992) |
| 1984 | Sextant (Crouzet)/ Mirage 3 | 10.6µm/CW/ 4W | Focused reference-beam velocimeter | Airspeed measurement at 40 meters. First supersonic laser velocimeter flight test |

Many applications were to obtain airspeed and flow direction angles without using the traditional air data boom. The applications were initially driven by two requirements; (1) the need to measure flow direction at extreme flight attitudes, and (2) the need to reduce the cost for calibrating and maintaining air data systems. In the late 1980s and early 1990s another requirement became important; to avoid protuberances on military aircraft designed for stealth radar characteristics. To achieve high maneuverability, high-performance aircraft were flying at unusual attitudes exceeding the ability of conventional air data measurement techniques to measure accurately. Cost studies revealed that substantial resources were devoted to calibrating and maintaining air data systems. Optical measurement systems offered the possibility of substantially reducing these costs for the airspeed measurement and improving the accuracy of the information. Flow-direction measurement probes disturbed the carefully designed shapes consistent with the low radar cross-section characteristics of military aircraft. A non-intrusive measurement technique was needed, and optical techniques offered an attractive solution to meet the requirements.

### 1.1.2 Challenges for flight applications

Moving from a controlled environment in a wind tunnel to a less-controlled setting in flight brings additional challenges, not all of which are addressed by improvements in technology. Some of the challenges in the flight applications are described below.

#### *1.1.2.1 Natural aerosol backscattering*

Since most applications utilize optical scattering from natural aerosols entrained in the flow, one of the more challenging aspects of using optical techniques in a flight environment is utilizing the natural aerosol environment to provide the scattering for tracing the flow motion. The atmosphere is a highly complex system and a natural by-product of this complexity is the constant addition and removal of aerosols from a myriad of physical and chemical processes, all of which proceed independently of the desires and activities of the flow researcher (see also 3.3.2 and 3.4). No feasible control is possible over the natural aerosol number density or any of the aerosol physical characteristics. Measurement systems using aerosol backscattering must accommodate the natural situation to be useful. Occasionally the available aerosols are not present in sufficient density or are not of a useful size to provide adequate backscatter values for an acceptable signal-to-noise ratio of a given system design. This condition results in reduced quality data and limits

operating range. Some concepts in the early stages of development rely on molecular scattering and do not require the presence of aerosols to trace flow motion. These molecular scattering concepts bring their own set of challenges, including requirements for different operating wavelengths, and alternate methods of signal processing.

#### *1.1.2.2 Low signal-to-noise ratio (SNR)*

Obtaining an adequate signal-to-noise ratio requires capturing the maximum level of signal and optimizes the rejection of extraneous noise. In the flight environment, unlike the more controlled wind tunnel situation, extraneous noise can enter the system from natural sources within the system field of view. Wavelength filtering and tight control of the field of view are often used to restrict the entry of undesired radiation.

Some flight applications require measurements from long ranges (10s of kilometers). Light energy scattered back from aerosols at long ranges is (from first principles of optical physics) diminished by being proportional to the inverse square of the range. Flight optical systems have limited ability to collect the reflected energy, thereby causing low signal levels and low SNR. Averaging is often used to improve the SNR at the expense of spatial and temporal resolution. Of course the emitted energy should be as high as possible for high SNR (limited by laser power capability and safety considerations). All else being equal, the SNR for long-range measurements is proportional to the received energy (and by inference the emitted energy). Equation 3-4 in section 3.6.1 identifies factors that influence the SNR of a system.

#### *1.1.2.3 Eye and skin hazards*

Since the laser beam is projected into the free atmosphere, it creates a potential eye hazard for personnel on the ground or in other nearby aircraft. This same eye hazard is present with wind tunnel systems, but it is far easier to control by limiting access for at-risk operator staff. A serious eye hazard may be created by lasers operating at wavelengths that are not sensed by the human eye (invisible). The normal “blink” reaction to a bright light provides a degree of protection when a bright visible wavelength enters the eye. When invisible beams enter the eye, the “blink” reaction is inoperative and serious damage can occur with no awareness. It should be emphasized that not all visible and invisible wavelengths are equally dangerous and the risks must be assessed on a case-by-case basis using the series Z136 of ANSI standards or other applicable national standards. The subject of eye hazards is an evolving area and the series Z136 standards are updated on a regular basis. For example, flash blindness, glare, and startle reactions associated with low levels of laser energy are covered in a US Government publication ANSI Z136.6 *Standard for the Safe Use of Lasers Outdoors*,[1] a particularly applicable reference. Another good reference is the publication standard ANSI Z136.1 *Safe Use of Lasers*[2] for readers involved in the design and operation of laser-based flow measurement systems for flight use.

**It is important that the most recent version of the appropriate standard be used during a design project and for developing safety procedures to protect system operators. If system developers have limited expertise in laser technology it is advisable to seek the services of a consultant to assure that laser safety matters are properly addressed.**

Assessing the hazard for a laser measurement system is a complex process that involves several factors, including power output, wavelength, mode of operation (continuous wave or pulse), pulse duration, and aperture (or cone angle). This process involves the use of a wavelength-based maximum irradiance, which is termed the maximum permissible exposure (MPE). For minimum risk, the laser should qualify as a Class I, which causes no damage to either vision or skin under continuous exposure. Lasers in Class II may often be applied with limited restrictions as a result of the natural blink reaction. Laser system operators are required to undergo eye examinations prior to initial service as an operator, and periodically as long as the service continues.

Most in-flight measurements have used infrared laser sources. There is some safety advantage to using wavelengths longer than 1.4 micrometers since the cornea and the vitreous humor in the eye absorb a substantial fraction of the incident energy prior to its reaching the retina. Irradiances beyond 1.4 micrometers result in MPE levels on the order of 15 times the levels in the visible range. This means that about 15 times the power level at visible wavelengths can be used and the laser source can still qualify as a Class I. The term "eye-safe" is sometimes applied for laser radiation with wavelengths beyond 1.4 micrometers, but as explained, this is a simplification because both the power level and wavelength must be specified to qualify as "eye safe." Although it is theoretically possible to cause eye damage from radiated laser light from an aircraft in flight, the authors know of no injuries caused by accidental in-flight laser radiation. For class III and class IV lasers, overall system safety is more effective with an emphasis on development of safe system maintenance procedures and disabling the laser against accidental activation on the ground.

Newer systems using molecular backscatter require shorter wavelengths in the ultraviolet (UV) range. Compared to visible wavelengths, the eye is much less tolerant of shortwave ultraviolet radiation (especially below about .3 micrometers). For ultraviolet light (and to a lesser degree for all radiation) the effects of radiation effects on the skin should also be taken into account (see the ANSI standards noted earlier in this section).

### 1.1.3 Component technology developments

As suggested in the prior section, the practicality of using optical measurements in flight is strongly limited by the available technology of the system components. Therefore, improvement in component technology often paces flight applications. Improvement in optics and signal processing technology as well as the widespread availability of powerful, rugged, and compact computer technology has opened doors to many flight applications not previously feasible.

#### *1.1.3.1 Optical state-of-the-art technology*

State-of-the-art developments in optical technology, primarily in the area of solid-state lasers, detectors, and integrated optics make possible small, power-efficient systems that can be used in flight. Solid-state lasers that operate at near-infrared wavelengths are much less dangerous to the eye than others with visible outputs and are rapidly becoming available, spurred on by requirements from the communications industry for components and systems optimized for these wavelengths. Wavelengths longer than 1.3 micrometers have received relatively more attention, at least for long-range measurements. Most solid-state lasers are substantially more efficient and more compact than earlier gas or dye lasers; therefore, less power is required for operation and the resulting smaller systems can be installed within the restricted space and power constraints typical of most aircraft. An often overlooked side benefit to more efficient systems is the reduced heat that must be dissipated. The more effective systems enable flow measurement with optical techniques in flight, thereby introducing to flight applications the advantages previously only experienced in the wind tunnel. In addition to the advantages for fluid dynamics research, optical flow measurement gives the potential for less disturbance to air data measurements and to measurements of the atmosphere in the vicinity of the aircraft. Examples of these applications are turbulence and wind shear detection systems under development. 1-micrometer Nd:YAG lasers using non-linear quadrupling crystals operate at .25 micrometers in the ultraviolet spectrum and make use of the increased molecular scattering at the shorter wavelength. While posing a risk of eye damage, these UV systems can provide non-intrusive measures of ambient air temperature and density. These measurements round out the full suite of "air data" parameters that are needed by most flight vehicles. Conventional temperature and pressure probes introduce errors resulting from the flight vehicle motion in the atmosphere, while the UV-based measurement approach avoids this particular source of error.

*1.1.3.2 Signal processing*

Improved high-speed signal processing capability, primarily from electronic digital signal processors, provides detailed test results in real time. This allows applications in operational flight settings where results must be rapidly analyzed to support operational decisions. This capability strongly supports the research application by providing results to the investigator, so that an inefficient experiment protocol may be altered quickly to obtain more effective use of expensive flight time.

*1.1.3.3 Spin-off developments*

In most cases, improved technology has resulted in reductions in size, and increases in efficiency for system components. Reductions in size usually imply reductions in weight as well. All of these characteristics associated with improved technology make the application of optical measurements much more feasible in the flight environment. Smaller components mean smaller systems, systems that can be more fully integrated into robust designs capable of operating in the sometimes harsh vibration and temperature extremes encountered in flight

## 1.2 Objective

The general objective of this AGARDograph is to provide an introductory overview of in-flight optical flow measurement techniques. The focus of this AGARDograph is to identify the basic knowledge and techniques that system designers need to assess the applicability of optical measurements and to address effective optical measurement techniques in flight. Key aspects of optical measurements in flight are discussed and tradeoffs are identified, as they are currently understood. Examples of specific applications are provided.

Instrumentation design engineers usually have an educational background including a major in some branch of engineering. Understanding the principles of making optical measurements in flight requires knowledge of basic optical concepts, electronic concepts, optoelectronic interfaces, and some understanding of atmospheric processes associated with natural aerosols. It is not often that an engineer will have the necessary background knowledge in all these areas to begin effective work in acquiring optical measurements in the flight environment immediately after an assignment has been made. This AGARDograph is intended to provide the initial information that will be useful in understanding the basic concepts.

Because this is an introductory document, theoretical treatment is not emphasized and the reader is encouraged to use the references provided at the end of the document for more comprehensive and detailed treatment of various aspects of optical flow measurements. Equations are occasionally used to illustrate relationships, but the majority of the discussion is focused on describing processes in a way that is physically understandable for a reader with a limited background in optical theory and technology.

## 1.3 Organization

The volume is organized, in keeping with the objective of providing an introductory overview of the subject, to provide a basic vocabulary and understanding of fundamental principles governing the operation of optical flow measurement in Chapters 1, 2, and 3. Chapters 4 and 5 treat the individual components of typical optical flow measurement systems and discuss how these components may be combined into operating systems. Chapters 6 and 7 describe how systems may be designed for specific applications and highlight the basic requirements for these applications. Also reviewed are several examples of systems that have been designed for flight applications. Chapter 8 identifies trends in the technology for optical measurements in flight and speculates on the effects this may have on future systems capabilities. An outline of the volume follows:

## Chapter 1. Introduction

A brief historical background of optical flow measurements in flight is reviewed for reader insight. Examples of past systems are included to provide an understanding of optical systems development over the past 30 years as technology has progressed, in both optics and in many of the supporting disciplines for flight-based optical flow measurements.

## Chapter 2. Terminology and definitions

The terminology used for the different optical flow measurement techniques in literature is not uniform. Therefore a clear definition of the terms to be used in this volume is provided. The authors have attempted to define the terminology to conform to the definitions of the majority of authors in the literature.

## Chapter 3. Basic principles

The physical principles of optics and their implications for optical flow measurement in flight are reviewed.

Light source – Light source properties that bear on the performance of an optical measurement system are discussed. Factors considered include coherence, pulsing, and power effects.

Measurement volume discrimination – Several methods are considered for selecting the volume from which the optical measurement is obtained. Optical methods, including focusing and masking, are considered as well as timing techniques that rely on pulsed sources and detector gating.

Scattering from seeded flow – All optical flow measurements being applied in flight depend on light scattering. Basic theory concerning the light scattering is summarized. The requirements on aerosols in the flow or molecules that comprise the flow are reviewed. Also considered are the characteristics of scattering from an ensemble of scatterers and the effects upon the detected signal

Detection – Detector requirements are reviewed for optical flow measurement systems. Factors considered include sensitivity, frequency response, and noise characteristics.

Signal processing – Most aspects of signal processing are discussed because of its importance in optical system performance. Signal processing before detection and after detection is reviewed. Tradeoffs for many optical configurations and measurement applications are also discussed.

## Chapter 4. System components

In this chapter an overview is provided of the essential system components encountered in optical flow meters. The principles identified for system components in chapter 3 are translated into practical specifications.

Optical components – Optical components are reviewed, together with the interactions that occur between the light source, the focusing elements, the pulsing characteristics, and the detector in these optical systems.

Mechanical construction – For flight applications, the mechanical construction of flight systems takes on an overriding importance. Small size and stiffness of the flight system are critical for reliable in-flight optical system operation.

Signal processor – The electrical signal from a detector must be processed to derive the flow information. Different signal processors are compared in order to identify tradeoffs for optimal system performance.

**Chapter 5. Types of laser anemometers**

The basic forms of different laser anemometers are categorized and described. Some implicit characteristics are mentioned.

Laser Doppler anemometers – This category includes dual-beam laser Doppler anemometers, reference-beam Doppler anemometers (homodyne and heterodyne) and Doppler global velocimeters. These anemometers are based on the measurement of the frequency-shift of light being scattered on a moving particle.

Time-of-flight anemometers – The laser two-focus anemometer and the sheet-pair anemometer are distinct members of this category. These anemometers are based on the measurement of time intervals between successive scattering events on one particle.

**Chapter 6. Applications**

Optical flow measurements in flight are used in several applications that set various requirements on the anemometers. A structured overview of the various application fields follows.

Air Data Systems – Velocities derived from light scattering, just outside the range of the flow disturbance from the aircraft, enable the calibration of air data sensors. The airspeed of the aircraft in three components, the angle of attack, and the angle of sideslip can be determined by using this method, with a high degree of accuracy and without the use of other sensors. This is particularly useful under conditions of dynamic maneuvering and unusual flight attitudes.

Safety Hazard Detection and Atmospheric Research – By measuring the airspeed at a considerable distance in front of the aircraft, a wind shear or turbulence hazard detection system can be created. This detection can trigger procedures for protecting the aircraft occupants or a change in the setting of a supersonic aircraft engine to prevent engine inlet unstart. Clear air turbulence as well as wake vortices near runways can also be detected with far field anemometers. Improved passenger comfort and safety are expected as a result of this capability.

Aerodynamic Investigations – To determine the air flow very close to the aircraft is to learn about the aerodynamics at this range. Subjects of interest in this area include flow around wing-body junctions and flow around nacelles.

Atmospheric research – To determine the wind velocity field without flying through the air mass under investigation is possible with this technology.

Parachute drop accuracy improvement – To measure wind velocity fields for the accurate determination of high-altitude release points for parachutes (and similarly for release points of ballistic munitions) is another possible application of this technology.

**Chapter 7. Existing systems**

An overview of existing systems is provided, based on a literature survey and the findings from travels by the authors through the USA and Europe. Some examples of existing optical anemometers are described in detail. Since the science (and art) of obtaining optical flow measurements in flight has not reached a mature state, some systems are included in Chapter 7 that are designed for flight applications, but have not yet reached flight status.

## Chapter 8. Future prospects and directions

Future potential of optical flow measurements is shown in a variety of application areas. Prospects of in-flight flow measurements may be advanced considerably by the development of suitable components of anemometers. The authors' viewpoint on future trends in optical air flow measurement in flight is included in this chapter.

# Chapter 2 – TERMINOLOGY AND DEFINITIONS

The terminology used for different optical flow measurement techniques is not uniform in the existing literature. Therefore it is necessary to provide a clear definition of the terms used in this volume. The definitions included here attempt to conform to terminology in common use by the majority of authors in the literature available on this subject.

**aerosol** — a microscopic solid or liquid particle in the atmosphere. Examples of natural atmospheric aerosols are; water droplets, stratospheric sulfuric acid droplets from volcanic eruptions, wind-borne dust particles from surface sources, natural or man-made by-products of incomplete combustion, and solid by-products of natural atmospheric chemical reactions. Natural aerosols of the appropriate size and with useful optical properties are used in optical measurements as flow tracers to determine the flow motion. Some aerosols absorb optical energy at specific wavelengths and under some circumstances these may attenuate the optical signal strength.

**backscatter coefficient** — the ratio of transmitted optical energy to energy scattered directly back to the transmitter, normalized by length and by the collected solid-angle field of view. This parameter is the result of optical energy scattering by molecules and an ensemble of particles entrained in an illuminated region of the atmosphere. This coefficient is affected by the particle number density and the particle size relative to the wavelength of the transmitted optical energy.

**bistatic optical configuration** — an optical configuration using different optics to shape the output pulse-beam and to collect the scattered light. Bistatic optics receive scattered light from an axis not aligned with the transmitted energy and thus provide information on flow motion along a different axis. Multiple receivers can measure several velocity components from the same region of interest and thereby provide three velocity components.

**coherence length** — the length, in the direction of the propagation of a light beam, over which the phase of light is correlated (the correlation function larger than 1/e). The coherence length is often specified for a light source. Adequate coherence length is an important factor for anemometers based on interference of light for detection. The coherence length of the light source is therefore often an important parameter in the design of such a meter.

**coherent detection** — a process that provides improved detection sensitivity to weak signal returns in low signal-to-noise ratio (SNR) environments. The received signal is mixed with the single-frequency reference signal from a local oscillator on the surface of a “square-law” detector to derive a beat signal with a frequency equal to the difference frequency between the reference and the received signal. This process provides a substantial effective signal gain and a derived signal with a frequency distribution equal to the difference between the signal of interest and the reference. This difference signal is particularly interesting (since it includes the information of interest) and effectively represents a signal translation from an extremely high frequency to a range much lower than the original that is more amenable to further signal processing. An example is noise reduction through low-pass filtering. This process provides the ability to detect a narrow band of frequencies with very high Doppler frequency resolution. Optical systems using coherent detection require precise optical alignment to transmit and receive planar waves for optimal sensitivity and are more complex than systems using direct detection. In the electronic disciplines, the term “product detection” is used to describe the coherent detection process. (see heterodyne and homodyne)

**coherent laser radar (CLR)** — a term increasingly used to describe a reference beam laser anemometer; See reference beam laser anemometer (for air flow measurement applications).

**continuous wave** — is a mode of system operation wherein the optical system radiates continuously as opposed to the pulsed mode of operation where radiation is intermittent. The continuous-wave mode of operation is often abbreviated “CW”.

**detection** — is the process of converting the optical signal into an electrical form, so that the flow information can be electronically processed and extracted for analysis.

**detector** — is the device that reacts to the impingement of optical energy on its surface by producing an electrical output signal. Detectors play a key role in all optical measurement systems. Important parameters for detectors include: quantum efficiency, dark current, sensitivity, and frequency response.

**differential laser Doppler anemometer** — See dual-beam laser Doppler anemometer

**digital signal processor (DSP)** — a specialized digital processor technology configured to efficiently perform algorithms commonly encountered in signal processing applications. Typical processes include averaging, correlating, and time-to-frequency domain conversions. DSP technology is often used to process flowmeter signals.

**direct detection** — a process that discriminates a frequency shift (Doppler) in scattered light by optically filtering signals before they impinge on the detector surface. A very narrow-band filter is used to convert the scattered signal frequency into an amplitude variation. Thus the detector output amplitude becomes a representation of the frequency shift. Optical filters that are commonly used for direct detection include optical etalons and molecular vapor cells, Iodine being one of the more popular choices.

**discriminator signal processing** — a signal processing technique modeled on conventional frequency-modulated telemetry techniques that convert frequency variations into amplitude variations. Optical discriminator signal processing relies on narrow-band filtering (usually accomplished with an etalon or a molecular filter) to provide a sharp and stable amplitude-to-frequency characteristic. See direct detection.

**Doppler global velocimetry (DGV)** — (also called planar Doppler velocimetry (PDV)) a flow velocimetry technique applying direct detection of frequency shifts of light scattered from aerosols in a light sheet. The three components of the velocity vectors can be determined by illuminating the plane in which the measurements are taken from three directions or by detecting frequency shifts in three directions on three different sets of detectors.

**Doppler shift** — is the key parameter used in nearly all optical flow velocity measurement concepts to measure velocity by comparing the scattered light frequency with transmitted frequency. The difference in these two frequencies, scaled by the inverse wavelength, is a direct measure of the velocity along the laser beam.

**dual-beam laser Doppler anemometer** — is an anemometer using intersecting laser beams to measure the difference in Doppler shift of light scattered from these beams by particles traversing the intersection volume. A simplified explanation of the anemometer operation considers the interference pattern often called “fringes” created in this beam intersection volume. As entrained particles in the focal region traverse the fringe pattern, bursts of light are returned to the detector. Frequency analysis of the fringe-crossing frequency defines the particle velocity component perpendicular to the fringe orientation. Other fringe patterns at other locations must be used to provide two additional flow velocity components for the three-dimensional flow field at one point in space. The single measured velocity component is perpendicular to the angle bisector of the crossed beams.

**etalon** — is a device using two parallel partly transparent mirrors providing a frequency and directionally dependent optical transfer function to incident light. Spectrometers with very high spectral resolutions can be realized with an etalon. Etalons are used to determine the light spectrum generated by a laser.

**far field** — is the region of the atmosphere about a moving aircraft that is at such a large distance from the aircraft so as to be uninfluenced by flow disturbances created by the aircraft motion. As used in this volume, far field is the region remote from the local flow field

**finesse** — is the ability of an etalon to resolve closely spaced frequency components of incident light. Finesse increases proportionally with the etalon plate reflectivity while the signal throughput decreases. In a typical Fabry-Perot lidar application, there is an optimal finesse that results in adequate spectral resolution to measure the Doppler shift, but that also achieves sufficient light throughput to the detector. Finesse and frequency stability are affected by other factors, including plate flatness, parallelism, and spacing, range of angles that can be transmitted, and in some cases, the diffraction limit of the system. Fabrication of the plates, and mounting of the etalon must be done with care to avoid environmental effects of temperature and pressure gradients.

**flow following** — is the ability of a light scattering aerosol to follow the motion of the fluid in which it is entrained, particularly under conditions of high flow-acceleration. Factors that enhance this ability include small size, aerosol and fluid density matching, high fluid viscosity, and fluid motion with low levels of acceleration. Flow following is more important for measurements in the local flow field, as flow at greater distances (free-stream and far field) is subject to relatively lower accelerations originating from normal atmospheric processes.

**free stream** — is, in essence, similar to “far field”, except as used in this volume it implies that region of the atmosphere about a moving aircraft that is just beyond the outer boundary of the local disturbed flow field.

**fringe anemometer** — See dual-beam laser Doppler anemometer

**heterodyne** — is a coherent detection technique using a reference signal that is offset from the transmitted signal to provide advantages over a simple homodyne technique. Typical advantages are: (1) reducing the Doppler signal frequency to accommodate the limitations of the signal detector bandwidth, and (2) providing the capability to easily differentiate changes in flow direction in a reference-beam anemometer.

**homodyne** — is a coherent detection technique that uses the transmitted signal as a reference for the coherent detection process. Homodyne systems are used in cases where the Doppler signal is well within the detector bandwidth capability and where detection of flow velocity reversal is not required.

**ladar** — is an acronym from the words LAser Detection And Ranging. Through common usage, the term “ladar” has come to refer to the optical analog of radar (which is used to measure position and motion of large hard objects such as aircraft or automobiles).

**laser** — is an acronym from the words Light Amplification through Stimulated Emission of Radiation. The laser is a light source utilizing the quantum effect called “stimulated emission of radiation” to provide light characterized by a narrow bandwidth, coherence, focusing ability, high power, and pulse capability.

**LDA** — is an acronym from the words Laser Doppler Anemometry. A technique for measuring the velocity of wind (anemos is Greek for wind) from the frequency shift occurring when laser light is scattered from moving particles in the air. Through common usage, the term LDA (synonymous with LDV, laser Doppler velocimetry) refers to the dual-beam laser Doppler anemometer

**lidar** — is an acronym from the words LIght Detection And Ranging. Through common usage, the term lidar has come to refer to a measuring process that provides information on the motion of the atmosphere and the atmospheric aerosol loading that is manifested in the scattering of light back to a detector (the so-called monostatic system). The process relies on scattering from an ensemble of natural aerosols from an illuminated region of the atmosphere and does not track single aerosol motion.

**LTA** — is an acronym from the words Laser Transit Anemometry. A technique for measuring the time it takes for a particle to move from one intense light area to another intense light area. The velocity of the particle can be derived from the distance between the locations where the light was scattered and the time interval between scatterings. Through common usage, the term LTA refers to the two-spot laser anemometer

**L2F** — is an acronym for laser two-focus anemometer or two-spot laser anemometer. See two-spot laser anemometer.

**masking** — is a technique that uses the intersection of a projected light beam and a detector optical field of view to define a measurement volume.

**maximum permissible exposure (MPE)** — is the maximum irradiance permissible from a laser source into the human eye or onto exposed skin that will not cause damage. Such irradiance may be accumulated under continuous exposure or through the effects of many pulses over a short period of time.

**Mie scattering** — is the optical scattering from aerosols having diameters with the same order of magnitude as the optical wavelength. Mie scattering is characterized by highly variable peaks and nulls in scattering as the scattering angle is varied and as small changes occur in the ratio of aerosol diameter to optical wavelength.

**measurement volume** — is the region of the flow field in question from which the flow measurement is obtained. For bistatic systems, the overlap of the projected beam and the detector field-of-view defines the measurement volume. With CW systems using a single beam such as the reference beam laser anemometer, the optical focal region determines the measurement volume. For CW intersection-beam systems such as the dual-beam laser Doppler anemometer, the region of beam intersection determines the measurement volume. For pulsed systems, either the optical focal region (mostly for near-field measurements) or the optical pulse spatial length dimension and beam diameter determine the measurement volume. Often both types of volume selection are used when optimal performance is required for a specific application.

**monostatic optical configuration** — a laser anemometer optical embodiment that uses the same optics to shape the output pulse beam and to collect the scattered light. By virtue of its configuration, this optical arrangement captures scattered light directed exactly opposite from the transmitted beam, hence the term “backscatter” which is applied to the received signal. Monostatic systems lend themselves to robust and compact designs for flight applications. With a monostatic system, it is difficult to adjust receiving parameters independently from transmitting factors. Pulsed monostatic configurations require special control over pulse timing to avoid capturing scattered energy from the transmitted pulse onto the detector.

**near field** — is the region of the atmosphere close to a moving aircraft that is disturbed by the aircraft motion. Examples of disturbances include pressure fields, boundary layers, shock waves, and wakes shed from lifting surfaces.

**number density** — is the number of aerosols per unit volume of the atmosphere. This is a parameter often used in the measurement of aerosols.

**particle** — a microscopic solid or liquid object providing optical scattering. In the natural atmosphere the scattering objects are termed aerosols.

**particle image velocimetry (PIV)** — is a flow velocity measurement technique utilizing two images of particles, slightly offset in time, in a plane defined by a laser light sheet to measure individual particle displacement during the time interval. Flow velocity at the location of each particle is obtained by dividing the particle displacement by the time interval.

**phase-locked loop signal processing** — is a signal detection technique that uses the output from a product detector to slave (lock) a variable frequency oscillator (VFO) (serving as the reference for the product detector) in a feedback control loop to the highest amplitude frequency component in the received signal of interest. The frequency of the VFO is then a duplicate of the frequency component of interest (Doppler shifted frequency) and the VFO then provides a noise-free duplicate of this signal. This technique has been largely supplanted by the digital signal technology.

**range gating** — is a technique for distance discrimination by the capturing of scattered signals, at times corresponding to the round-trip period from the transceiver to the measurement volume on the transmitted beam axis. This technique restricts the signal reception to only the scattering originating in the region of interest. Pulse length limits the distance resolution possible from this technique.

**Rayleigh scattering** — is optical scattering from molecules or aerosols having diameters generally more than an order of magnitude smaller than the optical wavelength. Unlike Mie scattering, Rayleigh scattering has a smooth angular variation and the amplitude is proportional to the 4th power ratio of scattering cross-section to optical wavelength for individual scatterers.

**reference-beam laser anemometer** — is an anemometer that applies interference between light scattered by aerosols and light from a reference beam, to derive the flow velocity in a laser-illuminated measurement volume. This reference beam has the light frequency of the laser illuminating the aerosols or a known offset frequency where the modification is known. The technique is commonly applied in a backscatter configuration that requires that the receiver and transmitter be collocated. The component of fluid motion measured by the reference-beam laser anemometer in the backscatter configuration is along the beam axis.

**scattering** — is the changing of the propagation of light as it encounters scattering objects in its path (aerosols or molecules). The distribution and strength of this re-direction is dependent upon the object size relative to the optical wavelength, the object shape, and the optical properties of the object. (See *3.4.1 Molecular scattering*, and *3.4.2 Aerosol scattering*.)

**seeding** — is the process of adding artificial optical scattering material (particles or aerosols) to a flow to assist in tracing the flow motion. Common examples of seeding particles are hollow Teflon spheres or olive oil droplets created from a special atomizer.

**sheet-pair laser anemometer** — a flow velocity measurement technique using the aerosol transit time between laser beams shaped into the form of light sheets. This approach is an extension of the two-spot anemometer concept, designed to measure one component of the flow velocity. Systems of this type have been fabricated using 3 sheet-pairs converging at a point to provide three-component flow velocity measurement.

**signal processing** — is the process of analyzing the optical and electrical signal from a flowmeter to determine the flow motion.

**signal-to-noise ratio** — is the ratio of signal power to noise power. This ratio limits the ability of a system to extract a reliable measurement. The lower the SNR, the more difficult the extraction process and the more averaging required to obtain a reliable signal estimate.

**size distribution** — is the distribution of aerosols sizes in a specific volume of the atmosphere. Rayleigh scattering governs the backscatter coefficient for aerosols substantially smaller than the probe optical wavelength. Mie scattering is the dominant effect when the aerosols are of the same general order of magnitude as the wavelength. Refraction, reflection, diffraction and interference play important roles for those aerosols much larger than the wavelength.

**spatial filtering** — is a special type of mask (pinhole) placed at the focus of a light beam. This mask has the property of limiting the depth of field of the viewing optics.

**stimulated emission** — is a process whereby a photon physically passes close to an excited atom inducing that atom to release a photon. This photon is the same wavelength as the stimulating photon, is emitted in the same direction, and has the same phase. This process leads to coherent light emission.

**two-spot laser anemometer** — is a flow velocity measurement technique using the aerosol transit time between laser beams shaped into highly focused spots as a means of determining the flow velocity vector along the axis parallel to a line connecting the spots. Flow direction is determined by rotating these spots about the midpoint until the autocorrelation function of the backscattered signals has reached a maximum. When this condition is achieved, the flow is deemed to be along the axis parallel to the line connecting the spots.

**This page has been deliberately left blank**

---

**Page intentionnellement blanche**

# Chapter 3 – BASIC PRINCIPLES

Material covered in this chapter is limited to only that necessary for describing underlying principles necessary for an engineering understanding of flight optical flow measurement. These principles are to assist in identifying the capabilities of the various techniques and associated tradeoffs between alternative methods of research. More complete theoretical treatment of these principles is covered in the references provided.

## 3.1 Introduction

All in-flight optical airflow velocity measurements use light scattering. Light is scattered on inhomogeneities in the optical refractive index of a medium from both air molecules and aerosols entrained in the air. The characteristics of molecular scattering and aerosol scattering are quite different and are reviewed in this chapter. Furthermore, some other physical topics are introduced when such topics are necessary for understanding the physics behind laser anemometry.

The basic principles of in-flight optical airflow velocity measurements are utilized differently for the various anemometry systems and a wide variety of anemometer types have been developed. The basic layout of an anemometer is (1) a light source, (2) optical elements, (3) a detector, and (4) signal processing electronics (although generally not considered a part of the anemometer, scattering media entrained in the flow field of interest are required for operation). As an introduction, components in this layout are discussed in the order noted above.

The following block diagram (figure 3-1) illustrates how the system components are interconnected in a variety of airborne flow-measurement systems. Most systems contain all of the components shown, however, all of the electronic connecting links may not be required for all systems.

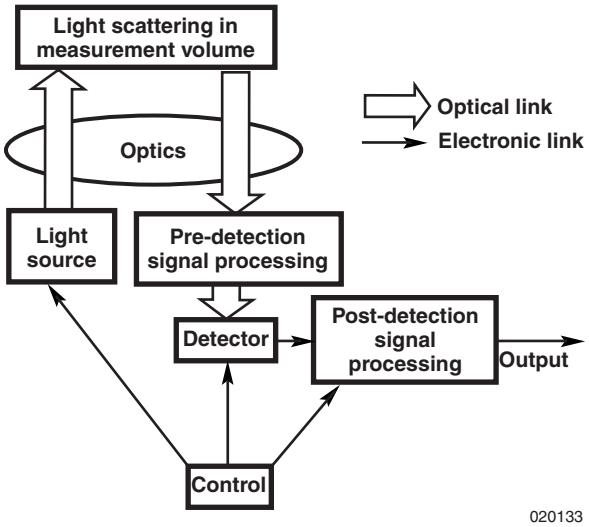


**Figure 3-1: Generic block diagram of an in-flight flow measurement system.**

## 3.2 Light Source

In many optical instruments the laser is introduced as the ideal light source for velocity measurements. Advantages of the laser compared with classical light sources are the coherence of light, the light beam shape, the high intensity of light produced, and the potential for very short pulses of light. In principle, classical light sources such as lamps can also be used for anemometry, but in practice the laser advantages prevail. Therefore, some words about the laser.

The laser (Light Amplification through Stimulated Emission of Radiation) is a light source in which a quantum effect of atoms (or molecules) is utilized. A large number of excited atoms is created in the optical cavity of a laser by optical excitation. For solid state lasers (i. e. ruby, NdYAG, sapphire, alexandrite) flash lamps or IR laser diodes provide the excitation. High-voltage is used to form a plasma excitation arc in gas lasers, such as HeNe, Argon-ion, Krypton, or $CO_2$. When excited atoms return to a lower energy state, a photon is produced. The emission of photons happens spontaneously at random moments and directions. A physical process called “stimulated emission” induces the return of excited atoms to a lower energy state, thereby producing a photon when a photon passes the exited atom. The photons created by stimulated emission are traveling in the same direction with the same wavelength, polarization, and phase as the photons stimulating the emission. All these factors together are what produce the so-called “coherence” and low angular dispersion associated with laser radiation. Low dispersion results from the optical cavity redirecting the light back through the laser medium along the optical axis. Spontaneous light emission will happen in all directions, as it is the process for light generation in a classical light source, such as a lamp or LED. Spontaneous light emission in a laser is not enhanced in directions away from the optical axis defined by the cavity mirrors, whereas the photons along the optical axis are redirected back and forth through the medium to stimulate more atoms to photon emission. This action produces the laser beam with its coherent light and low dispersion. The low angular dispersion of the beam allows for very narrow beams and very highly defined and localized regions of beam focus. The narrow light beams can be used for systems operating over long distances. Both the coherence and beam characteristics are very useful for optical velocimetry. Phase relations between photons generated in the stimulated emission process result in coherent light in which interference effects are much more pronounced than in light from classical light sources. Important factors of the light source include: wavelength, coherence, focusing ability, power, and pulse capability. (for further reading see Silfvast 1996,[3] Loudon 1983[4])

### 3.2.1 Continuous wave and pulse light sources

Continuous-wave (CW) light sources are the most straightforward and the obvious choice for many laser anemometer systems. This light source was available and was the first to be used in earlier systems; it is still commonly used in many applications today.

Pulsed light sources are often selected when power efficiency is a major consideration, or when the range must be determined using range gating techniques. Both of these issues become paramount with long-range systems, although pulsed (Q-switched) lasers may be used simply because that is the mode of operation for the available laser. The power relationships related to pulsed systems are discussed in the following section (3.2.2). With practical lens sizes for airborne applications, (~10 cm. diameter) at ranges beyond approximately 150 m, focusing is not effective as a range-discriminating technique. Therefore, range gating must be used to discriminate atmospheric velocity at long range. Narrow time windows of the scattered signal are sequentially processed to provide a range-discriminated velocity measurement along the axis of the laser beam. It should be noted that when measurements from a specific range are to be emphasized, focusing the beam optics at that same range will provide improved SNR.

### 3.2.2 Power effects

When long-range (1s to 10s of kilometers) operation is required, the signal-to-noise ratio (SNR) of the backscattered signal determines the effective range of the device. All other factors being equal, the SNR of the backscattered signal is proportional to the strength (power) of the received signal. To increase the efficiency

of operation, pulsing the laser is often used to increase the instantaneous transmitted power and thereby also the peak received power. The signal is acquired and processed during the short pulse duration when the SNR is higher than it would be if the energy were radiated on a continuous basis. Low-duty cycle pulses can improve the effectiveness of the radiated power; however, ever shorter and shorter pulses limit the velocity resolution attainable with a single pulse.

As the distance of operation increases, most systems revert to collimated beams, and the received power varies as the inverse square of the distance to the scattering source. Thus, to double the range of a system under the same atmospheric conditions with the same SNR, on average it requires four times the transmitted power.

When increased power levels (or high-pulse energy levels) are used, the risk of eye damage is increased. Eye safety is regulated in national standards (Ref. ANSI Z136.1 2000).[2] Some pulsed laser power limits are higher than CW power limits, which may be another reason for choosing a pulsed system.

## 3.3 Measurement Volume Discrimination

All optical velocimeters are required to obtain flow velocity from a known and well-defined region of the flow field, called the measurement volume. Several techniques are used to delineate the measurement volume depending on spatial resolution and range requirements.

### 3.3.1 Masking

For very short ranges (up to approximately 20 meters), masking is a technique sometimes used to define the measurement volume. This technique projects the light into a region of the surrounding atmosphere (the “illuminated” volume). The field-of-view volume from which the receiver accepts inputs is a separate volume from the illuminated volume, but the two volumes have a common region where the volumes intersect (the intersection region). It is from this intersecting region that the scattered received signal reaches the detector, as shown in figure 3-2. Masking is a measurement volume discriminator technique used in bistatic reference-beam anemometer systems.

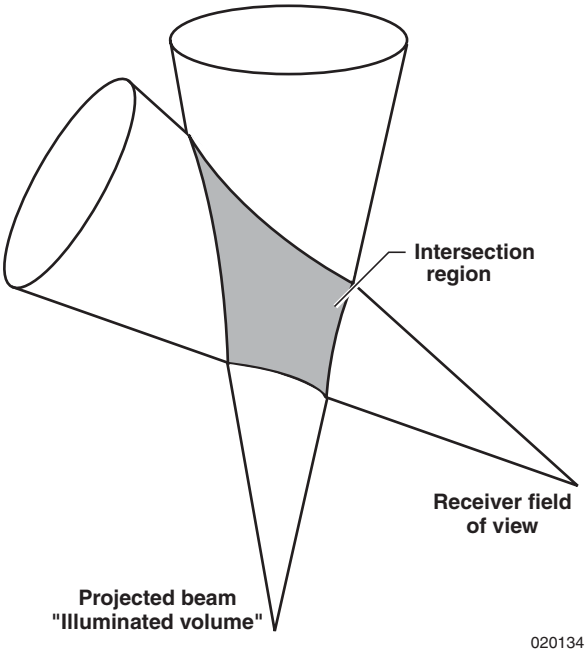


**Figure 3-2: Masking used to define measurement volume.**

### 3.3.2 Focusing

For short range applications (less than 150 meters) focusing is another technique used to define the measurement volume. By concentrating the optical energy in a small focal region, the vast majority of detected light is scattered from the aerosols within the measurement volume and propagates from this region back to the detector. Although not commonly applied, the optics used to concentrate scattered light on the detector can put an additional limit on the size of the measurement volume. Light is also scattered from aerosols located in regions of low energy density outside the focal region. When this light reaches the detector it adds small amounts of noise to the signal.

For focused systems, the measurement volume is delineated by the focal region of the light source, combined with phase effects of scattered light and reference-beam light for coherent systems (Vaughan and Forrester 1989).[5] The focal region is defined as the volume bounded by the surface where optical energy density has decreased to $1/e^2$ of the maximum intensity level encountered at the center of the volume. For a laser beam in the fundamental transverse mode the intensity profiles can be approximated as a Gaussian distribution. The focal region is an ellipsoid with the long axis coaxial with the axis of the focusing lens. The beam waist diameter $w_0$, for a light beam focused at distance r, with a lens or telescope with diameter D, is under ideal conditions:

Equation 3-1 $$w_0 = 4\lambda r / \pi D$$

and the measurement volume length $\Delta L$ is (Vaughan and Forrester 1989[5]) at 50 percent of maximum intensity:

Equation 3-2 $$\Delta L = 8\lambda r^2 / \pi D^2$$

Optical principles dictate that for a fixed lens diameter, the focal region increases as the distance to the focal point increases (Kogelnik -1966,[6] Silfvast - 1996,[3] Vaughan and Forrester 1989[5]). Note that ideal conditions are never encountered in practice. The focal region is larger when the laser is not in the fundamental transverse mode, when the Gaussian beam diameter does not match with the telescope diameter, and when the energy beam radiated is from a distributed light source (rather than from a point) or departs from a collimated condition. A larger lens diameter can be used to decrease the size of the focal region at a given range; however, flight applications usually limit the size of lens that is practical to use. In the case of very small focal volumes and low aerosol densities, the situation may arise where only one aerosol is illuminated. At first, this may appear to be an unfavorable situation, but when only one aerosol is illuminated, as opposed to an ensemble of aerosols, the SNR is improved, as no coherent cancellation is possible since no other scatterers are in the focal volume. Furthermore, the concentrated “burst” signal for single particles, instead of the more evenly distributed signal for multiple aerosols, allows other signal processing schemes to be used to achieve higher SNR (Harris - 2001)[7]. This single aerosol concept is practical only at short range because of the rapid signal strength fall-off with distance (as the inverse fourth-power of the distance from the radiating source). This single aerosol condition is closely related to that which exists in the dual-beam laser Doppler anemometer.

### 3.3.3 Range gating

As ranges increase beyond 150 meters where focusing is increasingly ineffective, range gating must be used to discriminate the measurement volume. A range-gated system transmits a short-duration light pulse (physical pulse length nominally from 3 to 500 meters) that scatters light back to the detector from aerosols as it moves through the flow field of interest. The detector is time-gated to capture the backscattered signal emanating only from a specific measurement region along the beam. This measurement region is defined as that cylindrical volume of space illuminated by the transmitted pulse during the time the detector gate is open. The cylindrical measurement volume diameter is the diameter of the collimated beam and the volume length is the sum of the transmitted pulse length plus the distance the pulse travels during the time that the detector

window is open. For example, a 300-nanosecond pulse (90 meters long) traveling 150 meters during the 500-nanosecond detector gate window defines a measurement volume 240 meters long. Because the light pulse is present during the gate window for a longer time in the middle of the measurement volume, the velocity of the middle aerosols is weighted more heavily than those on the ends of the measurement volume. Figure 3.3a illustrates the situation described above, where the gate length is longer than the pulse length. The graph below the pulse illustration shows the measurement weighting as a function of the pulse length. The length of the region in the center of the measurement volume (with constant 100 percent weighting) is defined by the excess of the gate length over the pulse length. A region with a high measurement weighting factor contributes more heavily to the Doppler velocity spectral average obtained during the gate time. This means that flow motion in the more heavily weighted regions of the measurement volume is emphasized in the spectral average. Figure 3-3b shows the condition where the gate length is shorter than the pulse length, and the graph illustrates the weighting for this configuration. The weighting distribution shown is the same as that for the prior situation where the pulse length is longer than the gate length.

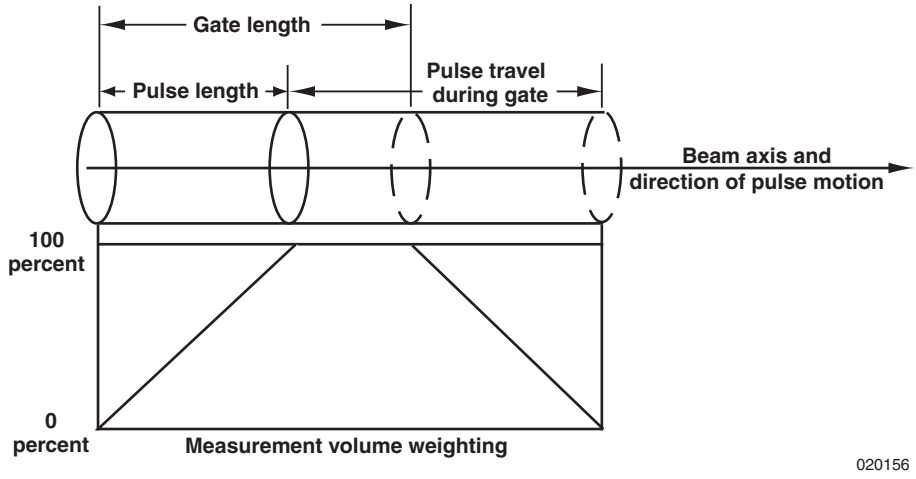


**(a) With pulse-to-gate length ratio more than 1.**

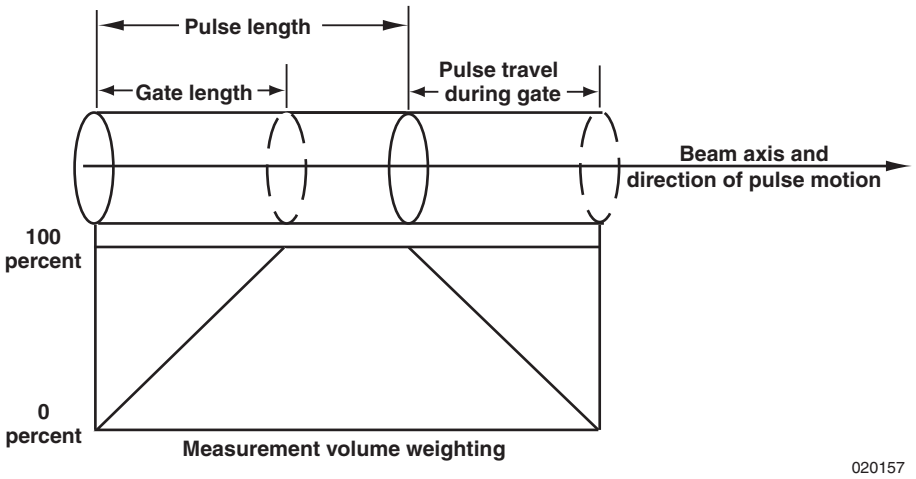


**(b) With pulse-to-gate length ratio less than 1.**

**Figure 3-3: Range-gated measurement volume.**

It is important to recognize the measurement effects of measurement volume for both size and weighting where range gating is used. For pulse systems using range gating, the measurement volume can be quite large (especially when long gating times or long pulse durations are used) and the resulting spectral measurement represents a weighted spatial average. In practical terms this means that for single pulse measurements using a nominal pulse length of 500 nanoseconds (150 meters long), measured atmospheric velocity conditions are a weighted average over what may be a large measurement volume. Furthermore, the weighting is not uniform and the velocity in the center of the measurement volume will be more heavily represented in the velocity average. Weighting of the measurement does not usually cause difficulty; however, using a short pulse relative to a long detector window length or a long pulse relative to a short detector window length can minimize any non-uniform weighting effects.

The volume weighting discussion and analysis presumes a uniform distribution of aerosols in the volume. Should aerosol density not be uniform within the measurement volume, the aerosol density distribution will overlay the above volume weighting functions. The always-present vertical atmospheric temperature gradient may create concentrated horizontal strata of aerosols as a result of condensation. Visible clouds are an obvious example of this effect and sub-visual cirrus ice-crystal clouds may also result from this process. Atmospheric temperature inversion may suppress normal vertical mixing activity to preserve horizontal aerosol stratification over extended periods of time and over large areas. Thus, non-uniform aerosol distributions may skew volume weights in range-gated measurement volumes. Stratification in vertical aerosol distribution is more prevalent and thus vertically oriented beam directions are more susceptible to the effects of non-uniform aerosol distribution

The averaging effects described above do not influence range-gated measurements obtained from an atmosphere without velocity gradients. For situations where turbulence exists and when the purpose of the measurement is to identify not only the presence of turbulence, but also the characteristic length(s) of turbulence structures, the measurement volume is an important factor.

## 3.4 Light Scattering

All optical flow measurements being applied in flight depend on light scattering, the basic theory of which is discussed in the following sections. The wavelength of the light has a dramatic effect on how the light is scattered. Although molecular and aerosol scattering is discussed separately, it should be remembered that the effects of the separate scattering sources are cumulative and the received signal is the total of the two. At the current time, most systems operate only through aerosol scattering. Some molecular-scattering-based systems use aerosol-based signals to enhance performance.

Light traveling through a medium with refractive index gradients is deviated (scattered) from the original direction in all directions. Both molecules and aerosols cause the light to be scattered, with molecules having only a small effect (per molecule) and aerosols having a relatively much larger effect (per aerosol). Partly compensating this imbalance between the relative scattering effects of molecules and aerosols is the fact that there is always a large supply of molecules in the atmosphere, but there may not always a be large supply of appropriate scattering aerosols. Atmospheric aerosol distribution is discussed in section 3.4.4 below.

### 3.4.1 Molecular scattering

Air molecules scatter light from an original direction in all directions. At visible wavelengths, the amount of light being scattered is low. Therefore the visibility in clear air is high. The scattering is much higher at UV wavelengths where electrons in molecules may be excited. At even shorter wavelengths in the X-ray bands, the energy is almost completely scattered (and absorbed) by atmospheric molecules. For this reason, X-ray astronomy must be conducted from satellites operating outside the atmosphere. Molecular scattering is even lower at the infrared wavelengths than in the visible range; however, the visibility in the atmosphere tends to be lower as a result of absorption of bands of energy from gaseous atmospheric constituents. This absorption is primarily from excitation of vibrations of water and carbon dioxide molecules. Taken together, these factors

cause the low levels of molecular scattering at infrared wavelengths with the resulting low SNR to be insufficient for effective flow measurements.

Scattered light from molecules includes the thermal molecular motion from a broad spectrum of Doppler-shifted photons in the detected signal. The air molecules are moving fast as a result of thermal motion. Air molecules have an average velocity of 459 m/s (about Mach 1.35) at 15 °C. This effect is superposed on the gas motion measurements relative to th

e anemometer and makes extracting the flow motion measurement that uses conventional techniques a formidable challenge to the measurement engineer.

*3.4.1.1 Characteristics of molecular scattered light*

Since molecular scattering cross-sections are much smaller than aerosol scattering cross-sections at the wavelengths commonly used in anemometers, Rayleigh scattering theory is used to predict molecular light-scattering behavior. Rayleigh scattered light extends in all directions. The scattered light intensity I from a light beam with intensity $I_0$ in a direction that has an angle θ with the initial propagation direction is

Equation 3-3 $$I = (1 + \cos^2\theta)|\bar{k}|^4|\bar{\alpha}|^2 I_0 / 2r^2$$

Where $\bar{k}$ is the wave number of the light, $\bar{\alpha}$ the polarizability, r the distance from the scattering where the intensity is measured. The Rayleigh scattering is dependent on the polarization of light and the detection angle. In this formula, polarization effects are neglected (“unpolarized light”). For more details refer to van de Hulst 1981[8]. This type of scattering has been termed “billiard ball” scattering because it behaves as if light photons are elastically bounced or deflected as they encounter individual molecules. No phase shift is created by the elastic collision. In the relatively dense atmospheric concentration of molecules, the variability of scattered light presents a smooth angular characteristic.

Molecules also scatter light inelastically. This means that the frequency of the photon is changed because of vibration excitation in the molecule or excitation of electrons during the scattering process (Raman scattering, fluorescence, etc.). In principle, airflow parameters can be derived from these processes. For example, the temperature and pressure of air can be derived from laser-induced fluorescence (LIF), (Mendoza 1998[9]). Proof-of-concept testing using oxygen fluorescence from flash-lamp excitation was conducted on an F-16 aircraft to measure temperature and density (Azzazy, 1990[10]).

As noted above, the thermal motion of molecules causes a major broadening of the scattered signal frequency. While this increases the difficulty of extracting a Doppler frequency from the bulk flow-field motion, it does offer the opportunity of obtaining the ambient temperature of the air causing the scattered signal. The width of the broadening is a direct measure of the mean velocity, which is directly related to the internal energy and the ambient air temperature. The mean molecular velocity, and therefore the broadening of the scattered signal frequency is directly proportional to the square root of the absolute temperature (see figure 3-4). Measuring temperature in this manner avoids many of the difficulties associated with conventional ambient air temperature measurement. This concept offers the possibility of remotely measuring the ambient air temperature at a distance from the flight vehicle in the flow surrounding the flight vehicle.

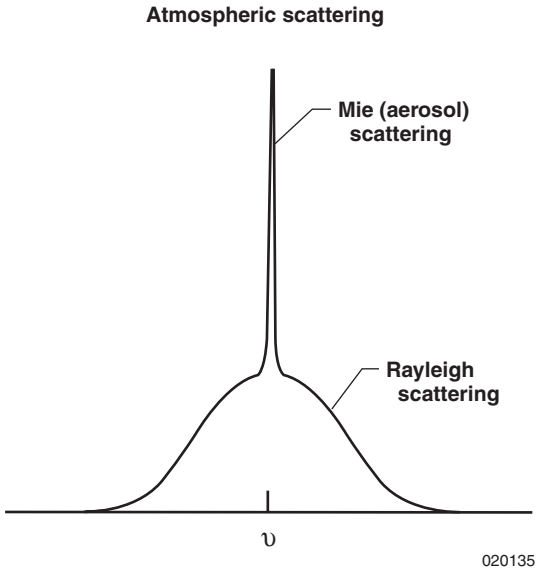


**Figure 3-4: UV atmospheric scattering with both molecular and aerosol scattering.**

*3.4.1.2 Molecular density variation in the atmosphere*

Unlike the highly variable atmospheric aerosol distribution, molecular density is well defined and highly predictable. The gaseous constituents of the atmosphere are uniformly distributed at all altitudes and the density of the atmosphere varies as an approximate logarithm of altitude. The density reaches half that of sea level at about 6000 meters and drops to 1/10 of the sea level value at about 17000 meters. The molecular scattering intensity is proportional to the density and a system based on molecular scattering must accommodate the scattering variation up to and including the design-operating altitude. This variation in the molecular scattering magnitude as the altitude changes offers the possibility of remotely obtaining the ambient air density at some distance from the flight vehicle. Combining the density with the temperature, as noted in the previous section through the universal gas law, provides the ambient pressure. Calibrations of the measured scattering intensity and spectral width are required to assure accurate ambient measurements of density and temperature respectively, however, these operations can be performed in a laboratory setting. A measurement obtained this way avoids the necessity for aircraft-specific calibrations and corrections that must be applied to measurements obtained with conventional sensors.

### 3.4.2 Aerosol scattering

Light scattering from aerosols is the basis of most flight optical anemometers. Lasers are used to illuminate the aerosols from a well-defined direction and wavelength. The amount of scattered light depends on the diameter, the shape, and the refractive index of the aerosol and the wavelength of light. Light scattering on aerosols is often categorized as a function of the quotient of the diameter of the aerosol and the wavelength of light. The characteristics of the light scattering are described below. A recommended textbook on this complicated matter is van de Hulst, 1981[8].

*3.4.2.1 Scattering from aerosols much smaller than the wavelength*

For aerosols much smaller than the wavelength of the light, the approximations of Rayleigh scattering applies (similar to molecular scattering). The intensity of light being scattered is proportional to the $4^{th}$ power of the ratio of the aerosol diameter over the wavelength. Equation 3-3 describes the scattering for these small aerosols also. The light is scattered in all directions with a smooth distribution. No phase shifts are introduced at the scattering of the light.

*3.4.2.2 Scattering from particles with sizes on the order of the wavelength*

The scattering of light is shape and refractive-index dependent for aerosols with sizes on the order of the wavelength of light. The exact relations for the scattering of light can be derived from Maxwell's equations for electromagnetic fields; however, this is impractical as the calculations are very complicated and time consuming and the shape and refractive indices are usually unknown. For spherical aerosols, Mie-calculated relations are computationally easier to use. In many investigations and design specifications the scattering aerosols are assumed to be spherical, which makes the Mie relations applicable. The assumption of spherical shape is realistic for liquids, which comprise a majority of the high-altitude aerosol population. Even for spherical aerosols the light scattering is not a simple expression where the scattered intensity, as a function of the scattering angle, shows large lobes. The phase of scattered light also depends strongly on the scattering angle and is related to the lobes. Examples of the intensity of scattered light as a function of aerosol radius and the angle are given in figure 3-5a and 3-5b (Mie 1908[11]). The multiple lines in the intensity graph (fig. 3-5a) show the effect of different aerosol indices of refraction.

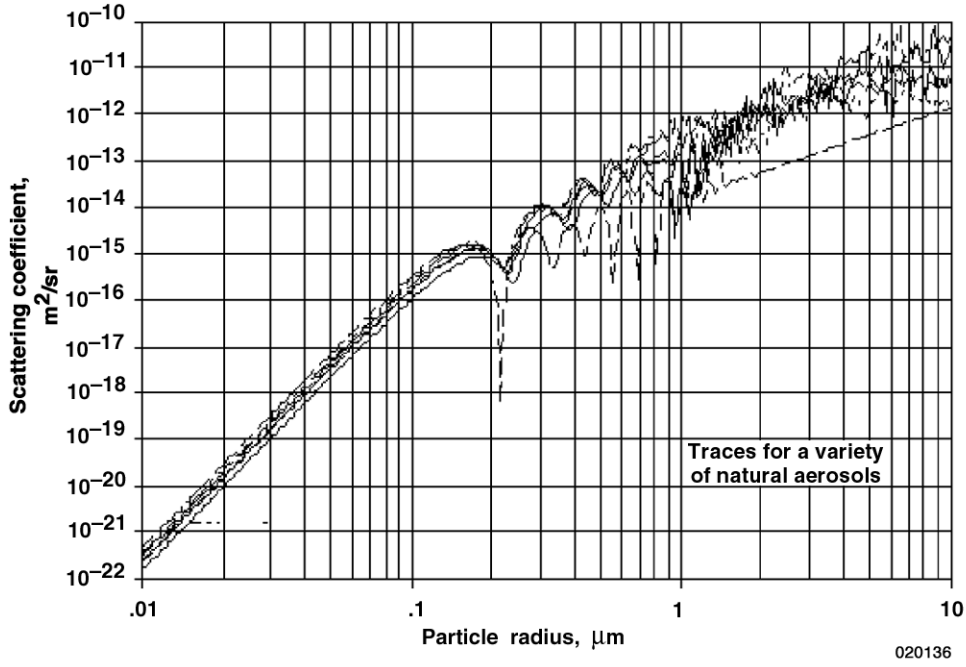


**(a) Characteristics for 0.81μm wavelength.**

**Figure 3-5: Mie scattering.**

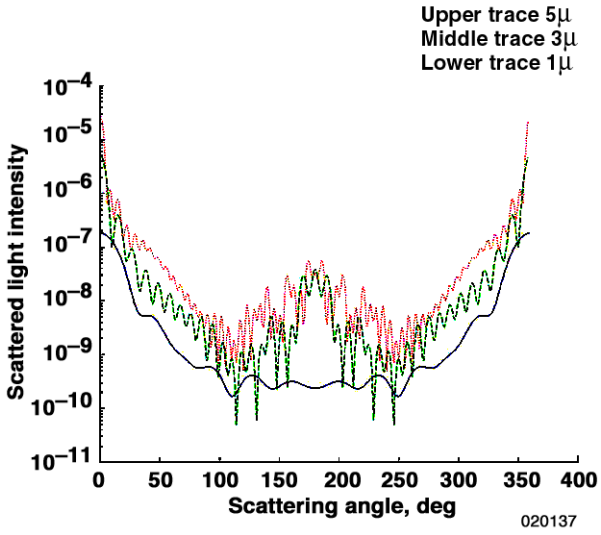


**(b) As a function of scattering angle.**

**Figure 3-5: Concluded.**

In figure 3-5b the upper line is for light scattering on a spherical droplet with a diameter of 5 μm. The middle trace and lower trace are for 3 μm and 1 μm respectively. All traces assume a refractive index of 1.33 representing water droplets in air.

#### *3.4.2.3 Scattering from aerosols with sizes larger than the wavelength*

For large aerosols optical effects such as refraction, reflection, diffraction and interference play important roles. Geometrical optics and interference, even if light is not monochromatic (think of the rainbow), determine the distribution of light over the different scattering angles. The properties of the aerosols, such as shape, refractive index, and refractive index gradients must be considered for exact calculations of light scattering. No straightforward general calculation method for scattering is available for this case. Mostly the scattering from aerosols with these sizes is not very relevant for optical flow measurement because there are very few aerosols with these sizes in the atmosphere. Moreover, as these aerosols are often too large to follow the flow adequately in situations with highly accelerated flow, most anemometers should not aim to measure the flow using these aerosols. Clouds and rain may even hamper optical airflow measurements as the optical access between the anemometer and the measurement volume is degraded.

### 3.4.3 Characteristics of scattered light from an ensemble of aerosols

Light scattered from an ensemble of aerosols is the sum of light-wave contributions of individual aerosols. In this situation, the phase of light waves and the associated interference plays a major role and must be taken into account. The scattered light intensity of an ensemble of aerosols may be small for some configurations of individual aerosols, whereas the intensity may be large for the same aerosols if positions are shifted even a small fraction of a wavelength. This phenomenon is also encountered if coherent (laser) light is scattered at diffusely scattering objects, where it is called the “speckle phenomenon” (Dainty 1975[12]). Taking all effects into account, the time-averaged (and therefore phase-averaged) light intensity of a moving ensemble of aerosols is larger than that of each single aerosol of the ensemble. Additional fluctuations of scattered light intensity are caused by the interference of the individual aerosol contributions.

### 3.4.4 Aerosol distribution in the atmosphere

Aerosol distribution in the atmosphere is one of the most highly variable factors facing the designer of anemometers. There are literally hundreds of atmospheric processes that create a myriad of aerosols of various compositions, sizes, and optical properties. Sources of these aerosols include; surface solid or liquid aerosols from high winds or volcanic activity, liquid or solid condensation from atmospheric physical processes, liquids or solids from atmospheric chemical reactions, and complex combinations of these three sources. Distributions of these aerosols have been measured, as have others, and reflected in terms of backscatter coefficients at a 10.6 micrometer wavelength (Vaughan and Brown 1995[13]) for various geographical regions of the world. The backscatter coefficients, and therefore also the atmospheric aerosol distribution, fluctuate considerably, not only as a function of the region but also as a function of time. Volcanic eruptions and the season play important roles in the amount of aerosols in the atmosphere. Other researchers determined the size distributions of aerosols in the atmosphere (Deirmendjian 1964[14]) that can be used for a theoretical analysis of aerosol velocimeter performance. Figure 3-6 illustrates the ranges of particle distributions and optical backscatter values associated with these situations. The numbers in parentheses indicate the relative magnitude of backscatter values at the selected altitudes in the atmosphere. It should however be noted that these "typical numbers" vary substantially under the influence of natural atmospheric processes. The references mentioned above present variations in aerosol distributions and are an example of several decades of backscatter coefficient measurements.

Backscatter values depend on the wavelength of light. In general the values are higher for shorter wavelengths. The choice of the wavelength for an anemometer is not a straightforward one, depending on the availability of lasers at different wavelengths and degrees of eye safety. Numerous studies have been published about this choice (Kane 1984[15], Targ 1996[16] and others).

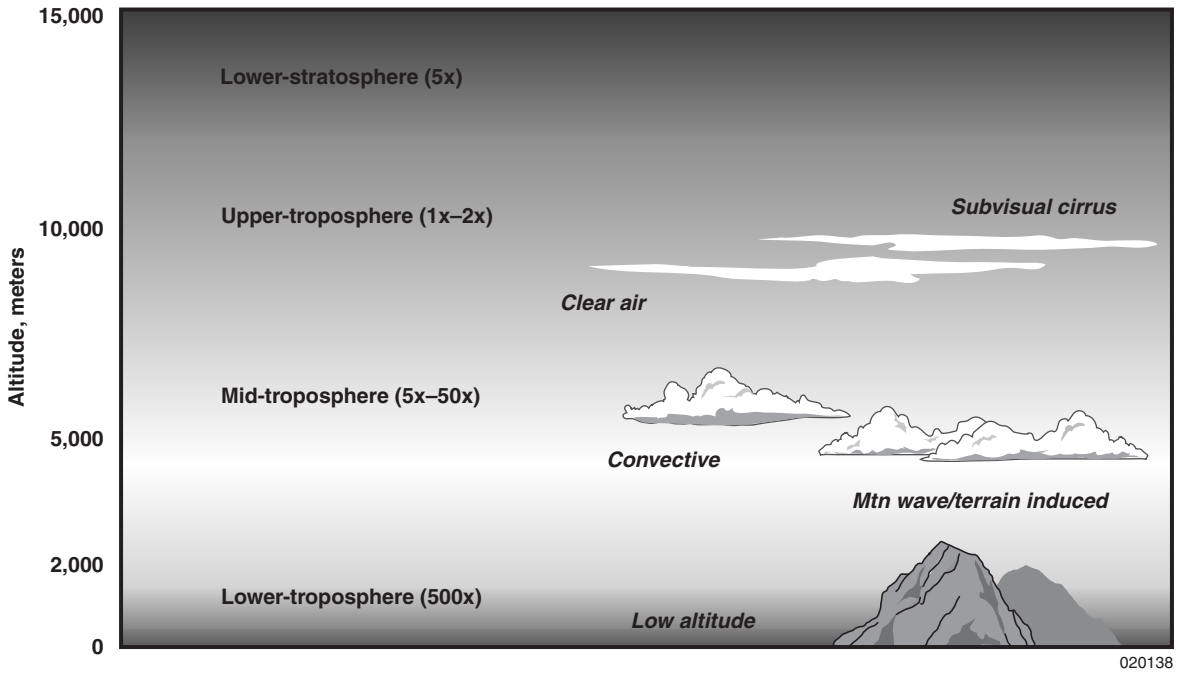


**Figure 3-6: Variation of backscatter values in the natural atmosphere.**

## 3.5 Detection

Information about the flow under investigation is encoded in the scattered light. A detector is used to convert relevant characteristics of scattered light into an electrical signal. In practice, the intensity of light (sometimes as a function of spatial position, sometimes not) is the relevant parameter to measure. Several types of detectors utilize the interaction between photons and different kinds of optically sensitive material. Detectors relevant for optical flow measurement produce electrons from impinging photons. The photons provide extra energy to the electrons as they are absorbed by the material. Different materials are used for detection and have optimized absorption characteristics, such that the maximum sensitivity for a specific wavelength of light is obtained. The optimum in sensitivity is reached if each photon impinging on the detector results in a signal. This ideal response of a detector leads to the ideal quantum efficiency ($\eta$) of 1. The quantum efficiency depicts the ratio of photons that result in a signal, which is dependent on the wavelength of the photon, and is an important parameter for the detector.

Detectors introduce several types of noise in signals. Signals are generated internally in the detector without any photons impinging to generate the signal. This is called the “dark-current”. Thermal excitation of electrons is one of the major reasons for this anomaly. As the effect is largest for detecting photons with low energy infrared (IR), many detectors used for these photons are cooled to low temperatures. The quantum character of light results in a random pulsed-noise character of the signal, the so-called shot noise. Even ideal detectors experience this noise. Therefore, it is important in system design to assure that detectors are not exposed to conditions that degrade their performance under either operating or nonoperating conditions.

Frequency response is a very important characteristic of a detector. The bandwidth should be sufficient for detecting the signal. Noise levels, however, increase typically with the square root of the bandwidth, so for this reason the detection bandwidth should be as small as possible consistent with detection requirements.

Video cameras are used as detectors in systems when it is necessary to acquire scattered light measurements in a plane. The fact that video cameras require array detectors limits the choice of detector materials to those available in a suitable array configuration. The same detector considerations noted above apply to the video configuration.

## 3.6 Signal Processing

Signal processing may be performed either prior to detection (pre-detection) where the signal is in optical form or after detection (post-detection) where the signal of interest is in electrical form. For simplicity, both pre-detection and post-detection signal processing are discussed in this section. Examples of signal processing include the five items listed below.

1. Optical wavelength filtering to remove extraneous noise signals, for example background light (pre-detection)
2. Heterodyne signal mixing to generate a difference signal with reduced noise level (pre-detection or post-detection)
3. Electronic fast Fourier transform processing or autocorrelation of electrical signals to extract the Doppler frequency shift (post-detection)
4. Direct processing using either a high-finesse etalon or a molecular filter (pre-detection)
5. Time-of-flight processing (post-detection)

Signal processing is a collection of operations performed on the signal at some point as it transits through the optical and electronic environments of the flight measurement system. The primary objectives of these operations are

1. To improve the signal-to-noise ratio (SNR) of the signal
2. To extract desired information contained in the signal

These primary objectives are both present in most signal processing operations, and it is not useful to categorize specific signal processing operations under one or the other of the above objectives.

Traditionally the term “signal conditioning” has been applied to processes that improve the SNR. However, with the advent of digital signal processing, the dividing line between improving SNR and extracting the desired information has been blurred. Many of the digital signal processes improve the effective SNR through digital time-averaging and other processes like time domain-to-frequency domain conversion. Signal conditioning, therefore, has been merged into the discussion of signal processing for this volume.

Light scattered from regions of low aerosol density is quite often very weak, particularly when scattered from particles located far away from the light source. Effective signal processing of weak signals is a critical factor in the performance of optical flow measurement systems. In this section a few basic processing techniques are presented as these techniques are applied in several anemometer configurations. The processing techniques specific for a single configuration are discussed together with configuration in chapter 4.

### 3.6.1 Coherent processing

Coherent processing is a powerful technique to increase the SNR of frequency-shifted Doppler signals. In the basic coherent processing approach, the received Doppler signal is first optically mixed (homodyned) with a small amount of the single-frequency transmitted signal immediately prior to signal detection. In most cases, the mixing occurs on the surface of the detector. The interference of these coherent optical signals creates an optical carrier signal modulated by the Doppler difference frequency component on the detector surface. Although strictly not part of the coherent processing, the detector responds to this mixed signal by generating a derived Doppler frequency shift as an electronic signal for further analysis and processing according to the requirements of the particular system. The amplitude of the detector output is proportional to the strength of the received signal and the frequency is the Doppler frequency shift.

This coherent processing technique is generally applied to atmospheric flight Doppler anemometers. SNR is a critically important system performance parameter, and yet it is difficult to accurately specify explicitly in an equation. The SNR of a heterodyne coaxial system is affected by several factors, and the system designer must be well acquainted with the important factors affecting SNR to achieve an optimal balance and provide the best performance. Theoretically it can’t be better than as follows (Sonnenschein 1971[17], Kane 1984[15], Keeler 1987[18], Vaughan and Callan 1989[19]).

Equation 3-4 $$SNR = [\{\eta P_T \beta_\pi \lambda\} / 2Bh\nu] F(D, L, \lambda, f)$$

Where F denotes a factor that is a function of the parameters in brackets.

$\eta$ = detector quantum efficiency

$P_T$ = transmitted power

$\beta_\pi$ = atmospheric backscatter coefficient

$\lambda$ = wavelength of light

B = System bandwidth

$h$ = Planck’s constant

ν = frequency of light

F( ) = function of...

D = diameter of collecting optic

L = range

*f* = focal distance of collecting optic

The configuration of the system determines the value of the variable F. As shown in the equation, collecting optic characteristics, wavelength, and range are each an influence on the magnitude of F. Unstated in the equation, but also influencing the magnitude of F, are the operating mode (pulse or CW) and the focused or unfocused state of the system. Unfortunately, all of the "component imperfections" conspire to reduce the SNR and there are no real tradeoffs that could be used to reach an optimum balance between competing factors. The strategy must be to make each factor as good as possible to get the best SNR. A few of the "component imperfections" include: detector noise, non-ideal signal processing algorithms, laser wave front distortions, and laser q-switch turn-on and turn-off characteristics. Among other factors affecting the SNR, and not explicitly identified in the equation, are the coherence length characteristics and wave-front characteristics described below

Optical alignment plays a critical role in coherent processing. It is important that the wave fronts of the signals mixed on the detector surface are parallel, to assure that the alternate destructive and constructive interference is realized simultaneously at all points on the sensitive detector area. Misalignment of optical elements that degrade the parallel wave front of the mixing signals can seriously reduce the sensitivity of the coherent detector, the primary reason for using this concept.

For long-range measurements, the coherence length of the laser source should be comparable to the range from which the measurement is obtained. If the coherence length is insufficient, an optically-delayed reference signal (from a long optical fiber for example) may be used in the coherent mixing process. The fiber length is determined by the required "range gate" delay for desired measurement range.

### 3.6.2 Direct processing of Doppler shifts

To extract the Doppler shift frequency, the direct processing approach requires a mechanism to convert the optical Doppler frequency shift to an amplitude shift prior to detection. This concept is used in frequency modulation (FM) radio applications and the translation of frequency shift to amplitude change is accomplished by a special filter device called a "discriminator". In optical applications, a filter device is used which has a region where the relationship between frequency and amplitude is single-valued and preferably linear. Typically, a high-finesse etalon or a molecular cell filter is used for this purpose.

Direct processing requires a very sharp frequency-amplitude characteristic to discriminate the relatively small Doppler frequency shift. The frequency of the light in a typical anemometer is approximately $10^{15}$ Hz. The Doppler frequency shift is approximately $5 \times 10^6$ Hz per m/s aerosol velocity. For velocity ranges from 50 to 300 m/s, the Doppler shift ranges from $250 \times 10^6$ to $1500 \times 10^6$ Hz. Thus, the frequency shift is approximately $10^9$ Hz at an absolute frequency of $10^{15}$ Hz or 1 part in $10^6$. This very small frequency shift requires high stability of both the frequency-amplitude filter characteristic and the illuminating laser frequency. High-resolution spectrometers have been developed and could well provide in-flight direct signal processing in the near future.

Except for the coherence-related factors, the signal-to-noise ratio of a direct processing approach is affected by many of the same factors as the coherent processing approach. No explicit closed-form equation is known to exist that describes the relationship between the overall SNR and the system and environmental factors.

### 3.6.3 Pulsed operation signal processing

Pulsed systems provide short excitation pulses (from tens of nanoseconds to a few milliseconds duration). Pulsed operation may be used to discriminate the measurement volume (see the Measurement Volume discrimination section earlier in this chapter) or to improve the signal-to-noise ratio. The reason for using pulsed operation does not influence the necessity to synchronize the signal processing with the pulse timing. In the case of short ranges the delay between pulse transmission and reception of the scattered signal is usually too short to make range gating a practical consideration. If this short-range situation is the case, the processing is initiated when the pulse begins. When range gating is used to discriminate the measurement volume, the signal processing is gated several times for each pulse to acquire information from selected regions along the length of the beam as the pulse reaches and scatters light from each successive region. Except for the synchronization of signal processing with pulse timing, the signal processing concepts discussed immediately above operate the same with CW signals as with pulsed signals.

### 3.6.4 Reduction of effects of sun light

As has already been noted, operating in the natural atmosphere requires that optical system design be compatible with the natural aerosol environment to provide the scattering necessary for velocity measurement. Another factor of the natural atmosphere is the presence of the sun (unless night flight is an option for the program), an uncontrolled source of light with the potential to substantially degrade optical system performance. The major hazard to avoid is the entrance of background light into the optical aperture. At a minimum, this direct or reflected background light has the potential to degrade system SNR and under worst-case conditions may saturate, or even destroy the detector and render the system inoperable. Good construction practices will exclude light from sources not on the system optical axis. However, natural background light from the clear sky, from clouds, or reflected from the ground may also enter the system. Signal processing can sometimes be used to suppress the effects of extraneous light to improve the SNR.

Both optical and spatial filtering are effective techniques for reducing extraneous light. Spatial filtering or masking is already mentioned in section 3.3. Most flow measurement systems use single frequency lasers as light sources. Therefore the most direct approach is to utilize an optical band-pass filter that excludes all light except that in the vicinity of the operating frequency.

### 3.6.5 Signal processing and detection challenges

In a flight environment, one of the more important issues is controlling extraneous noise sources. As contrasted with a wind-tunnel setting, the flight environment affords almost no control over measurement conditions. Ambient light from the sun must be suppressed for some situations. Background light can cause major difficulties as well.

In most situations, the primary issue in the detection process is achieving the highest possible signal-to-noise ratio (SNR). This situation is occasioned by the need to use backscattered light since forward scatter systems are usually not practical in flight. An additional situation in flight is often the desire to acquire long-range measurements. Light scattered from a long-range is usually weak and sensitive detectors with low internal noise levels, coupled with signal processing for improving the SNR, are usually required to obtain a reliable flow signal.

## 3.7 Summary

This chapter has addressed the most important concepts involved in optical flow measurement in flight. This discussion has been limited to only the most salient features of these concepts. For a more detailed description of any particular concept please refer to the list of sources in the References and Bibliography sections.

**This page has been deliberately left blank**

---

**Page intentionnellement blanche**

# Chapter 4 – SYSTEM COMPONENTS

## 4.1 Introduction

This chapter discusses the key system components required to implement flight-based optical measurement systems. Chapter 5 will discuss designs for a variety of optical measurement systems. Descriptions of these system components with salient performance requirements are reviewed in this chapter to provide a basic understanding of what is required to assemble an optical measurement system. Examples from textbooks giving more detailed information on system components are: Bass 1995[20], Silfvast 1996[3] or (theoretically) Born 1970[21].

## 4.2 Optical Components

A full systems approach is required to produce the optimal system for performing optical airflow measurement in flight. The challenge in developing an effective system arises in part from the fact that the support from many disciplines is required to arrive at a system that is a useful measurement tool for research purposes. A second factor to be considered is the need to clearly focus on the intended application in the design of the measurement system. In-flight flow measurement systems are highly dependent on accommodating the flight environment, and in some cases, the ability to design and construct compact and flexible systems is a key requirement in being able to perform the desired measurements. For the optical measurement of airflows, it is not possible to design a single system that will address all of the requirements of even a few applications. For long-range systems, signal-to-noise considerations assume a primary role, which leads to considerations of laser output power, transmitting and receiving optics, detector sensitivity, and signal processing. For short-range systems, such as those required for air data measurement and local flow measurement, high data rates are needed to understand rapid changes in the flow situation as well as relatively high spatial resolution. Requirements must be thoroughly understood and a balance reached in each aspect of the design.

### 4.2.1 Laser

As already mentioned in chapter 3 the laser is the best light source for optical airflow measurement in flight because of the ideal light beam characteristics. The requirements on the laser for the in-flight application significantly affect both the effectiveness and practicality of airborne laser systems. The size of the laser system, the electrical power consumption and the associated efficiency of converting electrical power into light power, the requirements on cooling air or water, and the capability to operate in a vibrating environment are, in general, more important than in ground applications. It should be noted that improving the light-conversion efficiency returns dividends not only by reducing the power required for this function but also by producing less heat, thereby lowering cooling requirements, resulting in potentially smaller size and further electrical power reductions. In most of the early in-flight systems the carbon-dioxide laser was applied. Nowadays several laser systems are applied, each with an emphasis on factors that are advantageous for flight applications as follows:

- the carbon dioxide laser is robust and proven technology

- the diode laser and the diode laser pumped solid-state lasers are small and convert electrical power efficiently into light power.

- the Nd:YAG and Ho:YAG efficiently generate pulsed high-power light, where Ho:YAG emits light with an “eye-safe” wavelength (see section 1.1.2.3)

There are many types of lasers available (see table 4-1 and Hecht 1996[22], Yu 1997[23]), of which virtually none are excluded for in-flight applications provided the system design can accommodate the size, weight, power, and environmental limitations.

**Table 4-1: Compilation of laser materials.**

| Active medium | Type and operating mode | Wavelength, nm |
|---|---|---|
| Argon Fluoride (ArF) | Excimer, pulsed | 193 |
| Krypton Fluoride (KrF) | Excimer, pulsed | 249 |
| Xenon Chloride (XeCl) | Excimer, pulsed | 308 |
| Helium Cadmium (HeCd) | Gas, CW | 325, 442 |
| Nitrogen (N) | Gas, pulsed | 337 |
| Argon ion (Ar) | Gas, CW | 350, 488, 514.5 |
| Krypton ion (Kr) | Gas, CW | 350, 647 |
| Xenon Fluoride (XeFl) | Excimer, pulsed | 351 |
| Copper vapor (Cu) | Gas, pulsed | 510, 578 |
| Helium Neon (HeNe) | Gas, CW | 543, 632.8 |
| Gold vapor (Au) | Gas, pulsed | 628 |
| Xenon ion (Xe) | Gas, pulsed | 540 |
| Indium Galium Arsenic Phosphide (InGaAsP) | Semiconductor, pulsed or CW | 600-1600 |
| Titanium sapphire ($TiAl_2O_3$) | Solid state, pulsed | 660-1200 |
| Ruby | Solid state, pulsed | 694 |
| Alexandrite * 1 ($Be(Al_{1-x}Cr_x)_2O_4$) | Solid state, pulsed | 700-800 |
| Galium Aluminum Arsenide (GaAlAs) | Semiconductor, pulsed or CW | 720-900 |
| Iodine (I) | Gas, pulsed | 1300 |
| Neodymium (Nd:YAG) * 2 | Solid state, pulsed | 1064, 532, 266 |
| Indium Phosphate (InP), often in conjunction with rare-earth metal doped fiber amplifiers | Semiconductor, pulsed or CW | 1300-1600 |
| Holmium (Ho:YAG) * 3 | Solid state, pulsed | 2127, 2850, 2920 |
| Hydrogen Fluoride (HF) | Gas, pulsed or CW | 2600-3000 |
| Erbium (Er:YAG) | Solid state, pulsed | 2940 |
| Deuterium Fluoride ($H^2F$) | Gas, pulsed or CW | 3600-4000 |
| Carbon Monoxide (CO) | Gas, pulsed or CW | 5000-7000 |
| Carbon Dioxide ($CO_2$) | Gas, pulsed or CW | 9000-11000 |
| Lead Tin Telluride (PbSnTe) and other lead salts | Semiconductor, pulsed or CW | 2000-30000 |

notes:

1 - Alexandrite, chemical formula

2 - Nd:YAG, chemical formula Nd:$Y_3Al_5O_{12}$, where 532 and 266 nm light is emitted through applying frequency doubling in a non-linear crystal

3 - Ho:YAG, chemical formula Ho:$Y_3Al_5O_{12}$, also other metals (rare-earth metals) are applied like Chromium (Cr), Thulium (Tm), and Erbium (Er) emitting light with wavelengths between 2000 and 3000 nm.

- The active media of semiconductor lasers contains many different atoms (Silvast - 1996). Rare earth doped fibers or solid state laser rods are sometimes used to boost laser power.

- Lasers emitting wavelengths higher than 1400 nm are often termed “eye-safe”. This is an oversimplification of reality (see 1.1.2.3). The danger for eye damage is less at these wavelengths for a given power level, but there are still dangers in exposing eyes and other parts of the body to powers high enough to damage tissue (ANSI Z136.1 2000)

### 4.2.2 Detector

Detectors are used for the conversion from photons to electrical signals. The most important requirements on detectors are; (1) high response to light, (2) low noise levels, and (3) sufficient bandwidth to accommodate the light intensity variations. In table 4-2 some characteristics of commonly applied detectors are provided. Both the photo-multiplier tube (PMT) and the semiconductor detectors generally are available with sufficiently high bandwidths for most in-flight applications. For Doppler applications with coherent detection, the combination of large velocity measurements and a short operating wavelength requires the largest detector bandwidth. The choice of detector is mostly governed by the light wavelength sensitivity, which is different for different materials. Modern detectors have nearly ideal photon detection response, leading to the best possible signal-to-noise ratio. In general, far infrared detectors need to be cooled to reduce the noise caused by the thermal excitation of electrons.

**Table 4-2: Compilation of light detectors.**

| Material | Type | Typical wavelength range, (nm) |
|---|---|---|
| Vacuum tube with metal elements | Photo-Multiplier Tube (PMT) | 110–1100 |
| Gallium Arsenide (GaAs) | Semiconductor | 400–900 |
| Germanium (Ge) | Semiconductor | 500–1800 |
| Indium Gallium Arsenide (InGaAs) | Semiconductor | 900–1700 |
| Indium Antimonide (InSn) | Semiconductor | 1000–5500 |
| Lead Selenide (PbSe) | Semiconductor | 1000–7000 |
| Mercury Cadmium Telluride (HgCdTe) | Semiconductor | 2000–20000 |

### 4.2.3 Lenses

To receive the maximum optical power for the detector the most important requirement for lenses and focusing systems is to use a lens with as large a diameter as possible. Furthermore, the optics should have efficient optical transmission at the wavelength applied. For UV and far IR wavelengths, materials like quartz (for UV) and zinc selenide or germanium (for IR) have to be used for lenses and windows. Using high-quality optical components, high-performing focusing systems may be built with techniques similar to those used for building conventional optical telescopes. Infrared materials may require coatings to protect lens surfaces from scratching.

### 4.2.4 Windows

Optical windows are necessary to give optical access to the atmosphere. Obviously the windows should be transparent, which leads to material requirements as mentioned in the section above. Additionally, measures are usually required to prevent condensation of water on the window. Temperature differences over the window makes condensation of water likely from cabin air contact with the inside surface. Ice or a thin layer of water can accrete on the outside surface under certain meteorological conditions. The water or ice will degrade the optical properties of the window and often strongly attenuate optical transmissions. Measures taken to prevent condensation are typically the creation of a dry air or nitrogen atmosphere on the warmer side of the window. Ice removal may require heating the window and may require substantial heater power to maintain an unobscured view. If ice accretion is even a remote possibility, a means to detect window ice formation, such as a video camera is a wise investment. This capability can resolve mysterious in-flight performance anomalies.

### 4.2.5 Filters

Very narrow-band filters are required to perform the direct detection operation. Etalons have been used for this purpose; however, maintaining dimensional stability under conditions of variable temperature can present substantial problems. Achieving a high finesse at short wavelengths (less than 0.3 micrometers) is difficult. Molecular vapor cells can provide a more stable frequency characteristic; however, tight temperature control or other measures are often needed to stabilize the attenuation characteristic under varying environmental conditions.

Band-pass filters are sometimes applied to reduce the influence of daylight. Daylight may contribute significantly to noise, as the intensity of detected light is typically small compared to daylight levels. The reduction of daylight noise with band-pass filters is typically only part of the solution.

Polarization filters, quarter-wavelength plates, and half-wavelength plates are often applied to differentiate between transmitted and reflected light and scattered light.

### 4.2.6 Optical frequency shifter

Bragg cells are often used to shift the optical frequency input to a coherent detector. This is necessary when the raw Doppler frequency shift is higher than the band-pass of the signal detector. The transmission frequency is offset to a value closer to the Doppler-shifted return signal so that the difference frequency that appears on the detector is within the detector band-pass. Of course, the Doppler-shift output frequency from the detector is adjusted upward (often accomplished computationally) by the offset value to compensate for the Bragg shift.

## 4.3 Mechanical Construction

Robustness is very important, and by clever design, the requirements can be achieved using structures that maintain dimensions within the order of a wavelength while in operation. The task of making systems for flight applications is simplified when the size can be as small as possible and the stiffness as high as possible.

Conventional materials (like aluminum) usually require precise temperature control to maintain dimensions within the required tolerance. Thermal control for these systems adds considerable weight to the overall system. Recently developed components (for example, carbon-fiber optical benches) offer very high stiffness and light weight combined with very low thermal expansion such that precise temperature control is not necessary

## 4.4 Signal Processors

System requirements determine the signal processor selection. Where it is necessary to operate in conditions of low signal-to-noise ratio, coherent detection is usually selected to give the best performance in a low-density aerosol environment. Coherent detection is used when an averaged measurement is required from a single measurement volume in a reference-beam system. Direct detection is another option, and is the technique of choice for some systems, e. g. when a multi-point measurement is obtained such as in Doppler Global Velocimetry systems or available space cannot accommodate a coherent detection system. Regardless of the mode of detection (coherent or direct), signal processing is done partly in the optical domain (pre-detection) and partly in the electronic domain (post-detection). These concepts are described in sections 3.4 and 3.5.

### 4.4.1 Coherent detection signal processors

The optical portion of the coherent signal processor is integrated into the laser transceiver. A small portion of light from the transmitter is routed to, and mixed with, the received signal on the surface of the detector. This may be accomplished by mirrors and beam splitters, fiber optics, or combinations thereof. The output from the detector is more useful when it is presented in the frequency domain and most systems provide the means for frequency conversion as a part of the system design. Custom-designed fast Fourier transform signal processors utilize digital signal processor (DSP) technology to accomplish these transformations. For pulsed systems, the computation must be synchronized with the pulse start. Figure 4-1 shows a real-time flight qualified digital signal processor. Figure 4-2 shows a block diagram of a typical signal processor.


**Figure 4-1: Flight-qualified real-time advanced signal processor (RASP) and display.**

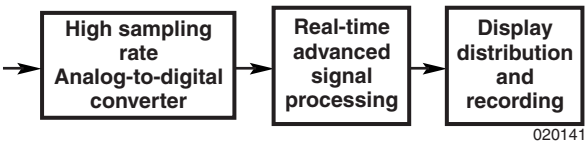


**Figure 4-2. Digital signal processing block diagram.**

### 4.4.2 Burst frequency signal processors

Burst frequency signal processors are commercially available and may be used in flight applications with appropriate packaging and power conversion support. These processors are used to analyze data from dual-beam laser Doppler anemometers (also known as LDA in wind tunnel applications). The output from the burst frequency signal processor is a digital readout of the fundamental burst frequency from the LDA installation.

# Chapter 5 – LASER ANEMOMETER CONFIGURATIONS

## 5.1 Introduction

A large number of laser anemometers have been developed and many of those have been used in-flight. In this chapter different configurations of anemometers are presented and the working principles are explained. Many applications of laser anemometers require far field measurement of flow, as described in chapter 6. The capability of measuring far field flow is, at the current state of development, limited to the reference-beam anemometer. Therefore the reference-beam anemometer will be discussed in more depth than other types of anemometers, within the framework of this document.

Two velocimetry methods are identified in the description of the configuration of laser anemometers.

- Doppler techniques measure the frequency of scattered light. Light is scattered from a moving particle thereby altering the frequency. This altered frequency of light can be determined directly with frequency-dependent optical processing using a spectrometer or an optical filter. The common approach for detection is converting light frequency changes into light intensity fluctuations using interference of light.

- Transit time techniques, measure the time it takes for a particle to move from one intense light area to another intense light area. The velocity of the particle can be derived from the distance between the locations where the light was scattered and the time interval between scatterings.

These techniques seem totally different. However, Doppler techniques can be viewed as projecting an intensity-modulated pattern in space, which can be interpreted as a transit anemometer. This interpretation is widely used for the dual-beam laser Doppler technique. The merits and limitations of this view are addressed in this chapter. The basic difference between the transit anemometer and Doppler anemometer is that light frequency-shifts and interference are essential for the Doppler technique, whereas in the transit anemometer these effects contribute to noise only.

The various types of laser anemometer configurations together with typical system characteristics and performance capabilities are summarized in Table 5-1. There is no common approach for naming optical system configurations. Some systems are described based on the optical configuration, others use the type of signal processing as a basis for the configuration nomenclature.

Table 5-1: Anemometer configurations.

| Type | Configuration | Detection | Signal Processing | Range | Comment |
|---|---|---|---|---|---|
| Doppler | reference-beam anemometry | coherent | DSP or burst frequency processor | near field, free stream, and far field | most widely applied in-flight concept |
| | spectrometry | direct | optical filter in combination with image processing | far field | also potential for near field applications, never implemented in flight |
| | dual-beam laser Doppler anemometry | coherent | burst frequency analyzer, correlator | near field | also called LDV and LDA |
| | Doppler global velocimetry | direct | optical filter in combination with image processing | near field | never implemented in flight |
| transit | two-spot anemometry | direct | correlator, analog scope | near field | |
| | sheet-pairs anemometry | direct | DSP correlator | near field | |
| | particle image velocimetry | direct | gated DSP | near field | never implemented in flight |

## 5.2 Doppler Anemometry

The frequency-shift of light scattering from a particle is dependent on the frequency of the light, on the scattering angle, on the velocity of the particle, and on the angle between the scattering angle and the velocity vector of the particle.

The frequency change of light with a wave number $\bar{k}$, scattered in direction $\bar{k}_s = \bar{k} + \delta\bar{k}$, by a scatterer with velocity $\bar{v}$, is:

Equation 5-1 $$\delta f = (\bar{v}, \delta\bar{k})/\pi,$$

where $(\bar{v}, \delta\bar{k})$ denotes the inner product of the vectors $\bar{v}$ and $\delta\bar{k}$.

For laser light with frequency f, traveling in direction $\bar{o}$, that is scattered by a particle in a measurement volume in direction $\bar{i}$, so that the frequency-shift at the detector is

Equation 5-2 $$\delta f = f(\bar{v},(\bar{o} - \bar{i}))/c,$$

For the velocity component $v_{los}$ of a particle moving towards the light source, the backscattered light has a frequency shift of:

Equation 5-3 $$\delta f = 2fv_{los}/c$$

The detection and processing of the frequency-shift in Doppler anemometry is accomplished using either direct or coherent methods. The setup of the instrumentation can be chosen such that the scattering angles of light are clear and the particle velocity can be derived. An overview of Doppler anemometers relevant for in-flight application is given in the next sections.

### 5.2.1 Reference-beam anemometer

In the reference-beam anemometer, Doppler scattered light is focused on a detector. A reference beam from the laser is also focused on the detector (see Fig. 5-1). The coherent detection is realized, and an intensity fluctuation with a frequency equal to the difference of the frequencies is available on the detector. There are two embodiments of the reference-beam anemometer. By far the most common is the monostatic version, wherein the transmitted beam and the received signal share the primary optical path (see definitions in Chapter 2). The second embodiment is termed the "bistatic" version, wherein transmitting and receiving optics are completely separate. Both versions of the reference-beam anemometer are discussed below.

Figure 5-1(a) shows the monostatic anemometer configuration together with a spectrum of the received scattered signal relative to the transmitted signal. This configuration is well suited for long-range applications. The flow velocity component parallel to the emitted beam and to the backscattered light beam is determined by the Doppler frequency-shift between the transmitted and received signals. This Doppler shift is illustrated by the graph in figure 5-1(b). Light scattered in any other direction (except forward) can be utilized in a bistatic configured reference-beam anemometer. The airspeed component measured with the monostatic anemometer is in the direction of the light beam, as shown in fig. 5-1(a).

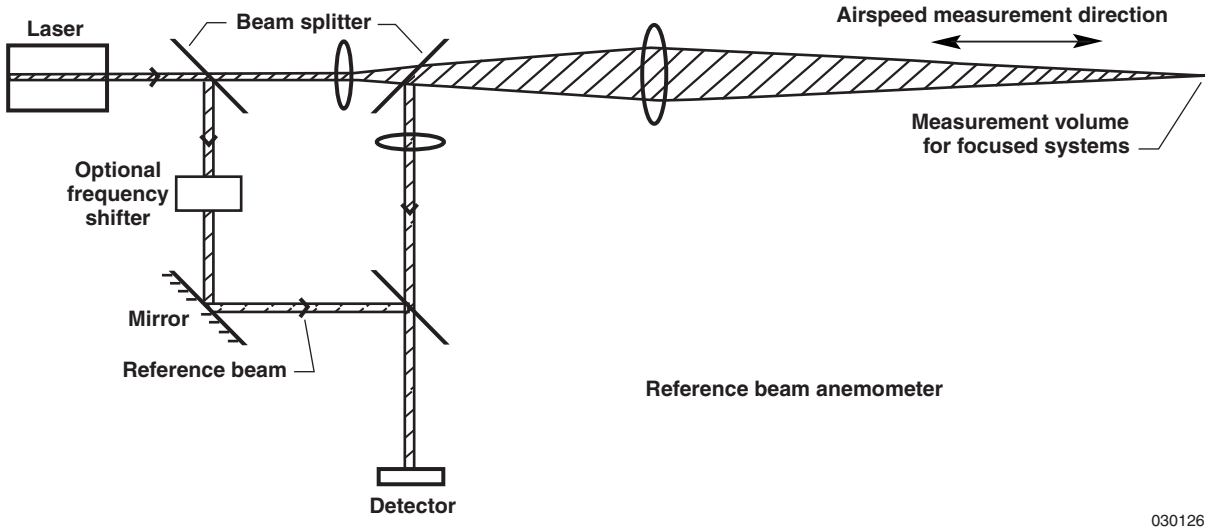


**(a) Monostatic reference-beam configuration.**

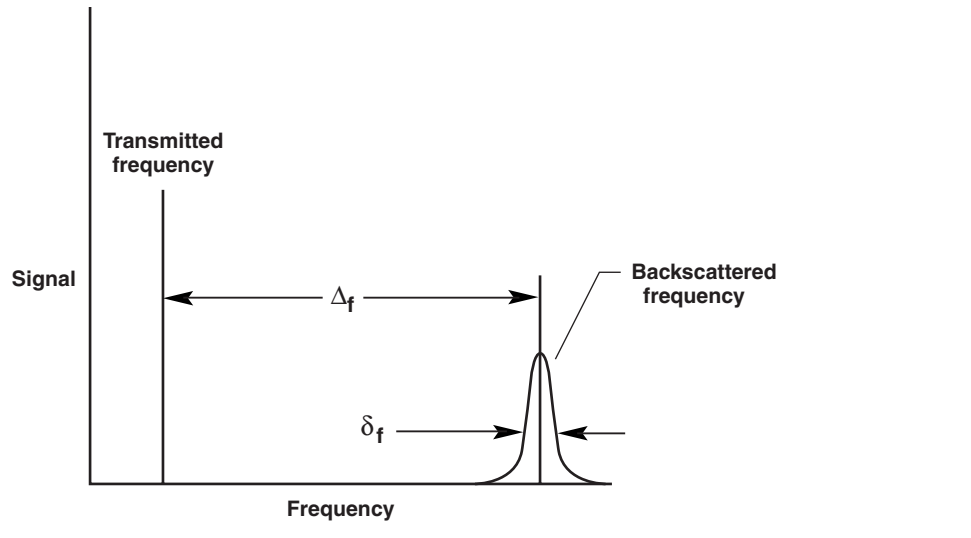


**(b) Reference-beam Doppler frequency shift.**

**Figure 5-1: The monostatic reference beam configuration in backscatter.**

Reference beam anemometers in backscatter configuration have a monostatic optical design in which the transmitting and receiving paths utilize the same optical systems as illustrated in fig. 5-1(a). The monostatic reference-beam configuration probably has the broadest measurement range of any anemometer and is used in applications at distances from a few centimeters up to 10s of kilometers. All reference-beam anemometer systems require a method of defining the region from which the velocity measurements are obtained. Focusing the beam is one method of defining the selected region. Focusing of the beam can be used to define this area of interest for short-range systems from a few centimeters up to about 150 meters and is limited by the size and shape of the focal region of the beam. A focused system can be operated in either pulsed mode or continuous wave (CW) mode and focusing offers the only means for defining the measurement volume in a monostatic system operated in the continuous wave mode. The technique for defining the pulse mode measurement region transmits a pulsed beam and gates the reception, so that the received signal is captured from the desired region (see section 3.3.3). This is called range-gating (adjusting the reception time window) and can be used to acquire information from any point along the beam path at distances out to the farthest point from which signals are received. Measurement resolution is limited by the "optical time length" of the pulse, which is also the physical length of the pulse as it travels through the atmosphere. Range-gating uses a gated detector to time-select the distance along the laser beam from which the scattered light is obtained. Laser pulse energy and pulse length must be matched to the requirements of the system (pulse length, in nanoseconds, defines the minimum length resolution according to the relationship: L = .3t, where L is in meters, and t is in nanoseconds).

With this broad range of application, typical systems exhibit substantial performance variation depending upon the requirements. Long-range systems require comparatively large collection optics, highly sensitive low-noise detectors, and high-speed digital signal processors. These long-range systems are typically constructed on an optical bench and require tight dimensional control and vibration isolation to maintain the optical integrity of the system, although lightweight, high-strength carbon fiber optical tables are re-defining the choices. Future systems are expected to be substantially smaller and lighter (except for the optics) than systems in use today.

Bistatic systems (where the transmitting and receiving paths utilize different optical systems off-axis from one another) measure the velocity vector along the line that bisects the angle between the axes of the transmitted beam and the collecting system. With bistatic systems, the measurement volume is defined by the masking and focusing approaches (see section 3.3 Measurement Volume discrimination). Bistatic designs (sometimes in conjunction with monostatic systems) can offer the advantage of measuring velocity in one or more directions from the same measurement volume (see Fig. 5-2). The on-axis detector measures the Doppler frequency shift from the upper (monostatic) system. The off-axis detector measures the Doppler frequency shift along the axis of the lower (bistatic) system. To obtain the magnitude of the off-axis airspeed it is necessary to combine the Doppler frequency shifts from both systems.

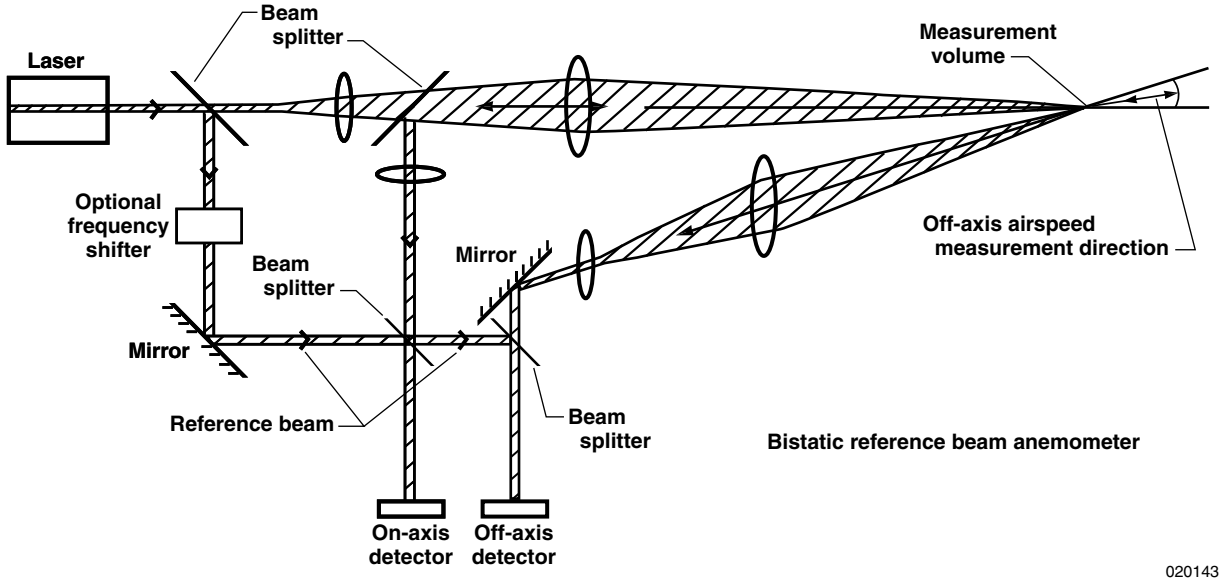


**Figure 5-2: Bistatic reference-beam laser velocimeter system.**

Some authors use the terms “homodyne” and “heterodyne” to categorize the reference beam laser Doppler anemometers, analogous to customs in radio technology. Regretfully, different definitions for homodyne and heterodyne are used in available literature, which makes these terms a source of confusion. In the most widely applied definition the reference beam of the homodyne laser anemometer has the same frequency for the laser and is mixed with the received Doppler signal on the detector. In the case of the heterodyne laser anemometer the frequency of the reference laser beam is shifted in optical components before impinging on the detector so that the two frequencies are different. Some characteristics of the reference-beam anemometer are:

- The measurement volume is defined by masking, focusing, or range-gating depending on the application.
- This anemometer is useful in a broad range of applications, from near field through far field.
- In the monostatic configuration, the velocity component parallel to the axis of the beam is measured.

### 5.2.2 Dual-beam laser Doppler anemometer

In a dual-beam laser Doppler anemometer two coherent light beams are crossed to create a measurement volume at the beam intersection (see fig. 5-3). Individual particles traversing through the measurement volume scatter light from both beams. A detector measures the intensity of scattered light. The frequency of intensity fluctuations is a constant, times the velocity component of the scatterer in the intersecting beam plane, perpendicular to the bisector of the beam propagation vectors. The frequency of intensity fluctuations is independent of the detection angle. The phase of detected intensity fluctuations is dependent on the detection angle only if phase shifts are introduced by the scattering, because a particle-dependent phase shift of light is added into each scattering direction according to Mie’s scatter relations (see section 3.3.2.2).

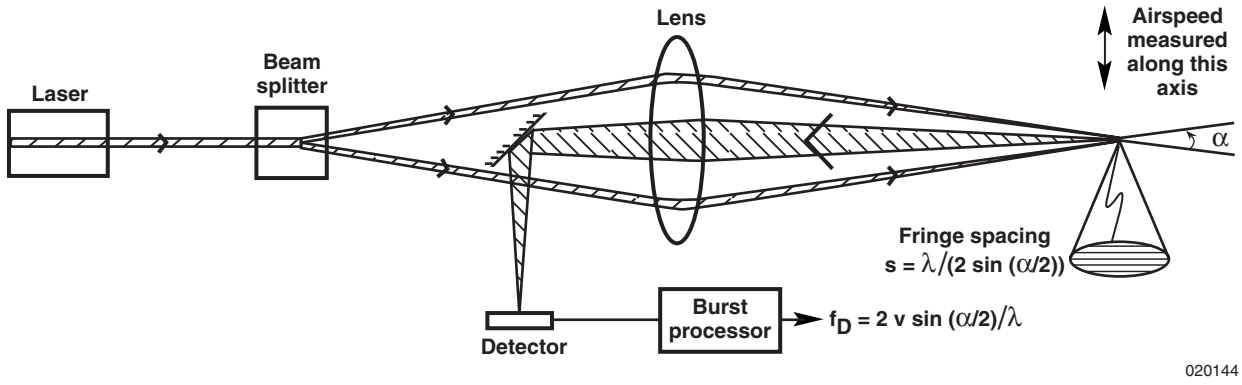


**Figure 5-3: The dual-beam laser Doppler configuration.**

A fringe model is widely in use to explain the principle of the dual-beam laser Doppler anemometer. The model considers an interference pattern formed by the two beams in the measurement volume. The interference pattern has parallel light and dark planes, called “fringes”, in the measurement volume as shown in figure 5-3. The distance between the fringes is

Equation 5-4 $$s = \lambda/(2\sin(\alpha/2))$$

where $\alpha$ is the intersection angle of the two light beams. The frequency fluctuation that results on the detector when a particle passes the interference pattern is

Equation 5-5 $$f_D = 2v_\perp \sin(\alpha/2)/\lambda$$

where $v_\perp$ is the particle velocity component in the plane of the two intersecting beams, perpendicular to the bisector of the beam directions.

The fringe model gives an easy insight into most of characteristics of the anemometer. The number of fringes in the measurement volume is constant and can be related to beam and measurement volume cross sections. The fringe model explains the signal shape and the relation between velocity and frequency of intensity fluctuations. Fig. 5-3 displays several of these features.

The fringe model does not provide an easy insight into the effects of the phase differences introduced by light scattering, mentioned in the first part of this section. The phase difference of scattered light results in a dependency of the position of the light and dark fringes on particle size and detector position. This dependence is demonstrated in Phase Doppler Anemometers (Bachalo 1984[24], Durst 1997[25]) which are used as standard equipment for particle size measurements in the laboratory and are being introduced into the flight environment (Bachalo 1984[24]).

The dual-beam setup is easily realized, with commonly available optical components. Coherence aspects are not stringent, which makes the dual-beam anemometer easy to apply in a wide variety of research applications. Dual-beam anemometers are available in many configurations on the market, for application in the laboratory, with fewer models suitable for the industrial production environment. There are few dual-beam Doppler anemometers developed for in-flight application and none marketed specifically for this. Some characteristics of this anemometer are:

- It has a small, well defined measurement volume.
- The measured velocity component is perpendicular to the crossed light beams in the plane of the light beams.
- The distance between the anemometer and the measurement volume must be limited (the anemometer cannot be used at long ranges).
- The best performance is achieved when only one particle at a time is in the measurement volume.
- The position and size of the detector are not critical for flow measurement.

These characteristics are well suited to near field applications in flight, described in chapter 6. However, the limited distance characteristic precludes use in far field applications. Intersecting two light beams at a large distance and the efficient collection of scattered light are very difficult for this type of anemometer.

This anemometer has a velocity measurement ambiguity. Velocities in either direction result in the same signal. To avoid this ambiguity a Bragg cell is used to introduce fixed frequency offset to one of the light beams. The frequency offset produces a measured velocity offset (the fringes move in the measurement volume at the velocity offset), and a new ambiguity emerges around this new velocity. The frequency shift is chosen such that the ambiguity leaves no inconvenient uncertainties for the experiment. There are many good

textbooks describing dual-beam laser Doppler anemometers in detail, see Durst 1981[26], Drain 1980[27], Rietmuller VKI LS 1991[28].

### 5.2.3 Spectrometric Velocimetry

Even for very high aircraft speeds the Doppler shifts of light are very small compared with the frequency of laser light. High resolution in the frequency domain is required for measuring the small shifts. Optical filter components such as molecular filters (Ref. Elliott-1999) and Fabry-Perot etalons can provide the required resolution. The molecular filters have been successfully applied in Doppler global velocimetry and will be further discussed in the next section. Velocimeters with Fabry-Perot etalons have been developed primarily for applications in space (Hays 1982[29], Korb 1992[30], McGill 1998[31], Korb 1997[32], Korb 1998[33], Skinner 1994[34], Abreu 1992[35], Rees 1982[36], Rees 1990[37]), and also have a potential for airborne applications.

Fabry-Perot etalons introduce a large dispersion of light frequencies in optical spectrometers caused by light interference that quenches light frequencies for most of the spectrum, except for some narrow bands. A thorough description of the Fabry-Perot interferometer is given in many optical textbooks (Hecht 1974[38], Born 1970[21]) and laser textbooks (Silfvast 1996[3]) as this device determines a key performance characteristic of a laser. The passive etalon version is described in the following paragraphs.

A Fabry-Perot etalon is constructed from two partly transmitting parallel mirrors. The transfer function of light passing through the assembly of the mirrors shows sharp peaks where the optical cavity length between the mirrors matches a multiple of the half-wavelength of light. The sharpness of the peaks depends primarily on the reflection coefficient of the mirrors and the precision of the parallel mirror alignment. The sharpness is reflected in a parameter called “finesse” and this determines the resolution of the spectrometer.

The sharp slope of the transfer function is used to discriminate the frequency of Doppler-shifted light and functions as a discriminator signal processor (see definitions in Chapter 2). The edge of a peak is used to modify the transmission as a function of light frequency, but by adding lenses and a camera to the optical configuration the etalon can also be used to disperse the different light frequencies in space. The spatial separation is measured by spectrometers with an imaging detector, to capture the fringe pattern.

The measurement of the frequency shift in the spectrometric velocimeter using an etalon requires a high mechanical stability of the cavity, which in turn requires special measures including temperature control as a minimum and possibly active mechanical feedback. Furthermore, for edge detection, the edge of the transmission peak should be matched to the laser frequency. These are the major challenges in the design of this spectrometrically-based velocimeter. (See discussion under 4.2.5 Filters).

### 5.2.4 Doppler global velocimetry

Doppler global velocimeters operate on the same principles as described for all Doppler velocimeters. A basic Doppler system with a single laser transmitter and single receiver is capable of resolving a single velocity component from a defined measurement volume. DGV provides a full 3-component velocity field measurement capability over a selected planar measurement region of the flow, and therefore requires more than a single transmitter and receiver pair to acquire the additional information (Meyers 1995[39]). A common implementation of DGV uses a single laser transmitter to project a plane of light in conjunction with three receivers positioned at three viewing angles to acquire the necessary three velocity components. Alternatively, the sheet can be illuminated intermittently from three different directions and analyzed with one receiver assembly (Roehle 1998[40], 1999[41], 2000[42], 2001[43]). This may be considered as three bistatic planar laser velocimeters with three laser transmitters, respectively, and a common receiver. Each of the

velocimeters obtains a separate flow velocity component at each point in the measurement plane. The ability to measure 3 components of velocity in an illuminated plane of interest is what sets DGV apart from other optical velocity measurement concepts.

A vary narrow-band optical filter serves as an optical discriminator signal processor and as discussed in the previous section (covering the range of Doppler shift) is used to convert the DGV Doppler frequency shift into an amplitude variation. This filter may be a high-finesse etalon or a molecular vapor filter, such as an iodine vapor cell, the transfer function of which is shown in figure 5-4 below (Meyers 1995[39]). This is a normal direct-detection process performed for the pixelated field of view. After passing through the filter, the intensity of the light reaching the pixel is determined by two factors, as suggested above: (1) the attenuation imposed by the optical filter (discriminator) as a function of the Doppler frequency shift, and (2) the scattering aerosol and particle density in the region from which the light originates. To extract the Doppler shift information at the pixel, the effect of the random amplitude must be removed so that the amplitude variation at the pixel location is caused only by the Doppler frequency shift.

Correcting for the aerosol and particle density variations requires the use of a compensating parallel video detection system, in principle matched pixel-for-pixel with the primary detecting video camera. With the compensating system, it is possible to remove the random amplitude variations by dividing the filtered signal level from the primary detector video camera by the unfiltered signal level from the compensating system, on a pixel-by-pixel basis. The ratio of the filtered signal level at the primary detector video camera pixel to the unfiltered signal level at the corresponding pixel in the compensating system camera, provides a measure of the Doppler frequency shift. On a pixel basis, this is the desired information needed to obtain the velocity shift distribution and thereby determine the velocity field variation for one of the three velocity components across the sensing pixel field.

For this approach, the primary detector camera and the compensating system camera must acquire the identical view to the point that the field of view for corresponding individual pixels must be very nearly identical. In practice, optical distortions between the two fields of view have made it impossible to match the scenes on a pixel-for-pixel basis. Scenes have been captured using video frame grabber technology and computer-based compensating optical corrections have been applied so that the processed scenes are sufficiently matched pixel-by-pixel to allow compensation for amplitude variations. Calibration of pixels in both systems has proven to be necessary to account for slightly different gains and to remove biases (Meyers 2001[44]).

Figure 5-4 shows the transfer characteristic of an iodine vapor cell with an acceptably linear frequency-amplitude region (Meyers 1971[45]). The vertical dotted line illustrates the situation where the scattered signal has no Doppler shift. When the Doppler shift is positive the response of the transfer function is to reduce (darken) the amplitude of the signal. When the Doppler shift is negative the response of the transfer function is to increase (brighten) the amplitude of the signal. Positive and negative Doppler shifts result when the flow moves generally toward and away-from the detectors respectively, keeping in mind that the component of the flow being measured is along the velocity measurement vector ($\bar{\mathbf{i}} - \bar{\mathbf{o}}$)(as described in figure 5-5).

The data from three bistatic velocimeters is combined using the geometrical layout of the plane(s) of the illuminating laser and the relative positioning of the receiver assemblies to provide 3-component velocity measurement. Figure 5-5 illustrates this concept and the relationship, with only one light sheet and one receiver assembly.

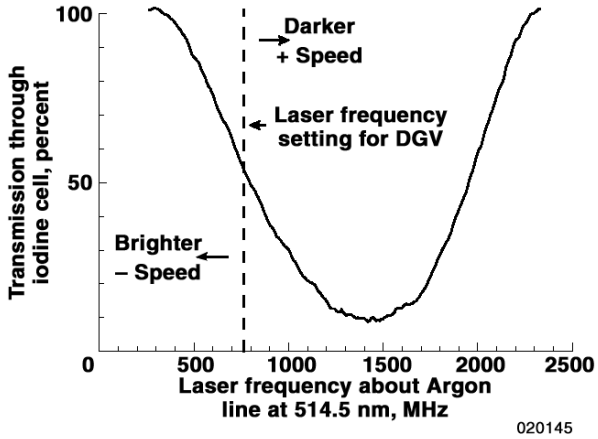


**Figure 5-4: Transfer function of the iodine vapor cell.**

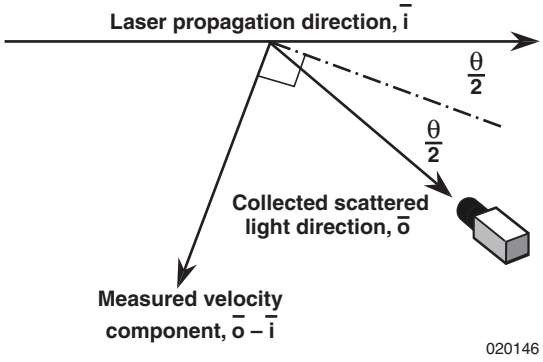


**Figure 5-5: Doppler global velocimeter layout.**

## 5.3 Laser Transit Anemometry

Laser transit anemometers derive the velocity of air from particles in the air by determining the travel distance of a particle in a short time. The principle is implemented in anemometers described in this section.

### 5.3.1 Laser two-focus anemometer (L2F)

The laser two-focus anemometer (Schodl 1986[46]) focuses two parallel beams in the airflow, where the airflow direction is perpendicular to the beams (fig. 5-6). Particles crossing the beams successively scatter light that is detected to establish the position of the particle in time. The time interval for the particles to travel between the foci is measured. The velocity of the particle is calculated from the time interval using the spatial separation of the foci. Normally the beams are rotated about the beam-pair rotation axis to determine the position with maximum successive light scattering from the two foci. This maximum is achieved only when the beams plane is aligned with the flow direction.

With the basic setup, the velocity component perpendicular to the light beams is measured, however, devices for three-component measurements have been developed as well (Schodl 2000[47]).

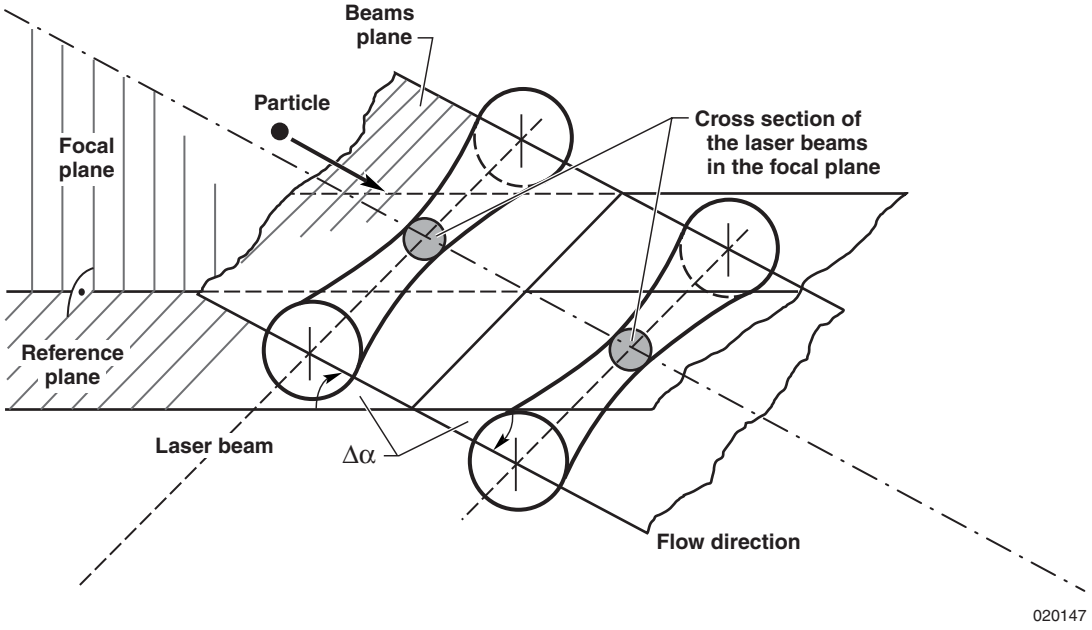


**Figure 5-6: The laser two-focus configuration.**

### 5.3.2 Sheet-pair anemometer

The sheet-pair anemometry concept is an extension of the laser two-focus anemometer that uses focused parallel sheets of light projected into the flow field of interest, as shown in fig. 5-7. For this anemometer, as a particle transits the sheets, a distinct reflection is detected and processed. A digital correlation process averages transitions and derives the average estimate of the time required for particles to ransition the distance between the sheets. Dividing the sheet separation distance by the average transition time provides an estimate of the velocity component perpendicular to the sheet-pair as shown in Equation 5-6.

Equation 5-6 $$v_x = d/\Delta t$$

Three sheet pairs can be configured to intersect in the region of a point at the desired distance from the surface of the aircraft to measure three velocity components. Each sheet pair is oriented to measure a velocity component, but physical constraints make it impractical to arrange the sheet configuration to measure orthogonal velocity components. Sheets are arranged to provide good velocity observability along the directions of the most common and largest flow velocity vectors. Since single particles are detected, the range is limited by the signal strength falloff as the inverse fourth-power of the distance. This system has been operated on the order of 1 meter from the surface of the aircraft.

The time-of-flight anemometer concept relies on the successive detection and timing of particles as they enter the spot or sheet illumination region as described below.

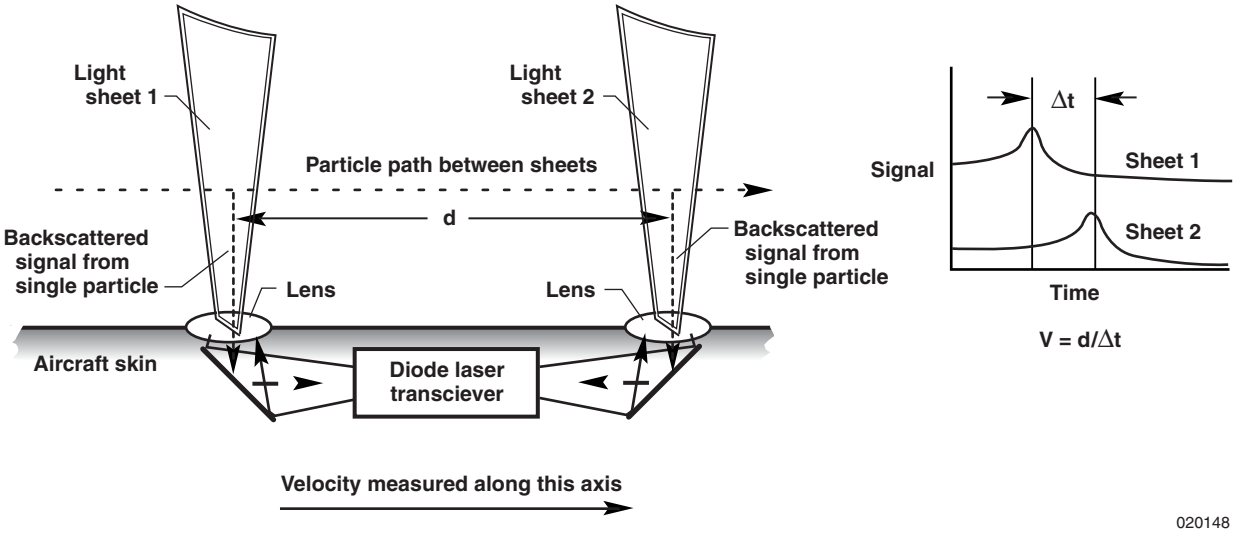


**Figure 5-7: The sheet-pair anemometer configuration.**

*5.3.2.1 Detecting Aerosol Presence*

It is necessary to discriminate between light energy scattered from legitimate particle targets and background noise from extraneous light sources, such as sky light. Optical filtering is often a useful technique to limit the amplitude of extraneous light sources by removing wavelengths different from the projected light wavelength. The detector signal from a legitimate particle will have both an expected signal amplitude and a persistence. Both expected amplitude and persistence must be determined from an analysis of the projected sheet-pair geometry, optical signal collection configuration, projected laser power, aerosol size distribution, and aerosol scattering characteristics. An amplitude threshold is often used to eliminate random system noise and scattered signals from aerosols below the design size-limit threshold. The implementation of this process is accomplished with high-speed analog-to-digital converters and digital processing that can identify legitimate aerosol presence as an “event”.

*5.3.2.2 Correlating events to establish time-of-flight*

Once events are confirmed, a time tag is attached and the event is loaded into buffer shift registers in preparation for the correlation process. Correlation is accomplished by a successive comparison of event times from the downstream sheet with those from the upstream sheet. A range of admissible times is accumulated and the average of this set of event-pair time differences is the time-of-flight estimate for the time window used to collect the events. The computation of the time-of-flight can be considered as a cross-correlation process. With the known sheet-pair spacing and the time-of-flight data, the component of the vector flow velocity perpendicular to the sheet-pair is computed by dividing the light-sheet spacing by the time-of-flight.

### 5.3.3 Particle image velocimetry (PIV)

A particle image velocimeter illuminates a plane field in the airflow with two light pulses. The illuminated plane is oriented to be as closely as possible to parallel to the airflow direction. Particles in the air scatter light, which enable recording of the image of the particles on the projected illuminated plane from a direction with a good viewing angle. The time between the light pulses is chosen, such that the faster particles move a considerable distance in the image field. By correlating the two images, travel distances can be determined in the recorded area. Together with the time interval of the two pulses, this information provides velocity information in the imaged plane.

The advantage of this technique is that it provides velocity information in a two-dimensional field, whereas many other techniques only give the velocity at a point. In wind tunnels this is very valuable. For in-flight applications the configuration seems less advantageous and no in-flight PIV application has been reported to the authors' knowledge.

# Chapter 6 – APPLICATIONS

## 6.1 Introduction

Optical air flow meters are applied in flight for different purposes. This chapter presents an overview of the different applications of laser anemometry in aircraft. Table 6-1 summarizes the applications and the laser anemometry techniques applied.

**Table 6-1: Overview of applications and measurement techniques applied.**

| Application | Measurement techniques applied in flight |
|---|---|
| air data systems | |
| helicopter | laser transit, coherent lidar |
| fixed wing aircraft | coherent lidar |
| air data system calibration | coherent lidar |
| safety systems | |
| wind shear | coherent lidar |
| clear air turbulence | coherent lidar |
| wake vortices | coherent lidar |
| aerodynamic investigations | Dual-beam LDA, laser transit, coherent lidar |
| atmospheric research | coherent lidar |
| parachute and ballistic trajectory control | coherent lidar |

## 6.2 Air Data Systems

The airspeed of aircraft can be measured with laser anemometry (Woodfield 1983[48], Smart 1992[49], McGann 1995[50]). The angle of attack and the angle of sideslip can also be derived through the three-component application of laser anemometry. If the measurement volume of the laser anemometer is located outside the local flow field of the aircraft, air speed can be measured without having to calibrate for installation errors. Measurements closer to the aircraft can also be used applying calibration factors to the sensor outputs, as is common practice for conventional air data systems.

Potential applications for optical air data systems exist, especially in fighter aircraft, stealth aircraft, and helicopters. In fighter aircraft the high-angle-of-attack maneuvers and the high dynamics put severe requirements on the performance of air data systems. For stealth aircraft, the optical systems remove the need for protruding pitot tubes, thereby preserving the low radar cross-section characteristics. Optical techniques also have advantages for the measurement of helicopter airspeed. Conventional air data sensors are installed on helicopters in the flow field generated by the rotor, which requires substantial flow corrections, especially at low speeds. Optical measurements (Mandle 1984[51]) made outside the influence of the rotor wash do not require flow corrections.

Laser anemometers are also used for calibrating air data systems. The errors in the conventional system (position error, airspeed influence, etc.) can be determined by measuring air data simultaneously with a conventional air data system and with a laser anemometer. Laser anemometers have been operated in

prototype aircraft for this purpose since 1991 (Mandle 1991[52], Alonso 1991[53], Cattin 1992[54]). Operating the anemometers in prototype aircraft from the first flight on provides accurate air data from the first flight, which is helpful, for example, in opening flight envelopes.

## 6.3 Safety Systems

In the pursuit of making aviation safer, unexpected atmospheric flow phenomena pose a considerable challenge. One of the options to make aviation safer in this respect is to install advanced detection systems for these phenomena. Laser anemometry for hazard detection is under development. Important requirements for the advanced detection system include (1) remote detection at a considerable distance (such that adequate action, such as fastening seat belts or avoidance maneuvers can be taken before entering a hazardous air mass) and (2) the ability to operate (complementary to radar) in clean air. Both requirements are feasible for laser anemometry.

Systems have been studied to detect the following phenomena.

- Wind shears – During landing or takeoff, abrupt changes of aircraft wind speed are particularly dangerous. Downbursts of air can cause rapid reductions in headwind, thereby causing rapid changes in descent rate and risking impact with the ground (Woodfield 1983[48], Köpp 1990[55], Fetzer 1990[56], Targ 1996[16]).

- Clear air turbulence – Clear air turbulence provides no visual cues of its presence and is often encountered during the cruise phase of a flight. The turbulence causes many injuries, especially among flight attendants and caused a fatality in a Boeing 747 over the Pacific Ocean enroute from Japan.

  Another need for detecting clear air turbulence may appear if new fuel-efficient supersonic aircraft are designed (Bogue 1995[57]). Turbulence can cause engine inlet unstarts that pose an unacceptable safety risk and reduce passenger comfort dramatically.

- Wake vortex – Every aircraft in the air generates wake vortices, posing a potential danger for an aircraft in trail flying through these hazardous conditions. Air traffic control at airports takes this potential danger into consideration in determining the safe distance between landing aircraft. A detection system close to the runway or onboard the aircraft can support the determination of safe distances as a function of atmospheric conditions (such as wind) and aircraft type. Many studies are in progress on this subject (Hannon 1994[58], Keane 1997[59], Combe 2000[60]). The feasibility of wake vortex detection has been demonstrated using laser anemometry technology.

The development of systems to detect the safety hazards listed above and also the potential threats of volcanic ash and ice crystals is in progress (Köpp 1997[61], Combe 2000[60]). The detection of all these hazards in one system is an extra challenge, but makes the system much more cost-effective for commercial aviation applications.

## 6.4 Aerodynamic Investigations

Measuring airflow very close to the aircraft provides information useful for aerodynamic research. In-flight feasibility of this kind of measurement was demonstrated in Jentink 1995[62], and Becker 1999[63]. Investigations of, for instance, the vortices generated by the aircraft (Meyers 1995[39]), the flow behind propellers, laminar-to-turbulent flow transition (Becker 1999[63]) and flow in the wing-body junction may benefit from applying laser anemometry.

## 6.5 Atmospheric Research

Aircraft have been used as platforms to carry laser anemometers investigating atmospheric phenomena (McCaul 1986[64], Kristensen 1987[65], Reitebuch 2001[66], Werner 2001[67], Rahm 2001[68]). Thunderstorm investigations, wind shear characterizations and particle density measurements have been reasons for flight campaigns. A considerable number of air masses can be reached in a short period of time in flight campaigns and the remote measurement capability of this technique is valuable when potentially hazardous atmospheric conditions such as thunderstorms and wind shear are to be investigated.

## 6.6 Parachute Drop Accuracy Improvement

During the UN missions in Bosnia it was necessary to drop parachutes from considerable altitudes to avoid the small arms threats for aircraft. The drop accuracy from these altitudes was reduced because of wind uncertainties. Development of laser anemometry technology for measurement of the wind field below the drop aircraft was initiated to adjust the cargo release point for wind drift compensation (Richmond 1997[69], Ott 1996[70]).

Similarly for ballistic munitions, the influence of wind on the trajectory can be determined with laser anemometry. By correcting for these influences the first-round accuracy can be improved (Richmond 1997[69]).

**This page has been deliberately left blank**

---

**Page intentionnellement blanche**

# Chapter 7 – EXISTING SYSTEMS

## 7.1 Introduction

Existing systems illustrate how designers have approached and used optical principles to construct systems to solve a specific set of requirements. This chapter provides the reader with examples of concepts that have proven to be viable in a specific application. As with other chapters in this document, this provides a short overview description of the application and the salient design features. Further reading from the referenced literature listed at the back of this document is encouraged to more fully understand the design issues and approaches.

## 7.2 Air Data System Calibration and Air Data Operational Measurement

With all conventional pneumatic air data systems the objective is to measure free stream values (see definition of free stream in Chapter 2). Because it is often impractical to install air data booms with sufficient length to obtain free stream samples, errors are present as a result of flow field disturbances caused by the aircraft movement through the air. These errors are repeatable and are functions of measured air data parameters. Although several techniques have been developed over the years, the most direct and probably the most accurate way to directly obtain the correction factors is to compare the aircraft air data measurements with optically derived measurements obtained non-intrusively from the free stream region in front of the aircraft. Two of the applications in this section are intended for use as calibration systems.

### 7.2.1 Thales air data calibration system

For air data system calibration European Aeronautic Defense and Space Company (EADS) applies a reference-beam laser anemometry system named ALEV 3 (Alonso 1991[53], Cattin 1992[54]). This system measures the airspeed of the aircraft in three directions and is installed in prototype aircraft of new aircraft types. The calibrations of the pitot static system and vanes using a laser anemometer have an increased accuracy compared with those obtained with conventional techniques, such as using a towed cone, tower-fly-by, or a pacer aircraft. Furthermore the availability of true airspeed, angle of attack and angle of sideslip from the first flight moment of a new aircraft type onwards is a valuable feature of the system. It precludes the necessity to install a boom on the aircraft. The simplifications in the flight-test program of a new aircraft type result in fewer flight test hours and also yield economic benefits.

Figure 7.1 shows the locations from which the airspeed measurements are taken. The focal length of the optical system defines the distance of the measurement volume (see section 3.2.2). The focal distance is different for different directions. The distance is chosen such that the airflow in the measurement volume is not disturbed by the presence of the aircraft, but is not so far away that air turbulence introduces differences between the air speeds experienced by the aircraft and in the measurement volume. Figure 7-2 shows a photograph of the system installed in the Airbus A340. To provide optical access for the infrared energy exchange from the cabin to the air in the measurement volume, a cabin window is replaced with a germanium metal plate for a window insert. An atmosphere with dry air is created on the cabin side of the insert to prevent condensation of water on this insert. The characteristics of the system are summarized in table 7-1.

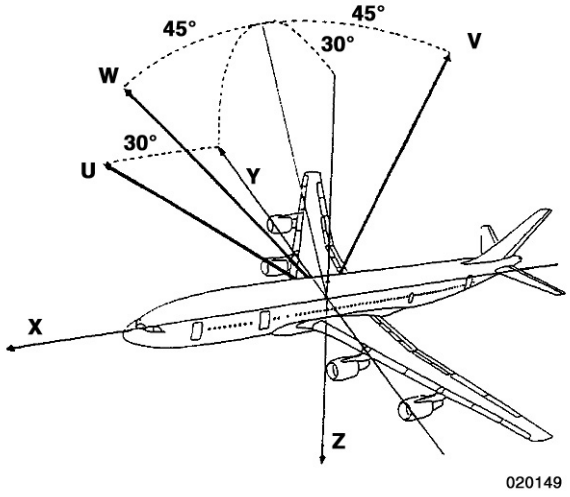


**Figure 7-1: Typical location of measurement volumes.**

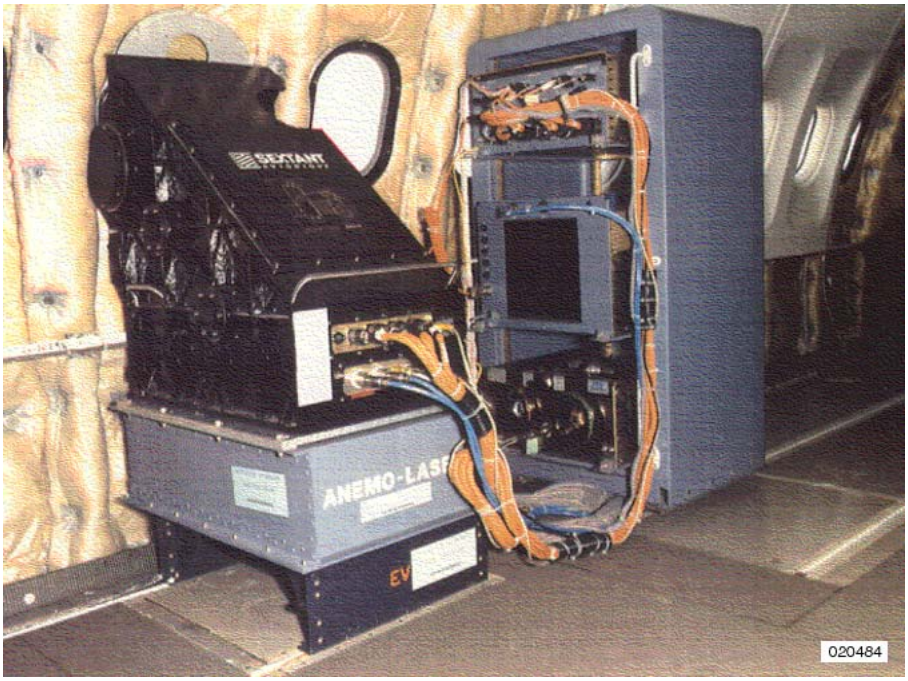


**Figure 7-2: Installation of ALEV 3 system in the Airbus A340.**

**Table 7-1: Characteristics of the ALEV 3 system.**

| Factor | Detail |
|---|---|
| anemometer type | reference-beam laser anemometer |
| laser | $CO_2$ gas laser |
| wavelength | 10.6 μm |
| operating mode | continuous wave (cw) |
| power | 5 Watts |
| detection | coherent mode using a HgCdTe detector cooled to 77 K |
| detector cooling | Thompson cooling, expansion of pressurized nitrogen gas |
| measurement | vector true airspeed (TAS) angle of attack (AoA), and angle of sideslip (AoS) |
| focal distance | between 50 and 100 m |
| velocity range | 10 m/s to 400 m/s |
| altitude range | up to FL 250 without signal loss, at FL 250 to FL 350 signal is occasionally lost because of insufficient atmospheric backscatter |
| TAS uncertainty | 0.25 m/s (including system and installation uncertainties) |
| update rate | 2, 4, or 8 measurements per second (measurements in the three directions are taken intermittently) |
| format | ARINC 429 |
| physical characteristics | |
| scanning | scanning mirror |
| size (optical unit) | 0.75 x 0.5 x 0.75 m |
| weight (optical unit) | 70 kg |
| developed by: | Crouzet, Sextant, Thales |

The ALEV 3 system was developed by Crouzet and was delivered in 1991 (the company is now part of Thales). In that year the system was tested in an A320 prototype. The A340 was the first aircraft certified with ALEV 3. Since then, about ten new aircraft types have been certified using the system. The system has accumulated over 1000 hours of operation.

Several other interesting laser anemometer systems have been developed for true airspeed measurements, which are described in Woodfield 1983[48], McGann 1995[50], Mandle 1984[51], Mandle 1991[52].

### 7.2.2 Boeing Doppler lidar airspeed system

The continuous-wave Doppler lidar was developed to augment pitot-static-based systems with a state-of-the-art optical airspeed sensor system and the ability to measure true airspeed (TAS), angle-of-attack, and angle-of-sideslip outside of the influence of the airplane flow field. Before development of the current

system, conventional CW or pulsed Doppler lidar systems were used. Previous systems have required large, inefficient laser sources to achieve the power needed to maintain acceptable data rates under clear air (low aerosol density) atmospheric conditions. Unlike some earlier systems, this one is built around a diode-pumped, solid-state laser.

**Table 7-2: Characteristics of the Boeing Doppler lidar airspeed system.**

| Factor | Detail |
|---|---|
| anemometer type | reference-beam laser anemometer |
| laser | NdYAG |
| wavelength | 1.064μm |
| operating mode | continuous wave (cw) |
| power | 0.5 Watt |
| detection | coherent mode using an indium gallium arsenide detector |
| measurement | single component flow velocity at a point |
| focal distance | between 1 and 2 m |
| velocity range | 10 m/s to 400 m/s |
| altitude range | tested up to FL 410 |
| TAS uncertainty | 1 m/s |
| update rate | dependent upon particle passage rate |
| format | RS 232 |
| physical characteristics | |
| scanning | none |
| size (optical unit) | 7.5 x 17.5 x 27.5 cm |
| weight (optical unit) | <5 kg |
| developed by: | Boeing Information Systems |

Boeing Defense and Space Group, Seattle, Washington has been improving the enhanced mode lidar (EML) concept for use as a line-of-sight optical airspeed sensor (McGann 1995[50], Erwin 1993[71]). This concept exploits the fact that as the beam is focused to a small focal volume (fig. 7-3), obtaining a return signal from discrete aerosols is possible (see fig. 7-4). This signal is much greater than that predicted by the conventional lidar signal power equation. As the signal per aerosol increases with sharper focusing, the number of aerosols in the detection volume decreases proportionately, thereby increasing the backscattered signal variability. Under these conditions, aerosols pass individually through the detection volume. Each time an aerosol is present, a signal pulse of high-SNR is received. The high-SNR condition requires less power than a conventional lidar system and a low-power laser may be used. Using low power is a viable option when the required sensing range is limited, and the aerosol density is high enough to provide an adequate data rate (sufficient rate of aerosols transiting the focal region). Large aerosols in the focal region increase the signal level and partially offset the range limitation. The signal power returned from each individual aerosol is constant for a given size of aerosol regardless of the number density.

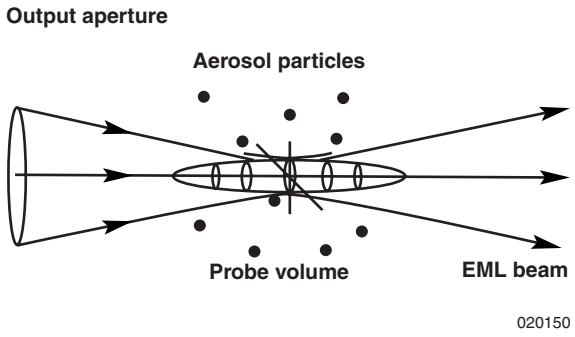


**Figure 7-3: Detection volume geometry.**

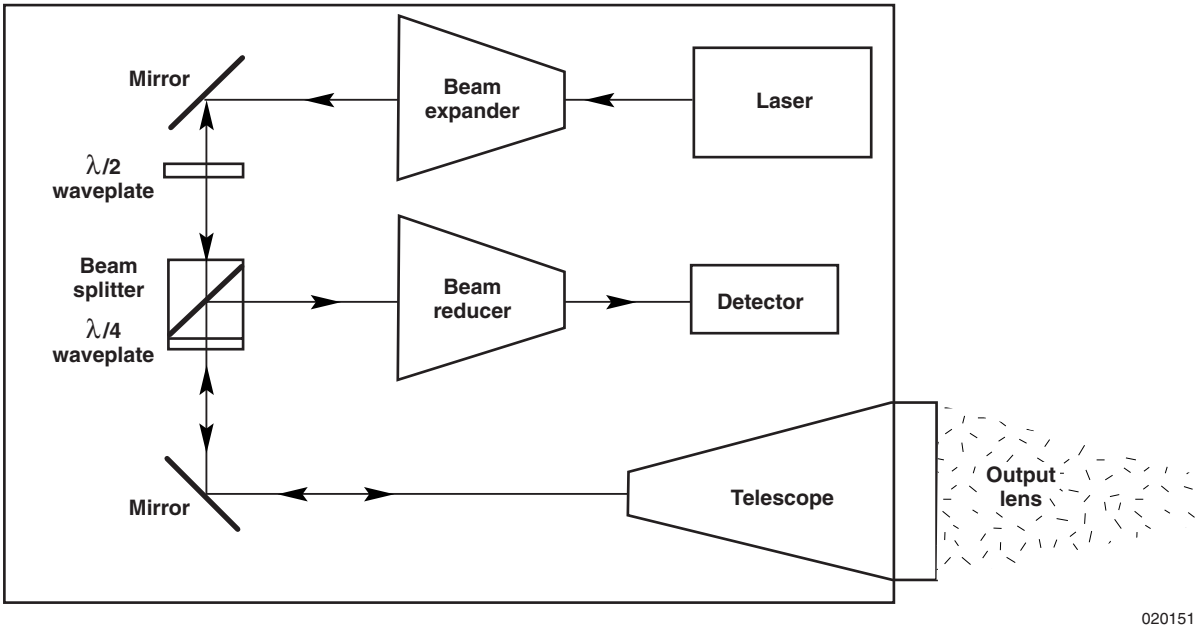


**Figure 7-4: Continuous-wave Doppler lidar brass board configuration.**

Successful velocity measurement demonstrations were performed in wind tunnel flow fields (with and without particulate seeding) and in local wind conditions using natural aerosol populations. Twelve hours of flight-testing over the course of three flights were completed onboard a University of Washington Convair C-131A test bed aircraft (McGann 1995[50]).

Figure 7-4 shows the optical configuration of the brass board sensor. The brass board employs a small, efficient, commercially available, diode-pumped solid-state NdYAG laser with a 500-milliwatt output power and a wavelength of 1.064 μm. Optics and hardware components in the brass board consist of commercially available off-the-shelf items. Although the brass board was not designed for minimum size or weight, the optical head measures only 7.5 x 17.5 x 27.5 cm, and weighs less than 5 kg. The output aperture is 50 mm and the final focal length of the system can be adjusted by changing the output lens. Performance was evaluated for 1-m and 2-m focal length corresponding to velocity measurements at 1 m and 2 m, respectively. The photo detector is a commercially available Indium Gallium Arsenide detector integrated into a detector-amplifier package.

### 7.2.3 Michigan Aerospace Molecular Optical Air Data System (MOADS)

MOADS is a direct detection lidar instrument that uses a Fabry-Perot interferometer as an optical discriminator to detect the (incoherent) Doppler shift from laser light backscattered by air molecules and aerosols. A significant advantage that MOADS has over similar air data system technologies is the ability to make measurements in clear air (air molecules only), without the presence of aerosols. It will, however, take advantage of aerosols when available to improve data quality. The instrument optical head is flush-mounted to the aircraft skin, minimizing the radar cross-section. Research is currently being performed to apply MOADS technology as a replacement for pitot-probe-based air data systems and for other applications that would benefit from the ability to operate in low-aerosol density environments.

The MOADS system design (Tchoryk-2001[72]) is the current result of a search by the US Department of Defense for an air data system capable of operating over a broad range of altitudes at any location worldwide, and at the same time preserving the radar stealth characteristics of the aircraft to which it is attached. An optical system was chosen to avoid the need for external pneumatic probes that make a significant contribution to the radar cross-section, thus increasing vulnerability by reducing the radar stealth characteristics. Concern for the global availability of aerosols led the designers to base their system on molecular scattering, wherein the presence of aerosols is not necessary for operation, however aerosol availability improves the system accuracy. The operating wavelength of the MOADS was chosen for effective molecular scattering properties, and for the fact that the wavelength extinction distance is short enough to preserve optical stealth features. MOADS has been ground tested in a wind tunnel and has not reached the flight prototype stage of development as yet, but the concept offers the opportunity for acquiring the full set of air data parameters such as airspeed, angle of attack, angle of sideslip, static pressure, and static temperature. MOADS is a proof-of-concept system built to confirm the viability and technical maturity of several design innovations including: static temperature and density measurement accuracy, the performance of the quad Circle to Line Image Optic (CLIO), direct detection etalon element stability, and overall system operability in an aircraft environment. Because the MOADS is a proof-of-concept effort, it is instructive to review the measurement performance that was achieved in a laboratory environment, but it is not possible or useful to obtain system size and weight specifications, because these parameters are not representative of a flight system. A study was performed under the Air Force Advanced Technology Air Data System (ATADS) program that resulted in a packaging design that met the installation and performance requirements for an F-117A upgrade. Additionally, a follow-on system called by the acronym “JOADS” (Joint Optical Air Data System), for existing and future military aircraft, is under consideration. Projected JOADS performance based on extrapolated MOADS laboratory experience and size, weight, and power projections can be used to provide a preview of future system performance. Projections are clearly identified and differentiated from actual laboratory results. Refer to Table 7-3 for a summary of the MOADS size, weight, and performance parameters.

**Table 7-3: Characteristics of Michigan Aerospace Molecular Optical Air Data Sensor (MOADS).**

| Factor | Actual Detail (as tested in the laboratory) | Projected Detail |
|---|---|---|
| anemometer type | spectrometric anemometer, bistatic configuration | |
| laser | NdYAG laser quadrupled | |
| wavelength | 1.064 mm quadrupled to 0.266 mm | |
| operating mode | continuous wave or pulsed | continuous wave or pulsed |
| power | .5 W (dependent on update rate) | .5 W |
| detection | direct mode detection by a high-finesse etalon using a charge-coupled-device (CCD) detector | |
| measurements | vector true airspeed (TAS, AoA, and AoS), static pressure, and temperature. Derived measurements include: Mach and Pressure Altitude | |
| measurement distance | 2m. and 10m. | 2m. and 15 m |
| velocity range | 0 to 25 m/s | 0 m/s to 1200 m/s |
| altitude range | Sea level (SL) | SL to FL 1000 |
| TAS uncertainty | ±0.57 m/s (1 sec. integration) (1W laser power) | ±.2 m/s (80 Hz update) (2 W laser power) |
| update rate | 1 Hz | 80 Hz for AoA and AoS<br>20 Hz for others |
| pressure uncertainty | ± 700 Pa (127mW laser power) | ± 63 Pa (80 Hz update) (2 W laser power) |
| temperature uncertainty | none quoted | ± .9 °C (10 Hz update) |
| format | RS 232 | MIL-1553 |
| physical characteristics | | |
| scanning | none (measurements from 3 separate axes) | |
| size | 0.127 $m^3$ (not including laser) | .04 $m^2$ |
| weight | 42 kg | 20 kg |
| developed by | Michigan Aerospace Corporation, Ann Arbor, MI and University of Michigan, Ann Arbor, MI | |
| funded by | US Navy and US Air Force (AFRL) | |

The MOADS sensor projects ultraviolet radiation in three directions, then senses the backscatter from the intersection of the beam volume and the detection optics fields of view. The system design is based on the bistatic concept as defined in chapter 2 and uses masking to delineate the measurement volume as described in section 3.2. Direct detection is accomplished using a high-finesse etalon to extract three velocities in the three directions of beam projection. Temperature is measured by assessing the spectral width of the backscattered signals from the three beam directions. The shift in the centroid of the

backscattered signal is indicative of the mean velocity of the air molecules, which is directly related to the static temperature of the air. Density is measured by assessing the magnitude of the backscattered signal after removing that component attributable to aerosol backscatter. Sections 3.4.1.1 and 3.4.1.2 of this document provide a short overview of density and temperature measurement using molecular backscatter. Pressure is computed by applying temperature and density into the perfect gas law. Figure 7-5 illustrates the prototype optical head and fiber optic coupled Signal Processor-Detector assembly.

The outputs from the three etalon detector channels are digitally encoded and processed to provide the air data parameters at the required update rate. MOADS update rate, measurement accuracy, and laser power are intimately interlinked as noted in Table 7.3. Measurement accuracy is inversely proportional to the inverse second-power of the laser power output.

The primary value of the MOADS activity was to confirm the theoretical assumptions regarding the laser system performance and the statistics that drive this performance. With the information confirmed regarding the laws governing the operation of an ultraviolet-based laser air data system, it has been possible to predict with a reasonable degree of certainty the expected performance of a future system designed according to the operating laws. A primary requirement is the laser power necessary for achieving the specified measurement accuracy. The next phase of MOADS development involves a low-dynamics flight demonstration of the current prototype and funding the production of a ruggedized laser capable of operating in a high-dynamics environment. This laser power requirement will await the maturation of this technology to allow production of these systems at reasonable prices.

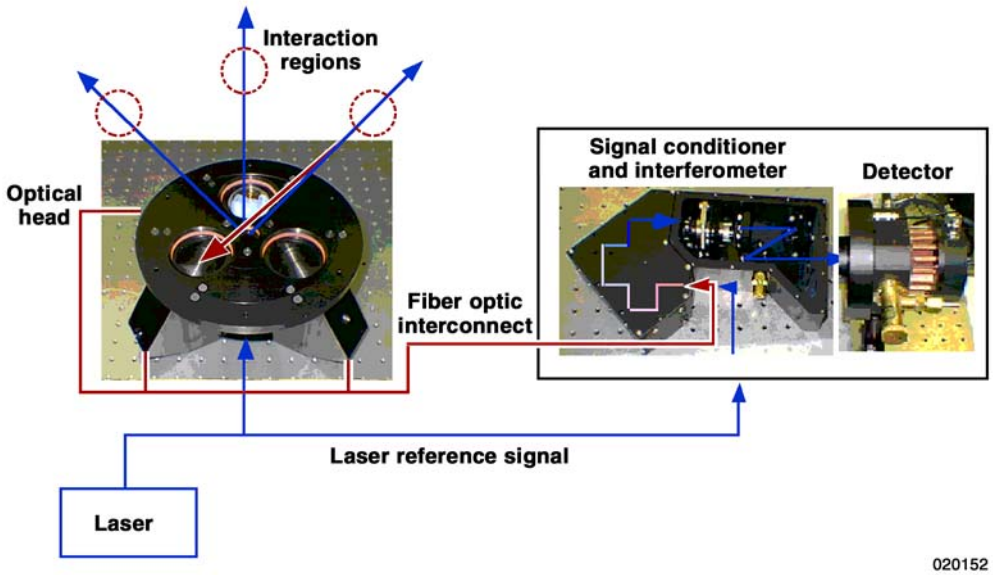


**Figure 7-5: MOADS prototype optical head and signal processor detector.**

## 7.3 Warning System for Atmospheric Threat

### 7.3.1 Thales wake vortex system

There are several systems under investigation for the detection of atmospheric threats to aircraft. A promising approach is followed by a European consortium under the leadership of Thales, Valence, France in the Multifunction Future Laser Atmospheric Measurement Equipment (MFLAME) project (Combe - 2000). The objectives of the project are to develop an airborne system for detecting wake vortices, wind shear, clear air turbulence, volcanic ash, mountain rotor, and hail with one system. These hazards are not detected with onboard weather radar. The system is based on a reference-beam laser anemometer. The pulsed laser of the system emits light at a 2-micrometer wavelength with a repetition rate of 500 pulses per second. An air mass in front of the aircraft at 800 m to 2300 m and in a 3-degree by 12-degree solid angle is scanned in three seconds. From each pulse the velocity distribution at 21 distances is derived using time-gating as shown in fig 7-6. In this way, 21 images with 1500 velocities are gathered by the system. In these image patterns characteristics for the different hazards are searched. If a hazard is detected, an alarm is generated for use in the cockpit.

The first experiments were done in early 2000 with a prototype system installed on the ground, 600 m before the runway threshold of Toulouse Airport, in Toulouse, France. Images of airflow behind landing aircraft were gathered with a system for optimizing vortex image recognition algorithms and are shown in fig 7-6. The eventual goal is to develop equipment for installation on commercial airliners.

Miniaturization of the system and implementation of a system for the correction of aircraft motion are the next steps in the development. For widespread application of this system, low cost is a requirement.

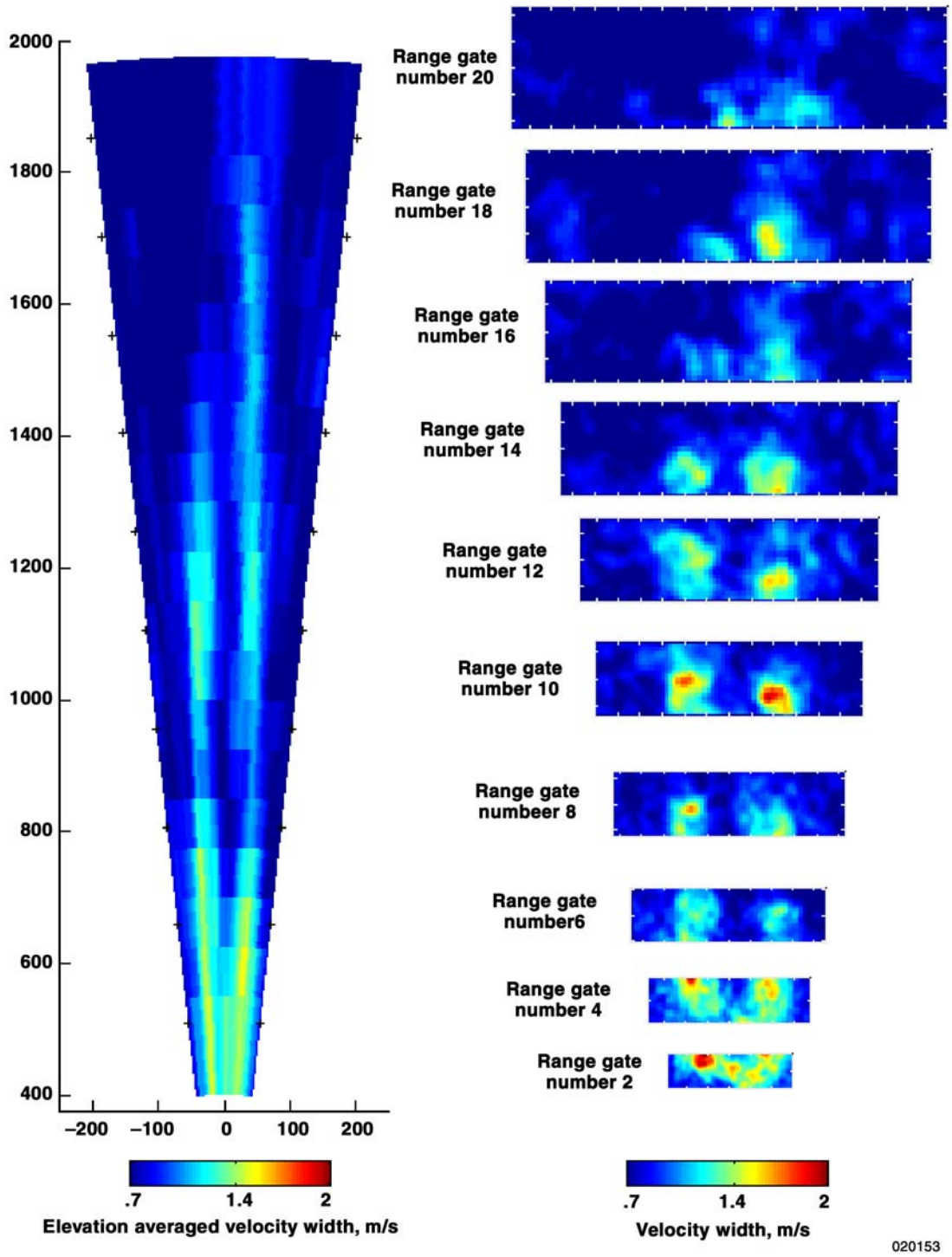


**Figure 7-6: Images of vortices obtained with the ground-based demonstrator.**

### 7.3.2 ACLAIM airborne forward-looking turbulence warning system

The detection of turbulence before it reaches the airplane has been a goal of the ACLAIM program since its inception in 1994. ACLAIM stands for Airborne Coherent Lidar for Advanced In-flight Measurements, and was a NASA/Dryden-led program to develop and demonstrate an airborne Doppler lidar system for look-ahead turbulence detection. Turbulence detection has several tangible benefits for commercial airplanes.

Aircraft engine inlets for supersonic aircraft are susceptible to an unstart condition that causes sudden dramatic changes in drag and thrust. These drag and thrust changes precipitate motions to the subject aircraft

that are clearly unacceptable for commercial revenue passenger operations. Atmospheric turbulence is a major factor in precipitating inlet unstart. The original objective for the ACLAIM program was to detect turbulence from supersonic aircraft with sufficient warning time to configure the inlet for safe transit of the turbulent atmospheric region. It was the need to operate in the high-speed supersonic flight regime with large Doppler frequency shift that generated a requirement to offset the transmitted frequency to keep the received difference frequency within the detector bandwidth. This approach is discussed in section 4.2.6. Table 7-4 is a summary of the ACLAIM characteristics.

**Table 7-4: Characteristics of the ACLAIM forward-looking turbulence warning system.**

| Factor | Detail |
|---|---|
| anemometer type: | reference beam laser Doppler anemometer |
| laser | Tm Ho YAG |
| wavelength | 2.012 μm |
| operating mode | pulsed |
| power | 12 mJ x 100 pps = 1.2 watts |
| detection | coherent mode using avalanche silicon photodiode |
| measurement | single component airspeed at 96 ranges to maximum range |
| distance | 0 to >10 Km |
| size of measurement volume | ~100m long × 0.1 m diameter |
| physical characteristics | |
| size (transceiver) | .5 m length, .4 m width |
| size (optical unit) | diameter 0.03 m, length 0.115 m |
| developed by | Coherent Technologies, Inc. |
| funded by | NASA Dryden Flight Research Center, Edwards, CA |

Clearly, if turbulence can be detected before it affects the airplane, warnings issued to the passengers and flight attendants can reduce injuries significantly. Operating in conjunction with to-be-developed flight control algorithms, the warning of turbulence can be used to change the autopilot mode, potentially reducing the peak vertical accelerations, or even used as input to the flight controls system to actively counteract the effects of turbulence.

The ACLAIM program has developed a lidar system for use in prototypes of the systems described above. In late March and early April of 1998 the first flight test of the lidar system was performed. These flight tests are the first in a series of tests of the lidar sensor. While future tests will include a system to scan the laser beam, for this test the laser beam was aligned with the airplane body axis and was directed forward moving with the aircraft. The aircraft was an L-188 Lockheed Electra operated by the National Center for Atmospheric Research from the Broomfield, Colorado facility. This aircraft has a sophisticated array of aerosol instrumentation, a gust probe, global positioning equipment, and data acquisition systems to allow comparisons between the lidar and other aircraft measurement systems. About 14 hours of flight data were acquired during 5 flights.

The purpose of the ACLAIM program is ultimately to establish the viability of lidar as a forward-looking sensor for turbulence. The immediate goals of this flight test were; 1) to demonstrate that the ACLAIM lidar system operates reliably in a flight test environment, 2) measure the performance of the lidar as a function of the aerosol backscatter coefficient ($\beta$), and 3) use the lidar system to measure atmospheric turbulence and compare these measurements to onboard gust measurements.

Figure 7-7 shows the outside folding mirror installation on the Electra aircraft. The system was installed in a staring mode, that is, the beam did not move relative to the aircraft, so any aircraft motion was reflected in corresponding beam motion.

The standard deviation of the lidar-measured velocity has been calculated from overlapping sets of 5 data points. In figure 7-8 this is compared with the normal acceleration. A 6-second lag is applied to the normal acceleration data to show the correlation between the lidar prediction and the airplane response. The lidar data provides a 6-second warning of the disturbance. It should be pointed out that this is not the maximum possible warning, but a convenient value for the analysis. Data was available out to warning times of up to 100 seconds. The turbulent encounter shown in this plot is from flight number 2, and the log records strong turbulence. The increase in vertical acceleration is predicted well by the velocity standard deviation as shown in the figure. For comparison purposes, the units on the vertical scale are nondimensional (obtained by dividing the 5-second rms average by the mean over the same time window).

Preliminary analysis of the flight data shows that there was no turbulence encountered on the flight that was not predicted from the lidar data. Further testing will be required at altitudes above FL 250 to confirm the performance at altitudes more commonly used by commercial airlines.


**Figure 7-7: Folding mirror housing on the Electra testbed aircraft.**

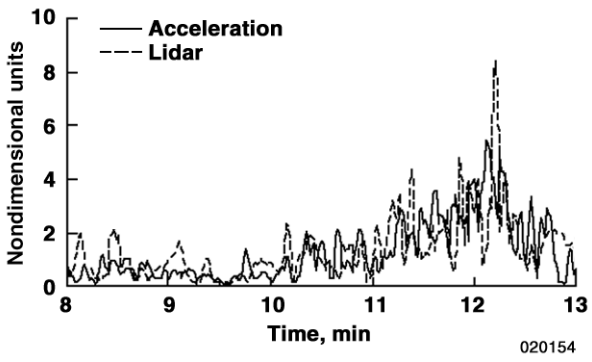


**Figure 7-8: Aircraft normal acceleration and lidar velocity standard deviation.**

## 7.4 Near Flow Field Investigation

Where the application of optical flow measurements is common practice for investigations of aerodynamics in wind tunnels, it is rarely applied for in-flight near-field investigations. Several techniques have been considered for the in-flight application and potentials have been demonstrated. ISL, Saint-Louis, France (Mainone-1978[73]); University of Erlangen, Erlangen, Germany (Becker-1999[63]); and NLR, Amsterdam, The Netherlands (Jentink-1995[62], Jentink-1994[74]) demonstrated the potential of the dual-beam laser Doppler technique. The DLR Cologne, Germany demonstrated the laser two-focus technique. NASA Langley, US (Meyers-1995[39]) considered the DGV technique for investigating the vortices generated by an F-18 in flight, but the concept was not demonstrated in flight. The dual-beam laser Doppler system described below and the measurement results using that system, indicate what is possible and what are problems for the application. Table 7-5 is a summary of the dual-beam Doppler characteristics.

The boundary layer on an NLR research aircraft was measured in flight to demonstrate the potential of dual-beam laser Doppler anemometry. The anemometer used in the demonstration has a small measurement probe that is connected with optical fibers to a unit with components for the generation and detection of light. A third unit provides the electronic signal processing and electrical power supply of the anemometer. The small robust measurement probe can be installed in various places where the aerodynamic flow field is to be measured. The disadvantage of the use of optical fibers are the optical power losses, 60 percent of the light is lost coupling light in the (singlemode) fibers for guiding the light to the measurement volume. Further characteristics of the instrument are given in table 7-2 and in reference 62.

**Table 7-5: Characteristics of the dual-beam laser Doppler anemometer.**

| Factor | Details |
|---|---|
| anemometer type | dual-beam laser doppler anemometer, CW |
| laser | diode laser |
| wavelength | 0.850 μm |
| operating mode | continuous wave |
| power | 0.12 W |
| detector | avalanche silicon photodiode |
| measurement | local flow velocity at a point |
| distance | between 0 and 0.12 m |
| size of measurement volume | diameter 56 μm, length 830 μm |
| physical characteristics | |
| scanning | mechanical displacement of the probe |
| size (optical unit) | diameter: 0.03 m, length 0.115 m |
| developed by: | University of Erlangen and Invent GmbH (Erlangen, Germany) |

The velocities in the boundary layer were measured in flight tests as shown in figure 7-9. The number of particles in the air appeared very critical for these measurements. In clear air the data rate for the measurements was too low for acquiring data in a reasonable time. Even polluted air from chimneys or in inversion layers contained an insufficient concentration of particles; the data rates were on the order of 1 to 10 measurements per second. In air with visible moisture (clouds) data were obtained with data rates considered sufficient for aerodynamic research (100 to 800 measurements per second).

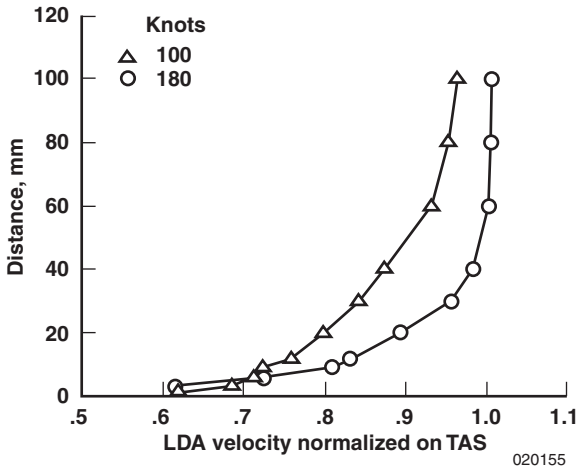


**Figure 7-9: Normalized air velocities measured with dual-beam LDA in the boundary layer.**

These measurements were obtained from the boundary layer of the fuselage of the NLR Cessna Citation II. The results are displayed as a function of the distance in the boundary layer, where 0 mm corresponds to the aircraft skin. Velocities are normalized on TAS and were measured at 100 kts TAS (Δ) and 180 kts TAS (O). Lines are drawn to guide the eye to the groupings of data points.

In very early experiments during the years from 1976 to 1984, ISL experienced similar limitations resulting from low particle concentrations with a dual-beam laser-pulsed Doppler anemometer (Mainone 1978[73]). Applying lasers with higher light power and with shorter wavelength than were used in these early experiments may reduce the limitations (Grosche 2000[75]), but the extent of the reductions is currently not clear. Applying seeding particles in the airflow, which is common practice for investigations in wind tunnels, is not an option for most in-flight applications, as this disturbs the flow that is to be measured.

Even smaller dual-beam laser anemometers have been developed, such as those at ISL (Damp 1991[76], Damp 1994[77]). The size of the optical head of the anemometer is 50 x 50 x 50 $mm^3$ and the electronics is integrated in a unit of the same size. As yet, the unit has not been flight tested.

# Chapter 8 – FUTURE PROSPECTS AND DIRECTIONS

## 8.1 Introduction

The future of optical airflow measurements in flight is discussed using an approach in which trends are analyzed from two different perspectives. On one hand there are several needs for in-flight measurements that may be met by applying optical airflow measurements. On the other hand the new technology developments in optical components, mostly for optical communication, provide the avionics design engineer and flight test instrumentation engineer a perspective of developing systems with low power consumption and small size. Both perspectives are discussed below, where the current and near future limitations and challenges for the introduction of optical airflow measurements in flight are also addressed.

## 8.2 The Need Perspective

The need for low radar cross-sections and the increased dynamics of modern fighter aircraft generate new requirements for optical air data systems. The introduction of optical airflow measurements for this flight-critical operational application requires that questions of system reliability must be answered, particularly regarding continuity of signals. Apart from the loss of signal because too few particles are in the air, there should also be a solution for the measurements in air with a very large number of scatterers. The availability of signals generated by aerosols needs further investigation, particularly in the upper troposphere where the aerosol density may sometimes be insufficient for some systems. Light scattering on air molecules instead of aerosols may be a solution for the insufficient aerosol condition, but these anemometers, that are based on Rayleigh scattering, are not mature and require further development and operational flight experience before the potential can be assessed. Further definition is required in the areas of size, cost, and maintainability. With new components becoming available, smaller size, less weight, lower cost, and higher reliability systems are easier to design and construct.

The request from society to improve flight safety stimulates the development of remote detection of atmospheric hazards that are not now detected with conventional weather radar. Optical airflow measurements are showing promise for this application. Optical measurements with onboard systems seem more promising than ground systems or satellite systems, as the air space in the vicinity of a specific aircraft can be searched for hazards instead of conducting more general overall searches of the atmosphere. Onboard systems face the high operational requirements that are mentioned above for air data system applications. As the application is directed more toward commercial airliner applications, the limitation on the cost of systems is probably even more stringent than for air data systems alone. Widespread application in this area may await the next generation of technology to achieve cost and operational requirements.

Needs for the other applications mentioned in this volume have a much smaller impact on aircraft operations in general. Laser anemometry has proven to be a valuable technique in many aviation research projects where remote detection in “clean” air (using only naturally occurring aerosols) is unique. For the authors there is no doubt that this technique will find further applications in flight research that utilize its unique features. In general, only a few tailored systems will be needed for the applications that support specific research goals.

Some systems can also be expected to be introduced for air data system calibrations. The maturity of reference-beam laser anemometry for this application has already been proven and expanded use of the technique is expected for calibrating air data systems of new aircraft types. The availability of small systems that are easy to operate will stimulate the use of this application.

The need for improved parachute drop accuracy is for only a few specialized operations. The optical airflow measurement technique seems to fulfill the requirements for these operations quite satisfactorily. Further applications of this technique seems likely.

## 8.3 The New Technology Perspective

The development of new lasers is expected to markedly increase the availability of very useful components for in-flight optical airflow measurement systems. Smaller lasers with improved optical performance, such as those with high-energy conversion efficiency, Gaussian beam profiles (at both the “eye-safe” wavelengths and in the blue and UV wavelengths) are expected to become available from developments in the optical communication community. Introduction of these new lasers in systems for optical airflow measurements is likely to alleviate several limitations for the installation and the operation of systems.

Technology to miniaturize systems, including optical systems, is found in the integrated circuit and silicon chip operations. Integrated optics and Microelectromechanical systems (MEMS) can provide a valuable spin-off for the development of optical flow meters. In the area of signal processing, the ever-increasing potential of digital signal processing can alleviate the burden of performing complicated processing and interpretation algorithms in real time.

Regretfully the methods to measure air flow for ground applications, such as wind tunnel settings, are not the same as the methods that are most promising for the in-flight application. The possibility to seed air with particles for optical flow measurements on the ground and the different requirements for the ground applications lead to the reference beam technique seldom being applied on the ground, whereas it is the most promising method in flight.

## 8.4 Concluding remark

In the future interesting research and development can be expected from optical airflow measurement in flight. Major improvements in avionics and flight test instrumentation can result from this research and development.

# Chapter 9 – REFERENCES

## 9.1 References cited in text

1. *Safe Use of Lasers in an Outdoor Environment*, ANSI Z136.6-2000, published by the American National Standards Institute, Washington, D. C. and New York, N. Y.

2. *Safe Use of Lasers*, ANSI Z136.1-2000, published by the American National Standards Institute, Washington, D. C. and New York, N. Y.

3. Silfvast, W. T.; *Laser Fundamentals*, Cambridge University Press, Cambridge, UK, 1996.

4. Loudon, R.; *The quantum theory of light*, second edition, Clarendon Press, Oxford, UK, 1983.

5. Vaughan, J. M.; P. A. Forrester; "Laser Doppler Velocimetry Applied to the Measurement of Local and Global Wind," *Wind Eng*., Vol. 13, No. 1, 1989, p. 1.

6. Kogelnik, H; Li, T.; "Laser beams and resonators," *Appl. Optics*, Vol. 5, 1966, p. 1550–1567.

7. Harris, M.; G. N. Pearson; K. D. Ridley, C. J. Karlsson, F. A. A. Olsson, D. Letalick; "Single-particle laser Doppler anemometry at 1.55 μm," *Appl. Optics*, Vol. 40, 2001, p. 969–973.

8. van de Hulst, H. C.; *Light Scattering by Small Particles*, 2nd ed., Dover Publications Inc., New York, 1981.

9. Mendoza, J.; I. Catton; and M. Azzazy; "The Feasibility of Evaluating Flowfield Temperatures and Pressures Using Broadband Excitation and Detection," *Proc. ASME FED Summer Meeting: Laser Anemometry & Experimental and Numerical Flow Visualization Symposium*, FEDSM98-5257, Washington DC, USA, June 21–25, 1998.

10. Azzazy, M.; J. B. Abbiss; and R. W. McCullough; "Determination of Aircraft Pressure, Altitude, and Ambient Temperature Using Fluorescence and Rayleigh Scattered Radiation from a Continuum Source." *Combusting Flow Diagnostics*, NATO Science Series E, Vol. 207, published by Kluwer Academic Publishers, April 1990.

11. Mie, G.; "Optics of Turbid Media," *Ann. Phys*., vol. 25, No. 3, 1908, pp. 377–445.

12. *Laser Speckle and Related Phenomena*, edited by J. C. Dainty. Series: Topics in Applied Physics, Vol. 9, Springer-Verlag, New York, 1975.

13. Vaughan, J. M.; D. W. Brown; C. Nash; S. B. Alejandro; and G. G. Koenig; "Atlantic atmospheric aerosol studies: 2. Compendium of airborne backscatter measurements at 10.6 μm," *Journal of Geophysical Research*, Vol. 100, No. D1, 1995, pp. 1043–1065.

14. Deirmendjian, D.; "Scattering and Polarization Properties of Water Clouds and Hazes in the Visible and Infrared," *Appl. Optics*, Vol. 3, No. 2, 1964, pp. 187–196.

15. Kane T. J.; B. Zhou; R. L. Byer; "Potential for coherent Doppler wind velocity lidar using neodymium lasers," *Appl. Opt*., Vol. 23, No. 15, 1984, p. 2477.

16. Targ, R.; B. C. Steakley; J. G. Hawley; L. L. Ames, Paul Forney; D. Swanson; R. Stone; R. G. Otto; V. Zarifis; P. Brockman; R. S. Calloway; S. Harrell Klein; and P. A. Robinson; "Coherent lidar airborne wind sensor II: flight-test results at 2 and 10 μm," *Appl. Optics*, Vol. 35, No. 36, 1996, p. 7117.

17. Sonnenschein, C. M. and F. A. Horrigan; "Signal-to-Noise Relationships for Coaxial Systems that Hetrodyne Backscatter from the Atmosphere," *Appl. Optics*, Vol. 10, No. 7, July 1971, pp. 1600–1604.

18. Keeler, R. J.; R. J. Serafin; R. L. Schwiesow; D. H. Lenschow; J. M. Vaughan; A. A. Woodfield; "An Airborne Laser Air Motion Sensing System, Part 1: Concept and Preliminary Experiment," *J. of Atm. and Oceanic Techn.*, Vol. 4, 1987, pp. 113–127.

19. Vaughan, J. M.; R. D. Callan; D. A. Bowdle; and J. Rothermel; "Spectral analysis, digital integration, and measurement of low backscatter in coherent laser radar," *Appl. Opt*., Vol 28, No. 15, 1989, p. 3008.

20. *Handbook of optics, Volume 1, Fundamentals, Techniques, and Design*, 2nd Ed. Edited by M. Bass, E. W. Van Stryland, D. R. Williams, and W. L. Wolfe. McGraw-Hill, Inc., New York, 1995.

21. Born, M.; E. Wolf; *Principles of Optics, Electromagnetic theory of propagation, interference and diffraction of light*, Seventh (Expanded) edition, Cambridge University Press, UK, 1970.

22. Hecht, J.; *The Laser Guidebook*, Optical and Electro-optical Engineering Series, 2nd ed., McGraw-Hill, New York, 1992.

23. Yu, F. T. S.; X. Yang; *Introduction to Optical Engineering*, Cambridge University Press, Cambridge, 1997.

24. Bachalo, W. D.; M. J. Houser; "Phase/Doppler spray analyzer for simultaneous measurements of drop size and velocity distributions," *Opt. Eng.*, Vol. 23, No, 5, 1984, pp. 583–590.

25. Durst, F.; G. Brenn; T. H. Xu; "A review of the development and characteristics of planar phase-Doppler anemometry," *Meas. Sci. Technol.*, Vol. 8, 1997, pp. 1203–1221.

26. Durst, F.; A. Melling; J. H. Whitelaw; *Principles and Practice of Laser-Doppler Anemometry*, 2nd ed., Academic Press, London, 1981.

27. Drain, L. E.; *The Laser Doppler Technique*, John Wiley & Sons, Chichester, U. K., 1980.

28. Rietmuller, M. L.; and A. Boutier, "Laser velocimetry," *VKI Lecture Series-05*, von Karman Institute for Fluid Dynamics, 10–14 June 1991, Chausée de Waterloo, 72, Rhode Saint Genèse, Belgium, 1991.

29. Hays, P. B.; "High-resolution optical measurements of atmospheric winds from space. 1: Lower atmosphere molecular absorption," *Appl. Optics*, Vol. 21, No. 6, 1982, pp. 1136–1141.

30. Korb, C. L.; B. Gentry; Chi Weng; "The edge technique: theory and application to the lidar measurement of atmospheric wind," *Appl. Optics*, Vol. 31, No. 21, 1992, p. 4202.

31. McGill, M. J. and J. D. Spinhirne; "Comparison of two direct-detection Doppler lidar techniques," *Optical Engineering*, Vol. 37, No. 10, 1998, pp. 2675–2686.

32. Korb, C. L.; B. M. Gentry; S. Xingfu Li; "Edge technique Doppler lidar wind measurements with high vertical resolution," *Appl. Optics*, Vol. 36, No. 24, 1997, pp. 5976–5983.

33. Korb, C. L.; B. M. Gentry; S. Xingfu Li; Cristina Flesia; "Theory of the double-edge technique for Doppler lidar wind measurement," *Appl. Optics*, Vol. 37, No. 15, 1998, pp. 3097–3112.

34. Skinner, W. R. and P. B. Hays; "Incoherent Doppler lidar for measurement of atmospheric winds," *Optical spectroscopic techniques and instrumentation for atmospheric and space research, SPIE vol. 2266*, 1994, pp. 383–394.

35. Abreu, Vincent J.; John E. Barnes; Paul B. Hays; "Observations of winds with an incoherent lidar detector," *Appl. Optics*, Vol. 31, No. 22, 1992, pp. 4509–4514.

36. Rees, D.; T. J. Fuller-Rowell; A. Lyons; T. L. Killeen; P. B. Hays; "Stable and rugged etalon for the Dynamics Explorer Fabry-Perot interferometer. 1: Design and construction," *Appl. Optics*, Vol. 21, No. 21, 1982, pp. 3896–3902.

37. Rees, D.; and I. S. McDermid; "Doppler lidar atmospheric wind sensor: reevaluation of a 355-nm Incoherent Doppler lidar," *Appl. Opt*., Vol. 29, No. 28, 1990, pp. 4133–4144.

38. Hecht, Eugene; Zajac, Alfred; *Optics*, Addison Wesley Publishing Company, 1974.

39. Meyers, J. F.; "Development of Doppler Global Velocimetry as a Flow Diagnostics Tool," *Meas. Sci. Technol.*, Vol.6, No. 6, 1995, pp. 769–783.

40. Roehle, I.; "Doppler Global Velocimetry," Lecture Series 1998-06: *Advanced Measurement Techniques*, von Karman Institute of Fluid Dynamics, Brussels, 1998.

41. Roehle, I.; "Doppler Global Velocimetry," paper 4, RTO-EN-6 RTO AVT Lecture Series, *Planar Optical Measurement Methods for Gas Turbine Components*, 1999.

42. Roehle, I.; R. Schodl; P. Voigt; C. Willert; "Recent developments and applications of quantitative laser light sheet measuring techniques in turbomachinery components," *Meas. Sci. Technol.*, Vol.11, 2000, pp. 1023–1035.

43. Roehle, I.; C. E. Willert; "Extension of Doppler global velocimetry to periodic flows," *Meas. Sci. Technol.*, Vol 12, 2001, pp. 420–431.

44. Meyers, J. F.; J. W. Lee; R. J. Schwartz; "Characterization of measurement error sources in Doppler global velocimetry," *Meas. Sci. Technol.*, Vol. 12, 2001, pp. 357–368.

45. Meyers, J. F.; *Investigation and Calculations of Basic Parameters for the Application of the Laser Doppler Velocimeter*, NASA Technical Note D-6125, April 1971.

46. Schodl, R.; "Laser-two-focus velocimetry." In *Advanced Instrumentation for Aero Engine Components*. AGARD-CP-399 (Philadelphia) p. 7, 1986.

47. Schodl, R.; W. Förster; G. Karpinski; H. Krain; I. Röhle; "3-Component Doppler Laser-Two-Focus Velocimetry Applied to a Transonic Centrifugal Compressor," *10th International Symp. on Application of Laser Techniques to Fluid Mechanics*, Lisbon, Portugal, July 2000, Paper 7-2, 2000.

48. Woodfield, A. A.; J. M. Vaughan; "Using an Airborne $CO_2$ Laser for Free Stream Airspeed and Windshear Measurements," *AGARDograph-AG-272, Advances in Sensors and Their Integration into Aircraft Guidance and Control Systems*, 1983, p. 7.

49. Smart, A. E.; "Optical velocity sensor for air data applications," *Opt. Eng.*, Vol. 31, No. 1, 1992, pp. 166–173.

50. McGann, R. L.; "Flight test results from a low-power Doppler optical air data sensor," *Proc. Air traffic control technologies, SPIE vol. 2464*, April 1995, pp. 116–124.

51. Mandle, J. and F. X. Weiss; "New calibration methods in air data measurement for low-speed helicopters," *AGARD CP 359*, p. 16, May 1984.

52. Mandle, J. and E. Fabacher; “Laser anemometry for flight test,” *Proceedings ETTC '91*, 25–26 June 1991, Toulouse, France, pp. 3–4.

53. Alonso, F.; “Anemometric Calibration Test Methods for Airbus A330/340”, *Proceedings ETTC 91*, 25-26 June 1991, Toulouse, France, pp. 2–7.

54. Cattin-Valsecchi, F.; C. Lopez; “Utilisation d’un velocimetre laser triaxe pour calibration anemometrique sur AIRBUS A340,” *AGARD-FMP-Symposium*, AGARD-CP-519, 1992, p. 26.

55. Köpp, F.; “Airborne $CO_2$ Doppler Lidar for Wind Shear Detection,” *Aircraft Integrated Monitoring Systems*, Oberpfaffenhofen, Germany, 1990, pp. 481–499.

56. Fetzer, G. J.; M. J. Post; “A low cost cw CO2 lidar system for low-level wind shear detection,” *SPIE Vol. 1222 Laser Radar V*, 1990, pp. 130–141.

57. Bogue, R. K.; H. R. Bagley; D. C. Soreide; “Coherent lidar solution for the HSCT supersonic inlet unstart problem,” in *Air Traffic Control Technologies, SPIE Proc. 2464,* March 1995, pp. 79–93.

58. Hannon, S. M.; J. A. Thomson; “Aircraft wake vortex detection and measurement with pulsed solid-state coherent laser radar,” *J. of Modern Optics*, Vol. 41, No. 11, 1994, pp. 2175–2196.

59. Keane, M.; M. Redfern; “Airborne Wind Shear Detection with the MFLAME 2 μm Lidar,” *Proc. 9th Conf. on Coherent Laser Radar*, June 23–27, 1997, Linköping, Sweden, 1997, p. 126.

60. Combe, H.; F. Köpp; M. Keane; “MFLAME On-Board Wake Vortex Detection: Definition, ground experimentation and results in the MFLAME EC Programme,” *3rd Wake-Net workshop,* Great Malvern, UK, 22-23 May 2000. On the Web at http://www.cerfacs.fr/~wakenet/instru/fields/Malvern-Article.htm.

61. Köpp, F.; G. Powilleit; “Investigation of the 3d wake-vortex velocity field for the development of airborne detection systems,” *Proc. 9th Conf. on Coherent Laser Radar*, Linköping, Sweden, June 23–27, 1997, p. 317.

62. Jentink, H. W.; M. Beversdorff; W. Förster; “Laser Anemometry for In-Flight Investigations,” *Proceedings 5th IEEE-ICIASF Conference*, Dayton, Ohio, USA, 18–21 July 1995, p. 23.

63. Becker, S.; F. Durst; H. Lienhart; “Laser Doppler Anemometer for In-Flight Velocity Measurements on Airplane Wings,” *AIAA Journal* Vol. 37, No. 6, 1999, pp. 680–687.

64. McCaul, E. W., Jr.; H. B. Bluestein; and R. J. Doviac; “Airborne Doppler lidar techniques for observing severe thunderstorms,” *Appl. Optics* Vol. 25, No. 5, 1986, p. 698.

65. Kristensen, L. and D. H. Lenschow; “An Airborne Laser Air Motion Sensing System. Part II: Design Criteria and Measurement Possibilities,” *J. of Atm. and Oceanic Techn.*, Vol. 4, 1987, p. 128.

66. Reitebuch, O.; Ch. Werner; I. Leike; P. Delville; P. Flamant; A. Cress; D. Engelbart; “Experimental Validation of Wind Profiling Performed by the Airborne 10-μm Heterodyne Doppler Lidar WIND,” *J. Atmos. Oceanic Technol.*, Vol. 18, No. 8, 2001, pp. 1331–1344.

67. Werner, Ch.; P. Flamant; O. Reitebuch; F. Köpp; J. Streicher; S. Rahm; E. Nagel; M. Klier; H. Herrmann; C. Loth; P. Delville; Ph. Drobinski; B. Romand; Ch. Boitel; D. Oh; M. Lopez; M. Meissonnier; D. Bruneau; A. Dabas; “Wind infrared Doppler lidar instrument”, *Opt. Eng*., 40, 115–125, 2001.

68. Rahm, S.; “Precursor experiment for an active airspeed sensor,” *Optics Letters*, Vol. 26, No. 6, 2001, pp. 319–321.

69. Richmond, R.; D. Jewell; J. Carr; and J. Root; “U.S. Air Force ballistic winds program,” *SPIE Proc*. Vol. 3065, *Laser Radar Technology and Applications II*, 21–25 April 1997, Orlando, FL, 1997. pp. 2–8.

70. Ott, J.; “Lidar 'reads' air-drop winds,” Aviation Week & Space Technology, 12 Feb. 1996, p. 44.

71. Erwin, L. L.; R. K. McGann; D. C. Soreide; D. L. Morris; “Enhanced Mode Lidar for Airborne Airspeed Measurement,” *Proceedings of the Seventh Conference on Coherent Laser Radar Applications and Technology*. Paris, France, July 1993.

72. Tchoryk, P. Jr.; C. B. Watkins; S. K. Lindemann; P. B. Hays; C. A. Nardell; “Molecular Optical Air Data System (MOADS),” *SPIE Proc. 4377, Laser Radar Technology and Applications VI*, 16–20 April 2001, Orlando, FL, Paper 4377-28.

73. Mainone, D. and X. Bouis; “Verwendung eines Farbstofflasers mit hoher Spitzenleistung und langer Pulsdauer zur Messung der ‘Luftgeschwindigkeit’ vom Flugzeug aus,” *Z. Flugwiss*, Weltraumforsch. 2, Heft 3, 1978, p. 151.

74. Jentink, H. W.; M. Stieglmeier; C. Tropea; “In-Flight Velocity Measurements Using Laser Doppler Anemometry,” *J. of Aircraft*, Vol. 31, No, 2, 1994, pp. 444–446.

75. Grosche, E. G.; N. Pape; H. Müller; V. Strunck; “Range and accuracy of a Laser-Doppler Anemometer for in-flight measurements,” *10th Int. Symp. on Appl. of Laser Techniques to Fluid Mechanics*, 10–13 July 2000, p. 4.2.

76. Damp, S.; “Miniature Laser Doppler Anemometer for Sensor Concepts,” *Proc. OE LASE '91, SPIE International Symposium vol. 1418*, Paper 52, *Laser diode technology and applications III*, Los Angeles, CA, USA, 20–25 Jan. 1991.

77. Damp, S. M.; E. Sommer; H. J. Pfeifer; “ASIC Based Signal Processing Unit in the Miniature LDA-Sensor Concept, Using Minimal Cross-Correlation,” *Proceedings of the 7th Int. Symp. on Applications of Laser Techniques to Fluid Mechanics*, Lisbon, Portugal, 11–14 July 1994.

## 9.2 Bibliography

Abreu, Vincent J.; John E. Barnes; Paul B. Hays; "Observations of winds with an incoherent lidar detector," *Appl. Optics*, Vol. 31, No. 22, 1992, pp. 4509–4514.

Alonso, F.; "Anemometric Calibration Test Methods for Airbus A330/340", *Proceedings ETTC 91*, 25-26 June 1991, Toulouse, France, pp. 2–7.

Azzazy, M.; J. B. Abbiss; and R. W. McCullough; "Determination of Aircraft Pressure, Altitude, and Ambient Temperature Using Fluorescence and Rayleigh Scattered Radiation from a Continuum Source." *Combusting Flow Diagnostics*, NATO Science Series E, Vol. 207, published by Kluwer Academic Publishers, April 1990.

Bachalo, W. D.; M. J. Houser; "Phase/Doppler spray analyzer for simultaneous measurements of drop size and velocity distributions," *Opt. Eng.*, Vol. 23, No, 5, 1984, pp. 583–590.

Becker, S.; F. Durst; H. Lienhart; "Laser Doppler Anemometer for In-Flight Velocity Measurements on Airplane Wings," *AIAA Journal* Vol. 37, No. 6, 1999, pp. 680–687.

Bilbro, J. W.; "Atmospheric laser Doppler velocimetry: an overview", *Opt. Eng.*, Vol. 19, No. 4, 1980 pp. 533–542.

Bilbro, J. W.; C. DiMarzio; D. Fitzjarrald; S. Johnson; W. Jones; "Airborne Doppler lidar measurements", *Appl. Opt.*, Vol. 25, No. 21, 1986, pp. 3952.

Bilbro, J. W.; S. C. Johnson; J. Rothermel; "Wind velocity measurement accuracy with highly stable 12 mJ/pulse high repetition rate $CO_2$ laser master oscillator power amplifier", NASA CP 2456, *Closed-cycle, frequency-stable $CO_2$ laser technology*, 1986, pp. 33–45.

Bogue, R. K.; H. R. Bagley; D. C. Soreide; "Coherent lidar solution for the HSCT supersonic inlet unstart problem," in *Air Traffic Control Technologies*, *SPIE Proc. 2464*, March 1995, pp. 79–93.

Bogue, R.; R. McGann; T. Wagener; J. Abbiss; A. Smart; "Comparative Optical Measurements of Airspeed and Aerosols on a DC-8 Aircraft", *Proceedings 5th IEEE-ICIASF Conference*, Dayton, Ohio, USA, 18-21 July 1995, pp. 56/1–56/25.

Born, M.; E. Wolf; *Principles of Optics, Electromagnetic theory of propagation, interference and diffraction of light*, Seventh (Expanded) edition, Cambridge University Press, UK, 1970.

Cattin-Valsecchi, F.; C. Lopez; "Utilisation d'un velocimetre laser triaxe pour calibration anemometrique sur AIRBUS A340," *AGARD-FMP-Symposium*, Agard-CP-519, 1992, p. 26.

Combe, H.; F. Köpp; M. Keane; "MFLAME On-Board Wake Vortex Detection: Definition, ground experimentation and results in the MFLAME EC Programme," *3rd Wake-Net workshop*, Great Malvern, UK, 22-23 May 2000. On the Web at http://www.cerfacs.fr/~wakenet/instru/fields/Malvern-Article.htm.

Damp, S.; "Miniature Laser Doppler Anemometer for Sensor Concepts," *Proc. OE LASE '91, SPIE International Symposium, Vol. 1418, Laser diode technology and applications III*, Los Angeles, CA, USA, 23–25 Jan. 1991, pp. 459–470.

Damp, S. M.; E. Sommer; H. J. Pfeifer; "ASIC Based Signal Processing Unit in the Miniature LDA-Sensor Concept, Using Minimal Cross-Correlation," *Proceedings of the 7th Int. Symp. on Applications of Laser Techniques to Fluid Mechanics*, Lisbon, Portugal, 11–14 July 1994.

Deirmendjian, D.; “Scattering and Polarization Properties of Water Clouds and Hazes in the Visible and Infrared,” *Appl. Optics*, Vol. 3, No. 2, 1964, pp. 187–196.

DiMarzio, C.; R. Chandler; M. Krause; J. O'Reilly; K. Shaw; J. Bilbro; “Airborne lidar dual wedge scanner,” NASA CP 2228, *Abstracts of papers presented at the 11th International Laser Radar Conf.*, 1982, p. 123.

Drain, L. E.; *The Laser Doppler Technique*, John Wiley & Sons, Chichester, U. K., 1980.

Durst, F.; G. Brenn; T. H. Xu; “A review of the development and characteristics of planar phase-Doppler anemometry,” *Meas. Sci. Technol.*, Vol. 8, 1997, pp. 1203–1221.

Durst, F.; A. Melling; J. H. Whitelaw; *Principles and Practice of Laser-Doppler Anemometry*, 2nd ed., Academic Press, London, 1981.

Elliott, G. S.; T. J. Beutner; “Molecular filter based planar Doppler velocimetry”, *Progress in Aerospace Sc.* Vol. 35, 1999, pp. 799–845.

Erwin, L. L.; R. K. McGann; D. C. Soreide; D. L. Morris; “Enhanced Mode Lidar for Airborne Airspeed Measurement,” *Proceedings of the Seventh Conference on Coherent Laser Radar Applications and Technology*. Paris, France, July 1993.

Fetzer, G. J.; M. J. Post; “A low cost cw CO2 lidar system for low-level wind shear detection,” *SPIE Vol. 1222 Laser Radar V*, 1990, pp. 130–141.

Förster, W.; “Laser-2-Focus Data Analysis Using a Nonlinear Regression Model,” DLR report D-51140, Köln, Germany.

Grosche, E. G.; N. Pape; H. Müller; V. Strunck; “Range and accuracy of a Laser-Doppler Anemometer for in-flight measurements,” *10th Int. Symp. on Appl. of Laser Techniques to Fluid Mechanics*, 10–13 July 2000, p. 4.2.

*Handbook of optics, Volume 1, Fundamentals, Techniques, and Design*, 2nd Ed. Edited by M. Bass, E. W. Van Stryland, D. R. Williams, and W. L. Wolfe. McGraw-Hill, Inc., New York, 1995.

Hannon, S. M.; J. A. Thomson; “Aircraft wake vortex detection and measurement with pulsed solid-state coherent laser radar,” *J. of Modern Optics*, Vol. 41, No. 11, 1994, pp. 2175–2196.

Hannon, S. M.; H. R. Bagley; R. K. Bogue; “Airborne Doppler Lidar Turbulence Detection: ACLAIM Flight Test Results,” SPIE Vol. 3707, March 1995, p. 234.

Harris, M.; G. N. Pearson; K. D. Ridley, C. J. Karlsson, F. A. A. Olsson, D. Letalick; “Single-particle laser Doppler anemometry at 1.55 μm,” *Appl. Optics*, Vol. 40, 2001, p. 969–973.

Hays, P. B.; “High-resolution optical measurements of atmospheric winds from space. 1: Lower atmosphere molecular absorption,” *Appl. Optics*, Vol. 21, No. 6, 1982, pp. 1136–1141.

Hecht, J.; *The Laser Guidebook*, Optical and Electro-optical Engineering Series, 2nd ed., McGraw-Hill, New York, 1992.

Hecht, Eugene and Alfred Zajac; *Optics*, Addison Wesley Publishing Company, 1974.

Huffaker, R. M.; R. Targ; “Performance Analysis and Technical Assessment of Coherent Lidar Systems for Airborne Wind Shear Detection”, SPIE Vol. 889 *Airborne and Spaceborne Lasers for Terrestrial Geophysical Sensing*, 1988, pp. 65.

Jentink, H. W.; M. Beversdorff; W. Förster; "Laser Anemometry for In-Flight Investigations," *Proceedings 5th IEEE-ICIASF Conference*, Dayton, Ohio, USA, 18–21 July 1995, p. 23.

Jentink, H. W.; M. Stieglmeier; C. Tropea; "In-Flight Velocity Measurements Using Laser Doppler Anemometry," *J. of Aircraft*, Vol. 31, No, 2, 1994, pp. 444–446.

Kane T. J.; B. Zhou; R. L. Byer; "Potential for coherent Doppler wind velocity lidar using neodymium lasers," *Appl. Opt.*, Vol. 23, No. 15, 1984, p. 2477.

Keane, M.; M. Redfern; "Airborne Wind Shear Detection with the MFLAME 2 μm Lidar," *Proc. 9th Conf. on Coherent Laser Radar*, June 23–27, 1997, Linköping, Sweden, 1997, p. 126.

Keeler, R. J.; R. J. Serafin; R. L. Schwiesow; D. H. Lenschow; J. M. Vaughan; A. A. Woodfield; "An Airborne Laser Air Motion Sensing System, Part 1: Concept and Preliminary Experiment," *J. of Atm. and Oceanic Techn.*, Vol. 4, 1987, pp. 113–127.

Kennedy, L. Z. and J. W. Bilbro; "Remote measurement of the transverse wind velocity component using a laser Doppler velocimeter," *Appl. Opt.*, Vol. 18, No. 17, 1979, pp. 3010.

Kogelnik, H; Li, T.; "Laser beams and resonators," *Appl. Optics*, Vol. 5, 1966, p. 1550–1567.

Köpp, F.; "Airborne $CO_2$ Doppler Lidar for Wind Shear Detection," *Aircraft Integrated Monitoring Systems*, 1990, pp. 481–499.

Köpp, F.; G. Powilleit; "Investigation of the 3d wake-vortex velocity field for the development of airborne detection systems," *Proc. 9th Conf. on Coherent Laser Radar*, Linköping, Sweden, June 23–27, 1997, p. 317.

Korb, C. L.; B. Gentry; Chi Weng; "The edge technique: theory and application to the lidar measurement of atmospheric wind," *Appl. Optics*, Vol. 31, No. 21, 1992, p. 4202.

Korb, C. L.; B. M. Gentry; S. Xingfu Li; "Edge technique Doppler lidar wind measurements with high vertical resolution," *Appl. Optics*, Vol. 36, No. 24, 1997, pp. 5976–5983.

Korb, C. L.; B. M. Gentry; S. Xingfu Li; Cristina Flesia; "Theory of the double-edge technique for Doppler lidar wind measurement," *Appl. Optics*, Vol. 37, No. 15, 1998, pp. 3097–3112.

Kristensen, L. and D. H. Lenschow; "An Airborne Laser Air Motion Sensing System. Part II: Design Criteria and Measurement Possibilities," *J. of Atm. and Oceanic Techn.*, Vol. 4, 1987, p. 128.

*Laser Speckle and Related Phenomena*, edited by J. C. Dainty. Series: Topics in Applied Physics, Vol. 9, Springer-Verlag, New York, 1975.

Loudon, R.; *The quantum theory of light*, second edition, Clarendon Press, Oxford, UK, 1983.

Mainone, D. and X. Bouis; "Verwendung eines Farbstofflasers mit hoher Spitzenleistung und langer Pulsdauer zur Messung der 'Luftgeschwindigkeit' vom Flugzeug aus," *Z. Flugwiss*, Weltraumforsch. 2, Heft 3, 1978, p. 151.

Mandle, J. and E. Fabacher; "Laser anemometry for flight test," *Proceedings ETTC '91*, 25–26 June 1991, Toulouse, France, pp. 3–4.

Mandle, J. and F. X. Weiss; "New calibration methods in air data measurement for low-speed helicopters," *AGARD CP 359*, p. 16, May 1984.

McCaul, E. W., Jr.; H. B. Bluestein; and R. J. Doviac; "Airborne Doppler lidar techniques for observing severe thunderstorms," *Appl. Optics* Vol. 25, No. 5, 1986, p. 698.

McGann, R. L.; "Flight test results from a low-power Doppler optical air data sensor," *Proc. Air traffic control technologies, SPIE vol. 2464*, April 1995, pp. 116–124.

McGill, M. J. and J. D. Spinhirne; "Comparison of two direct-detection Doppler lidar techniques," *Optical Engineering*, Vol. 37, No. 10, 1998, pp. 2675–2686.

Mendoza, J.; I. Catton; and M. Azzazy; "The Feasibility of Evaluating Flowfield Temperatures and Pressures Using Broadband Excitation and Detection," *Proc. ASME FED Summer Meeting: Laser Anemometry & Experimental and Numerical Flow Visualization Symposium*, FEDSM98-5257, Washington DC, USA, June 21–25, 1998.

Meyers, J. F.; "Development of Doppler Global Velocimetry as a Flow Diagnostics Tool," *Meas. Sci. Technol.*, Vol.6, No. 6, 1995, pp. 769–783.

Meyers, J. F.; *Investigation and Calculations of Basic Parameters for the Application of the Laser Doppler Velocimeter*, NASA Technical Note D-6125, April 1971.

Meyers, J. F.; J. W. Lee; R. J. Schwartz; "Characterization of measurement error sources in Doppler global velocimetry," *Meas. Sci. Technol.*, Vol. 12, 2001, pp. 357–368.

Meyers, J. F.; M. J. Walsh; *Computer Simulation of a Fringe Type Laser Velocimeter*, Project Squid Workshop on the Use of the Laser Velocimeter for Flow Measurements, March 27–29 1974, Purdue University.

Mie, G.; "Optics of Turbid Media," *Ann. Phys*., vol. 25, No. 3, 1908, pp. 377–445.

Mocker, H. W.; T. J. Wagener; "Laser Doppler optical air-data system: feasibility demonstration and systems specifications," *Appl. Optics*, Vol. 33, No. 27, 1994, p. 6457.

Munoz, R. M.; H. W. Mocker, L. Koehler; "Airborne laser Doppler velocimeter," *Appl. Optics*, vol. 13, 1974, p. 2890.

Ott, J.; "Lidar 'reads' air-drop winds," Aviation Week & Space Technology, 12 Feb. 1996, p. 44.

Post, M. J. and R. E. Cupp; "Optimizing a pulsed Doppler lidar," *Appl. Opt.* Vol. 29, No. 28, 1990, p. 4145.

Rahm, S.; "Measurement of a wind field with an airborne continuous-wave Doppler lidar," *Optics Letters*, Vol. 20, No. 2, 1995, pp. 216–218.

Rahm, S.; "Precursor experiment for an active airspeed sensor," *Optics Letters*, Vol. 26, No. 6, 2001, pp. 319–321.

Rees, D.; and I. S. McDermid; "Doppler lidar atmospheric wind sensor: reevaluation of a 355-nm Incoherent Doppler lidar," *Appl. Opt*., Vol. 29, No. 28, 1990, pp. 4133–4144.

Rees, D.; T. J. Fuller-Rowell; A. Lyons; T. L. Killeen; P. B. Hays; "Stable and rugged etalon for the Dynamics Explorer Fabry-Perot interferometer. 1: Design and construction," *Appl. Optics*, Vol. 21, No. 21, 1982, pp. 3896–3902.

Reitebuch, O.; Ch. Werner; I. Leike; P. Delville; P. Flamant; A. Cress; D. Engelbart; "Experimental Validation of Wind Profiling Performed by the Airborne 10-µm Heterodyne Doppler Lidar WIND," *J. Atmos. Oceanic Technol*., Vol. 18, No. 8, 2001, pp. 1331–1344.

Richmond, R.; D. Jewell; J. Carr; and J. Root; "U.S. Air Force ballistic winds program," *SPIE Proc*. Vol. 3065, *Laser Radar Technology and Applications II*, 21–25 April 1997, Orlando, FL, 1997. pp. 2–8.

Rietmuller, M. L.; and A. Boutier, "Laser velocimetry," *VKI Lecture Series-05*, von Karman Institute for Fluid Dynamics, 10–14 June 1991, Chausée de Waterloo, 72, Rhode Saint Genèse, Belgium, 1991.

Roehle, I.; C. E. Willert; "Extension of Doppler global velocimetry to periodic flows," *Meas. Sci. Technol*., Vol 12, 2001, pp. 420–431.

Roehle, I.; "Doppler Global Velocimetry," Lecture Series 1998-06: *Advanced Measurement Techniques*, von Karman Institute of Fluid Dynamics, Brussels, 1998.

Roehle, I.; "Doppler Global Velocimetry," paper 4, RTO-EN-6 RTO AVT Lecture Series, *Planar Optical Measurement Methods for Gas Turbine Components*, 1999.

Roehle, I.; R. Schodl; P. Voigt; C. Willert; "Recent developments and applications of quantitative laser light sheet measuring techniques in turbomachinery components," *Meas. Sci. Technol.*, Vol.11, 2000, pp. 1023–1035.

Rye, B. J.; R. M. Hardesty; "Time series identification and Kalman filtering techniques for Doppler lidar velocity estimation," *Appl. Opt.*, Vol. 28, No. 5, 1989, p. 879.

*Safe Use of Lasers,* ANSI Z136.1-2000, published by the American National Standards Institute, Washington, D. C. and New York, N. Y.

*Safe Use of Lasers in an Outdoor Environment,* ANSI Z136.6-2000, published by the American National Standards Institute, Washington, D. C. and New York, N. Y.

Schodl, R.; "Laser-two-focus velocimetry." In *Advanced Instrumentation for Aero Engine Components*. AGARD-CP-399, Philadelphia, 1986, p. 7.

Schodl, R.; W. Förster; G. Karpinski; H. Krain; I. Röhle; "3-Component Doppler Laser-Two-Focus Velocimetry Applied to a Transonic Centrifugal Compressor," *10th International Symp. on Application of Laser Techniques to Fluid Mechanics*, Lisbon, Portugal, July 2000, Paper 7-2, 2000.

Silfvast, W. T.; *Laser Fundamentals*, Cambridge University Press, Cambridge, UK, 1996.

Skinner, W. R. and P. B. Hays; "Incoherent Doppler lidar for measurement of atmospheric winds," *Optical spectroscopic techniques and instrumentation for atmospheric and space research, SPIE vol. 2266*, 1994, pp. 383–394.

Smart, A. E.; "Optical velocity sensor for air data applications," *Opt. Eng.*, Vol. 31, No. 1, 1992, pp. 166–173.

Sonnenschein, C. M. and F. A. Horrigan; "Signal-to-Noise Relationships for Coaxial Systems that Hetrodyne Backscatter from the Atmosphere," *Appl. Optics*, Vol. 10, No. 7, July 1971, pp. 1600–1604.

Soreide, D. C.; R. K. Bogue; L. J. Eherenberger; H. Bagley; *Coherent Lidar Turbulence Measurement for Gust Load Alleviation*, NASA Technical Memorandum 104318, 1996. Also presented at the SPIE 1996 International Symposium on Optical Science, Engineering, and Instrumentation, August 1996, Denver, CO.

Soreide, D.; R. K. Bogue; J. Seidel; and L. J. Ehernberger; *The Use of a Lidar Forward-Looking Turbulence Sensor for Mixed-Compression Inlet Unstart Avoidance and Gross Weight Reduction on a High Speed Civil Transport*, NASA Technical Memorandum 104332, 1997. Also presented at the 33rd AIAA/ASME/SAE/ASEE Joint Propulsion Conference and Exhibit, July 1997, Seattle, WA.

Soreide, David; Rodney K. Bogue; L. J. Ehernberger; Stephen M. Hannon; David A. Bowdle; *Airborne Coherent Lidar for Advanced In-Flight Measurements (ACLAIM) Flight Testing of the Lidar Sensor*, American Meteorological Society, Ninth Conference on Aviation, Range, and Aerospace Meteorology, September 2000, Orlando FL.

Targ, R. and R. K. Bowles; "Windshear Avoidance: Requirements Proposed System for Airborne Lidar Detection", SPIE vol. 899, *Airborne and Spaceborne Lasers for Terrestrial Geophysical Sensing*, 1988 p. 54.

Targ, R.; M. J. Kavaya; R. M. Huffaker; and R. L. Bowles; "Coherent lidar airborne windshear sensor: performance evaluation," *Appl. Opt*., Vol. 30, No. 15, 1991, p. 2013.

Targ, R.; B. C. Steakley; J. G. Hawley; L. L. Ames, P. Forney; D. Swanson; R. Stone; R. G. Otto; V. Zarifis; P. Brockman; R. S. Calloway; S. Harrell Klein; and P. A. Robinson; "Coherent lidar airborne wind sensor II: flight-test results at 2 and 10 μm," *Appl. Optics*, Vol. 35, No. 36, 1996, p. 7117.

Tchoryk, P. Jr.; C. B. Watkins; S. K. Lindemann; P. B. Hays; C. A. Nardell; "Molecular Optical Air Data System (MOADS)," *SPIE Proc. 4377, Laser Radar Technology and Applications VI*, 16–20 April 2001, Orlando, FL, Paper 4377-28.

van de Hulst, H. C.; *Light Scattering by Small Particles*, 2nd ed., Dover Publications Inc., New York, 1981.

Vaughan, J. M.; D. W. Brown; C. Nash; S. B. Alejandro; and G. G. Koenig; "Atlantic atmospheric aerosol studies: 2. Compendium of airborne backscatter measurements at 10.6 μm," *Journal of Geophysical Research*, Vol. 100, No. D1, 1995, pp. 1043–1065.

Vaughan, J. M.; J. O. Steinvall; C. Werner; and P. H. Flamant; "Coherent Laser Radar in Europe," *IEEE Proceedings*, Vol. 84, No. 2, February 1996, pp. 205–226.

Vaughan, J. M.; P. A. Forrester; "Laser Doppler Velocimetry Applied to the Measurement of Local and Global Wind," *Wind Eng*., Vol. 13, No. 1, 1989, p. 1.

Vaughan, J. M.; R. D. Callan; D. A. Bowdle; and J. Rothermel; "Spectral analysis, digital integration, and measurement of low backscatter in coherent laser radar," *Appl. Opt*., Vol 28, No. 15, 1989, p. 3008.

Wagener, T. J.; N. Demma; J. D. Kmetec; T. S. Kubo; "2 μm LIDAR for Laser-Based Remote Sensing: Flight Demonstration and Application Survey," *13th DASC, AIAA/IEEE Digital Avionics Systems Conference*, 30 Oct–3 Nov 1994, Phoenix, AZ.

Werner, Ch.; M. Klier; H. Herrmann, E. Biselli, R. Häring, "Compact Laser Doppler Anemometer," *AGARD CP 502, Remote Sensing of the Propagation Environment*, 1992, p. 27.

Werner, Ch.; "Applications of spaceborne Doppler and backscatter lidar: a critical review," *Opt. Eng.*, Vol. 34, No. 11, 1995, pp. 3103–3114.

Werner, Ch.; P. Flamant; O. Reitebuch; F. Köpp; J. Streicher; S. Rahm; E. Nagel; M. Klier; H. Herrmann; C. Loth; P. Delville; Ph. Drobinski; B. Romand; Ch. Boitel; D. Oh; M. Lopez; M. Meissonnier; D. Bruneau; A. Dabas; "Wind infrared Doppler lidar instrument," *Opt. Eng*., 40, 2001, pp. 115–125.

Woodfield, A. A.; J. M. Vaughan; "Using an Airborne $CO_2$ Laser for Free Stream Airspeed and Windshear Measurements," *AGARDograph-AG-272, Advances in Sensors and Their Integration into Aircraft Guidance and Control Systems*, 1983, p. 7.

Yu, F. T. S.; X. Yang; *Introduction to Optical Engineering*, Cambridge University Press, Cambridge, 1997.

## 9.3 Chapter-Specific Breakdown

### Further Reading Chapter 1

Smart–1992, ANSI Standard Z136, Munoz–1974.

### Further Reading Chapter 3

Mie–1908, Dainty–1975, Deirmendjian–1964, Drain–1980, Durst–1981, Hays–1982, Hughes–1973, Kane–1984, Kogelnik–1966, Korb–1992, Louden–1993, Mendoza–1998, Silfvast–1996, Sonnenschein–1971, Targ–1996, van de Hulst–1981, Vaughan–1995, Vaughan and Callan–1989, Vaughan and Forrester–1989.

### Further Reading Chapter 4

Damp–1994, Hecht–1992, Kane–1984, Köpp–1990, Silfvast–1996, Yu–1997.

### Further Reading Chapter 5

Abreu–1992, Bilbro–1986, Bilbro and Johnson–1986, Born–1970, Drain–1980, Durst–1981, Elliott–1999, Hays–1985, Hausamann–1990, Hecht–1992, Holmes–1988, Jentink–1994, Korb–1992, Komine–1994, Kristensen–1987, Latalick–1989, McGil–1998, Meyers–1971, Meyers–1974, Meyers–1995, Meyers–2001, Post–1990, Rietmuller–1991, Roehle–1998, Roehle–1999, Roehle–2000, Roehle–2001, Rye–1989, Schodl–1986, Schodl–2000, Silfvast–1996, Skinner–1994, Yu–1997.

### Further Reading Chapter 6

Alonso–1991, Becker–1999, Bilbro–1980, Cattin–1992, Combe–2000, Fetzer–-1990, Hannon–1994, Jentink–1995, Köpp–1997, Mandel–1984, McGann–1995, McCaul–1986, Ott–1996, Rahm–1995, Reitbuch–2001, Richmond–1997, Smart–1992, Soreide–1996, Soreide–1997, Soreide–2000, Targ–1991, Targ–1996, Tchoryk–2001, Woodfield–1983.

### Further Reading Chapter 7

Alonso–1991, Becker–1999, Bogue–March 1995, Bogue–July 1995, Cattin–1992, Combe–2000, Damp–1991, Damp–1994, Erwin–1993, Grosche–2000, Hannon–1994, Jentink–1994, Jentink–1995, Keane–1997, Köpp–1997, Mandle–1984, Mandle–1991, Manione–1978, McCaul–1986, McGann–1995, Meyers–1995, Ott–1996, Rahm–2001, Reitebuch–2001, Richmond–1997, Schodl–2000, Soreide–2000, Smart–1992, Targ–1996, Vaughn–1996, Wagener–1994, Werner–1992, Werner–2001, Woodfield–1983.

**This page has been deliberately left blank**

---

**Page intentionnellement blanche**

# Annex – AGARD and RTO
# Flight Test Instrumentation and Flight Test Techniques Series

## 1. Volumes in the AGARD and RTO Flight Test Instrumentation Series, AGARDograph 160

| Volume Number | Title | Publication Date |
|---|---|---|
| 1. | Basic Principles of Flight Test Instrumentation Engineering (Issue 2)<br>Issue 1: Edited by A. Pool and D. Bosman<br>Issue 2: Edited by R. Borek and A. Pool | <br>1974<br>1994 |
| 2. | In-Flight Temperature Measurements<br>by F. Trenkle and M. Reinhardt | 1973 |
| 3. | The Measurements of Fuel Flow<br>by J.T. France | 1972 |
| 4. | The Measurements of Engine Rotation Speed<br>by M. Vedrunes | 1973 |
| 5. | Magnetic Recording of Flight Test Data<br>by G.E. Bennett | 1974 |
| 6. | Open and Closed Loop Accelerometers<br>by I. McLaren | 1974 |
| 7. | Strain Gauge Measurements on Aircraft<br>by E. Kottkamp, H. Wilhelm and D. Kohl | 1976 |
| 8. | Linear and Angular Position Measurement of Aircraft Components<br>by J.C. van der Linden and H.A. Mensink | 1977 |
| 9. | Aeroelastic Flight Test Techniques and Instrumentation<br>by J.W.G. van Nunen and G. Piazzoli | 1979 |
| 10. | Helicopter Flight Test Instrumentation<br>by K.R. Ferrell | 1980 |
| 11. | Pressure and Flow Measurement<br>by W. Wuest | 1980 |
| 12. | Aircraft Flight Test Data Processing – A Review of the State of the Art<br>by L.J. Smith and N.O. Matthews | 1980 |
| 13. | Practical Aspects of Instrumentation System Installation<br>by R.W. Borek | 1981 |
| 14. | The Analysis of Random Data<br>by D.A. Williams | 1981 |
| 15. | Gyroscopic Instruments and Their Application to Flight Testing<br>by B. Stieler and H. Winter | 1982 |
| 16. | Trajectory Measurements for Take-off and Landing Test and Other Short-Range Applications<br>by P. de Benque D'Agut, H. Riebeek and A. Pool | 1985 |
| 17. | Analogue Signal Conditioning for Flight Test Instrumentation<br>by D.W. Veatch and R.K. Bogue | 1986 |
| 18. | Microprocessor Applications in Airborne Flight Test Instrumentation<br>by M.J. Prickett | 1987 |
| 19. | Digital Signal Conditioning for Flight Test<br>by G.A. Bever | 1991 |
| 20. | Optical Air Flow Measurements in Flight<br>by R.K. Bogue and H.W. Jentink | 2003 |

## 2. Volumes in the AGARD and RTO Flight Test Techniques Series, AGARDograph 300

| Volume Number | Title | Publication Date |
|---|---|---|
| AG237 | Guide to In-Flight Thrust Measurement of Turbojets and Fan Engines by the MIDAP Study Group (UK) | 1979 |

The remaining volumes are published as a sequence of Volume Numbers of AGARDograph 300.

| | | |
|---|---|---|
| 1. | Calibration of Air-Data Systems and Flow Direction Sensors<br>by J.A. Lawford and K.R. Nippress | 1988 |
| 2. | Identification of Dynamic Systems<br>by R.E. Maine and K.W. Iliff | 1988 |
| 3. | Identification of Dynamic Systems – Applications to Aircraft<br>Part 1: The Output Error Approach<br>by R.E. Maine and K.W. Iliff<br>Part 2: Nonlinear Analysis and Manoeuvre Design<br>by J.A. Mulder, J.K. Sridhar and J.H. Breeman | <br>1986<br><br>1994 |
| 4. | Determination of Antenna Patterns and Radar Reflection Characteristics of Aircraft<br>by H. Bothe and D. McDonald | 1986 |
| 5. | Store Separation Flight Testing<br>by R.J. Arnold and C.S. Epstein | 1986 |
| 6. | Developmental Airdrop Testing Techniques and Devices<br>by H.J. Hunter | 1987 |
| 7. | Air-to-Air Radar Flight Testing<br>by R.E. Scott | 1992 |
| 8. | Flight Testing under Extreme Environmental Conditions<br>by C.L. Henrickson | 1988 |
| 9. | Aircraft Exterior Noise Measurement and Analysis Techniques<br>by H. Heller | 1991 |
| 10. | Weapon Delivery Analysis and Ballistic Flight Testing<br>by R.J. Arnold and J.B. Knight | 1992 |
| 11. | The Testing of Fixed Wing Tanker & Receiver Aircraft to Establish Their Air-to-Air Refuelling Capabilities<br>by J. Bradley and K. Emerson | 1992 |
| 12. | The Principles of Flight Test Assessment of Flight-Safety-Critical Systems in Helicopters<br>by J.D.L. Gregory | 1994 |
| 13. | Reliability and Maintainability Flight Test Techniques<br>by J.M. Howell | 1994 |
| 14. | Introduction to Flight Test Engineering<br>Edited by F. Stoliker | 1995 |
| 15. | Introduction to Avionics Flight Test<br>by J.M. Clifton | 1996 |
| 16. | Introduction to Airborne Early Warning Radar Flight Test<br>by J.M. Clifton and F.W. Lee | 1999 |
| 17. | Electronic Warfare Test and Evaluation<br>by H. Banks and R. McQuillan | 2000 |
| 18. | Flight Testing of Radio Navigation Systems<br>by H. Bothe and H.J. Hotop | 2000 |
| 19. | Simulation in Support of Flight Testing<br>by D. Hines | 2000 |

| | | |
|---|---|---|
| 20. | Logistics Test and Evaluation in Flight Testing<br>by M. Bourcier | 2001 |
| 21. | Flying Qualities Flight Testing of Digital Flight Control Systems<br>by F. Webster and T.D. Smith | 2001 |
| 22. | Helicopter/Ship Qualification Testing<br>by D. Carico, R. Fang, R.S. Finch, W.P. Geyer Jr., Cdr. (Ret.) H.W. Krijns and K. Long | 2002 |
| 23. | Flight Test Measurement Techniques for Laminar Flow<br>by D. Fisher, K.H. Horstmann and H. Riedel | 2003 |

At the time of publication of the present volume, the following volumes are in preparation:

Flight Testing of Night Vision Systems

Unique Aspects of Flight Testing of Unmanned Aerial Vehicles/Unmanned Combat Aerial Vehicles

Aircraft-Stores Certification Testing

Selection of a Flight Test Instrumentation System

Testing of Precision Airdrop Systems

Flight Testing of Tactical Laser Systems

**This page has been deliberately left blank**

---

**Page intentionnellement blanche**

# REPORT DOCUMENTATION PAGE

| 1. Recipient's Reference | 2. Originator's References | 3. Further Reference | 4. Security Classification of Document |
|---|---|---|---|
| | RTO-AG-160<br>AC/323(SCI-033)TP/48<br>Volume 20 | ISBN 92-837-1112-2 | UNCLASSIFIED/<br>UNLIMITED |

**5. Originator**

Research and Technology Organisation
North Atlantic Treaty Organisation
BP 25, F-92201 Neuilly-sur-Seine Cedex, France

**6. Title**

Optical Air Flow Measurements in Flight

**7. Presented at/Sponsored by**

SCI-122, the Flight Test Technology Task Group of the
Systems Concepts and Integration Panel (SCI) of RTO.

| 8. Author(s)/Editor(s) | 9. Date |
|---|---|
| R.K. Bogue and H.W. Jentink | December 2003 |
| **10. Author's/Editor's Address** | **11. Pages** |
| Multiple | 106 |

**12. Distribution Statement**

There are no restrictions on the distribution of this document.
Information about the availability of this and other RTO
unclassified publications is given on the back cover.

**13. Keywords/Descriptors**

Aerodynamics
Air data systems
Aircraft instruments
Atmospheric disturbances
Atmospheric physics
Data acquisition
Flight safety
Flow measurement
Laser anemometers
Laser doppler velocimetry
Light scattering
Measuring instruments
Meteorological instruments
Optical detection
Optical measuring instruments
Optical properties
Pressure measurement
Turbulence
Velocity measurement
Wind shear

**14. Abstract**

Providing an introductory practical overview of in-flight optical flow measurement techniques is the goal of this AGARDograph. This document is written for instrumentation engineer or research scientist having a need for making non-intrusive flow measurements on an aircraft. It is hoped that this document will be particularly useful for the technologist with a limited background in optical theory and limited experience in applying optical technology. The experience of the authors and well as numerous other workers has been infused to provide guidance to avoid expensive non-productive diversions that may occur when applying optical technology for the first time in the flight environment. This AGARDograph provides basic knowledge and techniques necessary to assess the applicability of optical measurements and to address effective optical measurement techniques in flight. Key aspects of optical measurements are discussed and the tradeoffs are identified as they are currently understood. Basic components of optical measurement systems are discussed and key requirements are identified. Specific systems designed for a variety of applications are discussed to provide insight for the reader.

**This page has been deliberately left blank**

---

**Page intentionnellement blanche**

NORTH ATLANTIC TREATY ORGANISATION

RESEARCH AND TECHNOLOGY ORGANISATION

BP 25
F-92201 NEUILLY-SUR-SEINE CEDEX • FRANCE
Télécopie 0(1)55.61.22.99 • E-mail mailbox@rta.nato.int

**DIFFUSION DES PUBLICATIONS**

**RTO NON CLASSIFIEES**

Les publications de l'AGARD et de la RTO peuvent parfois être obtenues auprès des centres nationaux de distribution indiqués ci-dessous. Si vous souhaitez recevoir toutes les publications de la RTO, ou simplement celles qui concernent certains Panels, vous pouvez demander d'être inclus soit à titre personnel, soit au nom de votre organisation, sur la liste d'envoi.

Les publications de la RTO et de l'AGARD sont également en vente auprès des agences de vente indiquées ci-dessous.

Les demandes de documents RTO ou AGARD doivent comporter la dénomination « RTO » ou « AGARD » selon le cas, suivi du numéro de série. Des informations analogues, telles que le titre est la date de publication sont souhaitables.

Si vous souhaitez recevoir une notification électronique de la disponibilité des rapports de la RTO au fur et à mesure de leur publication, vous pouvez consulter notre site Web (www.rta.nato.int) et vous abonner à ce service.

## CENTRES DE DIFFUSION NATIONAUX

**ALLEMAGNE**
Streitkräfteamt / Abteilung III
Fachinformationszentrum der
Bundeswehr (FIZBw)
Friedrich-Ebert-Allee 34, D-53113 Bonn

**BELGIQUE**
Etat-Major de la Défense
Département d'Etat-Major Stratégie
ACOS-STRAT – Coord. RTO
Quartier Reine Elisabeth
Rue d'Evère, B-1140 Bruxelles

**CANADA**
DSIGRD2
Bibliothécaire des ressources du savoir
R et D pour la défense Canada
Ministère de la Défense nationale
305, rue Rideau, 9e étage
Ottawa, Ontario K1A 0K2

**DANEMARK**
Danish Defence Research Establishment
Ryvangs Allé 1, P.O. Box 2715
DK-2100 Copenhagen Ø

**ESPAGNE**
SDG TECEN / DGAM
C/ Arturo Soria 289
Madrid 28033

**ETATS-UNIS**
NASA Center for AeroSpace
Information (CASI)
Parkway Center, 7121 Standard Drive
Hanover, MD 21076-1320

**FRANCE**
O.N.E.R.A. (ISP)
29, Avenue de la Division Leclerc
BP 72, 92322 Châtillon Cedex

**GRECE (Correspondant)**
Defence Industry & Research
General Directorate, Research Directorate
Fakinos Base Camp, S.T.G. 1020
Holargos, Athens

**HONGRIE**
Department for Scientific Analysis
Institute of Military Technology
Ministry of Defence
H-1525 Budapest P O Box 26

**ISLANDE**
Director of Aviation
c/o Flugrad
Reykjavik

**ITALIE**
Centro di Documentazione
Tecnico-Scientifica della Difesa
Via XX Settembre 123
00187 Roma

**LUXEMBOURG**
*Voir* Belgique

**NORVEGE**
Norwegian Defence Research Establishment
Attn: Biblioteket
P.O. Box 25, NO-2007 Kjeller

**PAYS-BAS**
Royal Netherlands Military
Academy Library
P.O. Box 90.002
4800 PA Breda

**POLOGNE**
Armament Policy Department
218 Niepodleglosci Av.
00-911 Warsaw

**PORTUGAL**
Estado Maior da Força Aérea
SDFA – Centro de Documentação
Alfragide
P-2720 Amadora

**REPUBLIQUE TCHEQUE**
DIC Czech Republic-NATO RTO
VTÚL a PVO Praha
Mladoboleslavská ul.
Praha 9, 197 06
Česká republika

**ROYAUME-UNI**
Dstl Knowledge Services
Information Centre, Building 247
Dstl Porton Down
Salisbury
Wiltshire SP4 0JQ

**TURQUIE**
Milli Savunma Bakanlığı (MSB)
ARGE ve Teknoloji Dairesi Başkanlığı
06650 Bakanliklar – Ankara

## AGENCES DE VENTE

**NASA Center for AeroSpace Information (CASI)**
Parkway Center, 7121 Standard Drive
Hanover, MD 21076-1320
ETATS-UNIS

**The British Library Document Supply Centre**
Boston Spa, Wetherby
West Yorkshire LS23 7BQ
ROYAUME-UNI

**Canada Institute for Scientific and Technical Information (CISTI)**
National Research Council
Acquisitions, Montreal Road, Building M-55
Ottawa K1A 0S2, CANADA

Les demandes de documents RTO ou AGARD doivent comporter la dénomination « RTO » ou « AGARD » selon le cas, suivie du numéro de série (par exemple AGARD-AG-315). Des informations analogues, telles que le titre et la date de publication sont souhaitables. Des références bibliographiques complètes ainsi que des résumés des publications RTO et AGARD figurent dans les journaux suivants :

**Scientific and Technical Aerospace Reports (STAR)**
STAR peut être consulté en ligne au localisateur de ressources uniformes (URL) suivant:
http://www.sti.nasa.gov/Pubs/star/Star.html
STAR est édité par CASI dans le cadre du programme NASA d'information scientifique et technique (STI)
STI Program Office, MS 157A
NASA Langley Research Center
Hampton, Virginia 23681-0001
ETATS-UNIS

**Government Reports Announcements & Index (GRA&I)**
publié par le National Technical Information Service
Springfield
Virginia 2216
ETATS-UNIS
(accessible également en mode interactif dans la base de données bibliographiques en ligne du NTIS, et sur CD-ROM)

NORTH ATLANTIC TREATY ORGANISATION

RESEARCH AND TECHNOLOGY ORGANISATION

BP 25
F-92201 NEUILLY-SUR-SEINE CEDEX • FRANCE
Télécopie 0(1)55.61.22.99 • E-mail mailbox@rta.nato.int

**DISTRIBUTION OF UNCLASSIFIED RTO PUBLICATIONS**

AGARD & RTO publications are sometimes available from the National Distribution Centres listed below. If you wish to receive all RTO reports, or just those relating to one or more specific RTO Panels, they may be willing to include you (or your Organisation) in their distribution.

RTO and AGARD reports may also be purchased from the Sales Agencies listed below.

Requests for RTO or AGARD documents should include the word 'RTO' or 'AGARD', as appropriate, followed by the serial number. Collateral information such as title and publication date is desirable.

If you wish to receive electronic notification of RTO reports as they are published, please visit our website (www.rta.nato.int) from where you can register for this service.

## NATIONAL DISTRIBUTION CENTRES

**BELGIUM**
Etat-Major de la Défense
Département d'Etat-Major Stratégie
ACOS-STRAT – Coord. RTO
Quartier Reine Elisabeth
Rue d'Evère
B-1140 Bruxelles

**CANADA**
DRDKIM2
Knowledge Resources Librarian
Defence R&D Canada
Department of National Defence
305 Rideau Street
9th Floor
Ottawa, Ontario K1A 0K2

**CZECH REPUBLIC**
DIC Czech Republic-NATO RTO
VTÚL a PVO Praha
Mladoboleslavská ul.
Praha 9, 197 06
Česká republika

**DENMARK**
Danish Defence Research Establishment
Ryvangs Allé 1
P.O. Box 2715
DK-2100 Copenhagen Ø

**FRANCE**
O.N.E.R.A. (ISP)
29, Avenue de la Division Leclerc
BP 72
92322 Châtillon Cedex

**GERMANY**
Streitkräfteamt / Abteilung III
Fachinformationszentrum der Bundeswehr (FIZBw)
Friedrich-Ebert-Allee 34
D-53113 Bonn

**GREECE (Point of Contact)**
Defence Industry & Research General Directorate, Research Directorate
Fakinos Base Camp, S.T.G. 1020
Holargos, Athens

**HUNGARY**
Department for Scientific Analysis
Institute of Military Technology
Ministry of Defence
H-1525 Budapest P O Box 26

**ICELAND**
Director of Aviation
c/o Flugrad, Reykjavik

**ITALY**
Centro di Documentazione Tecnico-Scientifica della Difesa
Via XX Settembre 123
00187 Roma

**LUXEMBOURG**
*See* Belgium

**NETHERLANDS**
Royal Netherlands Military Academy Library
P.O. Box 90.002
4800 PA Breda

**NORWAY**
Norwegian Defence Research Establishment
Attn: Biblioteket
P.O. Box 25, NO-2007 Kjeller

**POLAND**
Armament Policy Department
218 Niepodleglosci Av.
00-911 Warsaw

**PORTUGAL**
Estado Maior da Força Aérea
SDFA – Centro de Documentação
Alfragide, P-2720 Amadora

**SPAIN**
SDG TECEN / DGAM
C/ Arturo Soria 289
Madrid 28033

**TURKEY**
Milli Savunma Bakanlığı (MSB)
ARGE ve Teknoloji Dairesi Başkanlığı
06650 Bakanliklar – Ankara

**UNITED KINGDOM**
Dstl Knowledge Services
Information Centre, Building 247
Dstl Porton Down
Salisbury, Wiltshire SP4 0JQ

**UNITED STATES**
NASA Center for AeroSpace Information (CASI)
Parkway Center, 7121 Standard Drive
Hanover, MD 21076-1320

## SALES AGENCIES

**NASA Center for AeroSpace Information (CASI)**
Parkway Center
7121 Standard Drive
Hanover, MD 21076-1320
UNITED STATES

**The British Library Document Supply Centre**
Boston Spa, Wetherby
West Yorkshire LS23 7BQ
UNITED KINGDOM

**Canada Institute for Scientific and Technical Information (CISTI)**
National Research Council
Acquisitions
Montreal Road, Building M-55
Ottawa K1A 0S2, CANADA

Requests for RTO or AGARD documents should include the word 'RTO' or 'AGARD', as appropriate, followed by the serial number (for example AGARD-AG-315). Collateral information such as title and publication date is desirable. Full bibliographical references and abstracts of RTO and AGARD publications are given in the following journals:

**Scientific and Technical Aerospace Reports (STAR)**
STAR is available on-line at the following uniform resource locator:
http://www.sti.nasa.gov/Pubs/star/Star.html
STAR is published by CASI for the NASA Scientific and Technical Information (STI) Program
STI Program Office, MS 157A
NASA Langley Research Center
Hampton, Virginia 23681-0001
UNITED STATES

**Government Reports Announcements & Index (GRA&I)**
published by the National Technical Information Service
Springfield
Virginia 2216
UNITED STATES
(also available online in the NTIS Bibliographic Database or on CD-ROM)

ISBN 92-837-1112-2